Piping in the Maasvallei

A possibility or far-fetched scenario?

P.G. van der Hulst

TUDelft

Piping in the Maasvallei

A possibility or far-fetched scenario?

by

P.G. van der Hulst

to obtain the degree of Master of Science
at the Delft University of Technology
to be defended publicly on Friday September 15, 2017 at 15:00 PM.

Student number: 4152530
Project duration: February 2017 – September 2017
Thesis committee: Dr. P. J. Vardon   TU Delft, chair
                    Prof. Dr. M. A. Hicks   TU Delft
                    Dr. Ir. W. Kanning   TU Delft and Deltares
                    Ing. R. Koopmans   Arcadis

Cover image: Photo of the dike at the research location near Beesel by Dagmar Haggenburg

An electronic version of this thesis is available at `http://repository.tudelft.nl/`.

TUDelft

Preface

This thesis, titled 'Piping in the Maasvallei', is written for the completion of my Master of Science degree in Geo-Engineering, at the faculty of Civil Engineering and Geosciences at the Delft University of Technology. The project was carried out in collaboration with Arcadis in the period between February 2017 until September 2017.

Arcadis is engaged in the ongoing project POV Piping, a research project investigating piping related issues on a national level. In the past, a lot of research into the subject of piping has been done. However, there is still a lot unknown. Soil is a natural material with highly variable properties. It is therefore difficult to accurately predict the behaviour of soil. The Maasvallei is an area for which it becomes clear that there is still much unknown about piping. In the recent assessment of the Dutch dikes many of the dikes along the Maas in Limburg were found to be unsafe against piping. However, early signs of piping have not been observed in this area during periods of high-water. The contradiction between the lack of observations and the assessment is the topic of this thesis. A topic combining soil mechanics and geohydrology. During my study in Civil Engineering I gained interest into the behaviour of soil. During my master in Geo-Engineering a specific interest in geohydrology joined the interest for soil behaviour. This thesis combines both fields.

Several people assisted, motivated, helped and inspired me during the project whom I would like to thank. First, my graduation committee, Phil Vardon, Michael Hicks, Wim Kanning and Rimmer Koopmans for their time, input, guidance and the thorough reading of the report for every meeting. They gave a direction when needed and the freedom to define the thesis in my own way. A special thanks to Rimmer who always gave priority to my questions.

In addition, I want to thank Arcadis for providing the opportunity to do my graduation project in collaboration with them. My colleagues at Arcadis, Hans Niemeijer for sharing his knowledge of piping and Lotte Hobbelt and Muriël Houdé for their assistance with PlaxFlow.

I would also like to thank Jon Nuttall (Deltares) for his extensive help with the D-Geo Flow software and Vera van Beek (Deltares) for answering all my questions.

Last but not least, I want to thank Koen, my parents and friends for their support and help during this project and throughout my years in Delft.

Patricia van der Hulst

Delft, September 2017

Summary

One of the failure mechanisms for water retaining structures is piping. Piping is an internal erosion mechanism creating hollow spaces underneath the dike as a result of the transport of soil particles due to seepage. In the recent assessment of the Dutch dikes, many of the dikes along the Maas in Limburg were found to be insufficiently safe against piping. However, the early signs of piping in the form of sand boils have not been observed during recent high-water periods. As a result of this contradiction the question arose whether dike-failure due to piping is realistic in the Maasvallei. That question is the main research question of this thesis.

The piping process is a combination of the subsequent occurrence of three mechanisms: uplift, heave and backward erosion. As a result of a high river water level with respect to a lower hydraulic head in the hinterland a horizontal groundwater flow through the aquifer underneath the dike establishes. This results in an increase of the water pressure in the aquifer. When the upward water pressure in the aquifer equals the weight of the blanket layer the blanket layer is lifted (uplift). Consequently, the soil particles cannot withstand the water pressure and the groundwater is forced upward through the blanket layer. Ruptures occur resulting in the formation of a vertical channel allowing the free exit of water. As a result of the high local flow velocity of the seepage flow, sand particles are eroded and transported through the vertical channel towards surface level (heave). The sand particles are deposited outside the well and small horizontal pipes start to form underneath the blanket layer. Once a critical head difference is reached, pipe formation continues (backward erosion) until the pipe reaches the upstream side and a continuous pipe is formed.

This study focussed on piping in the Maasvallei. The Maasvallei covers the northern part of the Maas, roughly between the Dutch towns Roermond and Mook. The subsoil in the Maasvallei typically exists of three components: a relative permeable top clay layer followed by coarse sand and a gravel package with a highly variable permeability. As the name of the area suggests, the Maas is situated in a valley. Therefore, the surface level in the hinterland increases further from the river, resulting in a seepage flow towards the Maas. The dikes in the Maasvallei are relatively new. They were constructed after the floods of 1993 and 1995. In 2011, again a high-water period occurred. No piping related observations such as sand boils are known from that period. Four research locations in the Maasvallei have been selected to study the piping likelihood of the Maasvallei. At the end of 2014, several piezometers were installed at these locations. In addition, a lot of field and laboratory tests were performed. The research locations are situated near the villages Well, Beesel, Buggenum and Thorn.

By means of these four cases, several analysis were performed, divided in two phases: the analytical analysis and the numerical analysis. The first phase concerned the analytical analysis. Three objectives were identified with respect to the analytical analysis: 1) the hindcast of past high water events and the forecast of a future high water event, 2) determining the influence of safety factors from the assessment guideline on calculation results, 3) determining the parameter sensitivity.

The analytical analysis has been performed based on the analytical groundwater flow model [TAW, 1999] as applied in practice and the calculation rule of Sellmeijer. The first step was to determine the critical head difference for each mechanism (uplift, heave and backward erosion). Based on these critical head differences, three water levels scenarios have been evaluated including a past scenario (water levels of 1993), a current scenario (water levels of 2011) and a future scenario (prediction for 2075). The effect of safety factors has been determined by a study of the influence of the safety factors on the critical head difference. The parameter sensitivity has been studied by means of a sensitivity analysis in which the parameters were varied based on a variation coefficient.

From the analytical analysis it followed that water levels have occurred in the past for which the critical limits would be exceeded at several 'critical locations' if they occur again. Besides, the number

of critical locations and thus the piping likelihood increases with a future increase of the river water level. Furthermore, based on the results concerning the water level scenario of 2011 and the historic observations, it seems that the critical heave gradient of 0.3 as applied in the assessment practice is conservative. However, this can not be ascertained with complete certainty. Furthermore, the analysis has shown that the influence of safety factors in the assessment guidelines is limited. The sensitivity analysis has shown that the blanket layer permeability is one of the most influential subsoil parameters with respect to the piping likelihood.

Several deficiencies regarding the analytical model have been identified, related to the assumptions underlying the analytical model. The analytical model incorrectly assumes that the subsoil consists of only two layers (blanket layer and aquifer) and that these layers are perfectly horizontal, homogeneous and continuous. In addition, the model incorrectly assumes a perfect horizontal flow path in the aquifer and vertical leakage through the blanket layer. In response to the identified deficiencies, two questions with respect to the applicability of the analytical model have been asked: 1) To what extent does the groundwater flow model correctly predicts the exit potentials in the Maasvallei? 2) To what extent is the Sellmeijer calculation rule applicable for the Maasvallei? These questions have been addressed in the second calculations phase, the numerical analysis.

The numerical analysis had two objectives: 1) determining the effect of model components on the piping likelihood, 2) validation of the analytical groundwater flow model and the Sellmeijer calculation rule. For this purpose a numerical model of the research location near Buggenum has been created and calibrated by means of the numerical finite element software PlaxFlow. Besides, the numerical model was implemented in the new software D-Geo Flow in order to model the pipe development.

The influence of the model components (layering and soil characteristics) has been studied by means of a variation study with respect to the original numerical model. The model variations showed that the most influential model component is the blanket layer. Both the permeability and the thickness of the blanket layer are of importance. A decrease of the permeability or the thickness of the blanket layer results in a higher exit potential and thus a higher piping likelihood. The opposite results in a lower piping likelihood. The second most influential component is the specific geometry of the aquifer. The presence of horizontal zones with highly varying permeability has a great effect on the exit potential. It is possible that a specific geometry reduces the exit potential locally, but the opposite is also possible.

The analytical groundwater flow model has been validated by means of a comparison with the numerical model based on the exit potential and model input. The analytical calculation resulted in a significantly lower exit potential than the numerical model, respectively 19.32 and 18.92 m + NAP. This difference can be explained by an evaluation of the flow pattern of both models. The analytical groundwater flow model is based on several assumptions leading to a horizontal schematisation of the aquifer groundwater flow, as previously described. However, in reality the flow path deviates from this perfect horizontal path causing a change in the exit potential. It can be concluded that when the groundwater flow deviates significantly from a horizontal flow path, the analytical model will most likely result in an exit potential that differs from the realistic exit potential.

The calculation rule of Sellmeijer is validated by means of a comparison of the analytical calculation rule and the numerical model in D-Geo Flow based on the critical head difference H_c. The calculation rules resulted in a lower head difference than the numerical model, respectively 2.45 m and 3.3 m. The difference can be explained by means of a comparison of the model configuration. The calculation rule is based on a standard dike configuration by means of a fit parameter in the calculation rule. If the actual geometry differs from the standard configuration, the calculation rule will result in a critical head difference that differs from the actual value. The fit factor can be re-determined for a different geometry by means of a numerical model in order to establish a calculation rule that is suitable for that particular dike configuration.

Based on the literature study and the results of both the analytical and numerical analysis it has been concluded that dike-failure due to piping is realistic in the Maasvallei. This does not apply to all dikes in the Maasvallei area, but to some critical locations. The study showed that in the past hydraulic circumstances have occurred for which piping would be a realistic scenario if they occur again. In

addition, it has been shown that the number of critical locations will increase in the future as a result of the rising river water level.

Samenvatting

Eén van de faalmechanismes voor waterkerende constructies is piping. Piping is een erosie mechanisme waarbij holle ruimtes worden gecreëerd onder een waterkerende constructie door het transport van zandkorrels als gevolg van kwel. In de meest recente toetsing van de Nederlandse dijken is een groot deel van de dijken langs de Maas afgekeurd met betrekking tot piping. Echter, zijn er geen tekenen van piping, zoals zandwellen, waargenomen tijdens de meest recente hoogwaterperiode. Naar aanleiding van deze tegenstelling is de vraag ontstaan of het falen van de dijken ten gevolge van piping realistisch is in de Maasvallei. Die vraag is de hoofdvraag van dit onderzoek.

Het piping proces is een combinatie van het opeenvolgend voorkomen van drie mechanismen: opbarsten, heave en terugschrijdende erosie. Een hoge rivier waterstand ten opzichte van een lagere stijghoogte in het achterland, resulteert in een horizontale grondwaterstroming door de watervoerende laag. De grondwaterstroming leidt tot een toename van de waterdruk in het watervoerende pakket onder de deklaag. Op het moment dat deze opwaartse waterdruk gelijk is aan het gewicht van de deklaag, barst de deklaag op. Er ontstaan scheurtjes waardoor het grondwater vrij naar het oppervlak kan stromen. Zo wordt een verticaal uitstroomkanaal gevormd. Zanddeeltjes worden geërodeerd en meegevoerd naar het maaiveld als gevolg van de hoge stroomsnelheid. Het geërodeerde zand wordt naast de wel afgezet waardoor kleine kanaaltjes onder de deklaag worden gevormd. Op het moment dat er een kritiek verval over de dijk wordt bereikt, zet deze kanaalvorming zich door totdat de pijp de rivier bereikt.

Dit onderzoek richt zich op piping in de Maasvallei. De Maasvallei betreft het Noordelijke deel van de Maas in Nederland en is grofweg gesitueerd tussen de plaatsen Roermond en Mook. De typische ondergrond in de Maasvallei bestaat uit drie componenten: een deklaag van relatief doorlatende klei, gevolgd door een laag grof zand en een grind pakket met een sterk variabele doorlatendheid. Zoals de naam van het gebied al suggereert, is de Maas gelegen in een vallei. De hoogte van het maaiveld neemt toe met toenemende afstand tot de dijk. Dit hoge achterland resulteert in een kwelstroom vanuit het achterland richting de rivier. De dijken in de Maasvallei zijn relatief nieuw. Ze zijn geconstrueerd na de overstromingen in 1993 en 1995. In 2011 is er opnieuw een periode van hoogwater geweest. Uit die periode zijn geen piping gerelateerde observaties bekend zoals zandwellen. Vier onderzoekslocaties in de Maasvallei zijn geselecteerd om de piping problematiek van het gebied te onderzoeken. Eind 2014 zijn op deze locaties verschillende piezometers geïnstalleerd die sindsdien de stijghoogtes meten. Daarnaast is uitgebreid veld- en labonderzoek uitgevoerd. De onderzoekslocaties zijn gesitueerd bij de plaatsen Well, Beesel, Buggenum en Thorn.

Aan de hand van deze vier cases zijn verschillende analyses uitgevoerd, opgedeeld in twee fases: de analytische analyse en de numerieke analyse. De eerste fase betrof de analytische analyse. Drie doelen met betrekking tot de analytische analyse zijn opgesteld: 1) de evaluatie van hoogwaterperiodes uit het verleden en een voorspelling voor de toekomst, 2) het bepalen van de invloed van veiligheidsfactoren uit de toetsingsrichtlijnen op de berekeningsresultaten, 3) het bepalen van de gevoeligheid van de parameters.

De analytische analyse is uitgevoerd op basis van het analytisch grondwaterstromingsmodel [TAW, 1999] zoals toegepast in de Nederlandse toetsingspraktijk en de rekenregel van Sellmeijer. De eerste stap betrof het bepalen van het kritieke verval voor ieder mechanisme (opbarsten, heave en terugschrijdende erosie). Op basis van deze kritieke vervallen zijn drie scenario's met betrekking tot de rivier waterstand geanalyseerd. Dit betrof een scenario op basis van de waterstand uit 1993, een scenario op basis van de waterstand uit 2011 en een scenario op basis van een voorspelling van de waterstand voor 2075. Het effect van de veiligheidsfactoren is onderzocht door middel van een analyse van het effect van de factoren op de kritieke limieten. De gevoeligheid van de parameters is geanalyseerd door middel van een gevoeligheidsanalyse op basis van een variatiecoëfficiënt voor iedere parameter.

Uit de analytische analyse is gebleken dat er in het verleden waterstanden zijn voorgekomen waarbij de kritieke limieten zouden worden overschreden wanneer deze omstandigheden zich opnieuw zouden voordoen. Dit geldt niet voor de gehele dijkring, maar voor bepaalde kritieke locaties. Daarbij is aangetoond dat het aantal kritieke locaties in de toekomst zal toenemen als gevolg van de toenemende waterstand. De analyse heeft tevens aangetoond dat het effect van veiligheidsfactoren beperkt is. De gevoeligheidsanalyse heeft laten zien dat de doorlatendheid van de deklaag één van de belangrijkste parameters is met betrekking tot piping.

Met betrekking tot het analytische model zijn een aantal onjuistheden geïdentificeerd, gerelateerd aan de uitgangspunten van het analytische model. Het analytische model veronderstelt onjuist dat de ondergrond uit slechts twee lagen bestaat (deklaag en watervoerende laag) en dat deze lagen perfect horizontaal, homogeen en continu zijn. Daarnaast veronderstelt het model onjuist dat de grondwaterstroming in de watervoerende laag perfect horizontaal is en dat de stroming (lek) door de deklaag perfect verticaal is. Naar aanleiding van deze onjuistheden zijn twee vragen gesteld met betrekking tot de toepasbaarheid van het analytisch model: 1) In hoeverre geeft het analytisch grondwaterstromingsmodel een juiste voorspelling van het potentiaal in de Maasvallei? 2) In welke mate is de rekenregel van Sellmeijer toepasbaar voor de Maasvallei? Deze vragen zijn aan bod gekomen in de tweede fase, de numerieke analyse.

De numerieke analyse had twee doelen: 1) het bepalen van het effect van modelcomponenten op de piping gevoeligheid, 2) het valideren van het analytisch grondwaterstromingsmodel en de rekenregel van Sellmeijer. Hiervoor is een numeriek model van de onderzoekslocatie nabij Buggenum gemaakt en gekalibreerd met behulp van de numerieke eindige-elementen software PlaxFlow. Tevens is het model geïmplementeerd in de nieuwe software D-Geo Flow om de ontwikkeling van een pipe te modelleren.

De invloed van modelcomponenten (gelaagdheid en grond karakteristieken) is onderzocht aan de hand van een variatie studie van het originele numerieke model. De model variaties hebben aangetoond dat de deklaag de meest invloedrijke modelcomponent is. Zowel de doorlatendheid als de dikte van de deklaag zijn van groot belang. Een afname van de doorlatendheid of de dikte van de deklaag resulteert in een hoger uittredepotentiaal en dus een grotere kans op piping. Het tegenovergestelde resulteert in een kleinere kans op piping. De tweede meest invloedrijke modelcomponent is de specifieke geometrie van de watervoerende laag. De aanwezigheid van horizontale zones met een sterk afwijkende doorlatendheid heeft een groot effect op het uittredepotentiaal. Het is hierdoor mogelijk dat de specifieke geometrie lokaal het uittredepotentiaal verlaagt. Het tegenovergestelde is ook mogelijk.

Het analytisch grondwaterstromingsmodel is gevalideerd aan de hand van een vergelijking van het analytisch en numeriek model op basis van het uittredepotentiaal en de modelinvoer. Het analytisch model resulteerde in een significant lager uittredepotentiaal dan het numeriek model, respectievelijk 19,32 en 18,92 m + NAP. Dit verschil kan worden verklaard door middel van een evaluatie van het stromingsbeeld van beide modellen. Het analytisch grondwaterstromingsmodel is gebaseerd op de aanname dat de grondwaterstroming in de watervoerende laag perfect horizontaal is, zoals hiervoor beschreven. Echter wijkt in werkelijkheid de grondwaterstroming af van dit perfecte horizontale pad. In dit onderzoek is aangetoond dat de vorm van de stroomlijnen een groot effect hebben op het uittredepotentiaal. Geconcludeerd kan worden dat wanneer het stromingsbeeld afwijkt van een horizontaal pad, het analytisch potentiaal zeer waarschijnlijk afwijkt van het werkelijke potentiaal.

De rekenregel van Sellmeijer is gevalideerd aan de hand van een vergelijking tussen de rekenregel en het numerieke model in D-Geo Flow op basis van het kritieke verval H_c. De rekenregel heeft geresulteerd in een lager kritiek verval dan het numerieke model, respectievelijk 2,45 m en 3,3 m. Het verschil kan worden verklaard aan de hand van een vergelijking van de model configuratie. De rekenregel is gebaseerd op een standaard dijk configuratie door middel van een fit parameter in de rekenregel. Wanneer de werkelijke geometrie verschilt van de standaard configuratie zal de rekenregel resulteren in een kritiek verval dat afwijkt van de realistische waarde. Om de rekenregel geschikt te maken voor een afwijkende dijk configuratie kan de fit factor opnieuw worden bepaald aan de hand van een numeriek model.

Op basis van een literatuurstudie en de resultaten van zowel de analytische als de numerieke analyse is geconcludeerd dat het falen van een dijk als gevolg van piping realistisch is in de Maasvallei. Dit geldt niet voor alle dijken in het gebied, maar voor een aantal kritieke locaties. Het onderzoek heeft aangetoond dat er in het verleden waterstanden zijn opgetreden waarbij piping een realistisch scenario is als deze waterstanden opnieuw zouden voorkomen. Tevens is aangetoond dat het aantal kritieke locaties zal toenemen als gevolg van de toenemende waterstand op de Maas.

Contents

1

Introduction

One of the failure mechanisms for water retaining structures is piping. Piping is an internal erosion mechanism creating hollow spaces (pipes) underneath, for example, a dike as a result of the transport of soil particles due to seepage. The formation of pipes can cause collapse of the structure once the erosion process reaches the outside of the dike. This study focusses specifically on the possibility of the occurrence of this failure mechanism in the Maasvallei area. The Maasvallei covers the area of the Maas roughly between the Dutch towns Roermond and Mook.

1.1. Motivation
The early signs of piping in the form of sand boils are frequently observed during periods of high water levels in the Dutch rivers. Although the total collapse of a dike in the Netherlands due to piping has not occurred in the past decades, the frequent observation of the early signs of the piping process has resulted in the inclusion of the piping failure mechanism in the Dutch legal safety assessment regulations for water retaining structures. During recent high-water periods in 2011 and 2012 sand boils were observed along several Dutch rivers except at the dikes along the Maas. The striking absence of sand boils in the Maasvallei area raised the question if the failure mechanism piping is relevant for this specific area.

In the recent assessment of the Dutch dikes, many of the dikes along the Maas in Limburg were found to be insufficiently safe against piping. The dilemma then becomes clear: the lack of early signs of piping contradicts the outcome of the safety assessment. Resources could be saved if the dikes do not need to be reinforced for piping, however, the safety should not be compromised.

1.2. Scope
In order for the water boards to make the right choices regarding the assessment of piping and reinforcement of the dikes in the Maasvallei, it is necessary to gain more insight into the piping likelihood for this specific area. This study has the objective of obtaining this knowledge. The main research question is as follows:

Is dike-failure due to piping realistic in the Maasvallei?

In support of the main research question, five sub-questions have been identified, all with respect to the Maasvallei:

1. *What are the processes leading to piping?*
2. *What is the sensitivity of model components (layering and soil characteristics) on the piping likelihood?*
3. *Which models are suitable for the evaluation of piping?*
4. *Does the assessment method match the actual situation in the Maasvallei?*
5. *What is the effect of a future increase of the water level on the likelihood to piping?*

1.3. Context

This study has been conducted in collaboration with Arcadis and is part of the already ongoing project POV Piping. The involvement of Arcadis in this project is focussed on research into the influence of clay and gravel layers [Koopmans and Janssen, 2016] and the influence of soil heterogeneity on the piping mechanism [Koopmans, 2016].

POV Piping

Currently, the Netherlands are engaged in the High Water Protection Program (HWBP), in Dutch 'Hoog-waterbeschermingsprogramma'. The aim of this program is to improve dikes that were rejected during the latest safety assessment. The HWBP includes, among others, several 'project transcending re-searches', in Dutch 'Project Overstijgende Verkenningen' or 'POV's'. The project POV Piping is one of these project transcending researches, which investigates piping related issues on a national level. POV Piping has two main goals: 1) the accurate identification of Dutch dikes that require reinforcement with respect to the failure mechanism piping, 2) the development of new accepted methods to solve piping related issues.

1.4. Outline

Figure 1.1 illustrates the outline of this report. The report is divided into three parts: literature, modelling and conclusion. Part I contains information about the piping mechanism (Chapter 2). Part II is the most comprehensive part. Chapter 3 introduces the cases that were studied as part of this research. Chapter 4 presents the analytical analysis and Chapter 5 the numerical work of this study. The report concludes with Part III where the discussion, conclusion and recommendations are discussed.
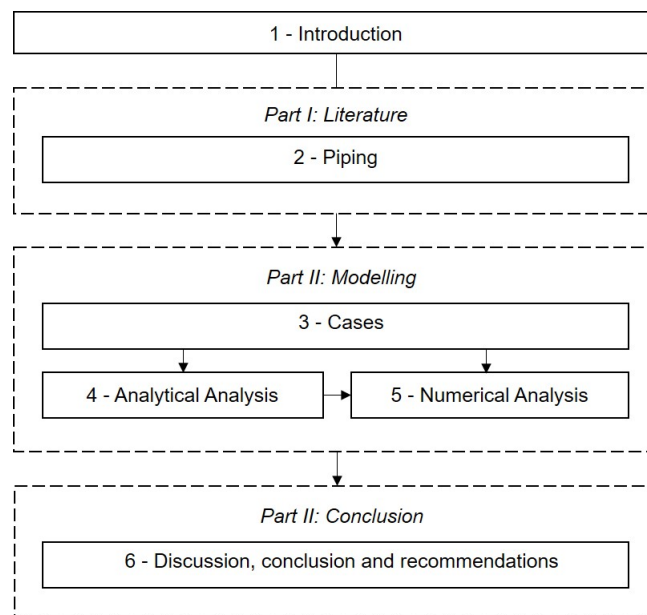

Figure 1.1: Research outline

I

Literature

2

Piping

Piping is an internal erosion mechanism creating hollow spaces (pipes) underneath the dike as a result of the transport of soil particles due to seepage. The formation of pipes can cause collapse of the structure once the erosion process reaches the upstream side of the dike. The total collapse of a dike as a result of a continuous pipe occurred, according to human observations, only three times in recent Dutch history. In 1880 the Heidijk in Nieuwkuijk failed due to piping as well as a dike of the Nieuw-Strijen polder in 1894 and a dike in Zalk in 1926 [Förster et al., 2012]. Although, these collapses are rare and have been a long time ago, the signs indicating the possible formation of pipes are observed regularly during high-water periods. For example, during the high-water periods in 1993 and 1995 the water reached a level of 0.50 to 1.50 meter below the design water levels. More than 300 sand boils were observed along the Rhine, Waal and IJssel. In addition, several cases are known where a critical situation was reached and the dikes did not fail merely due to timely measures [Förster et al., 2012].

(a) Uplift

(b) Seepage

(c) Heave

(d) Backward Erosion

(e) Continuous pipe

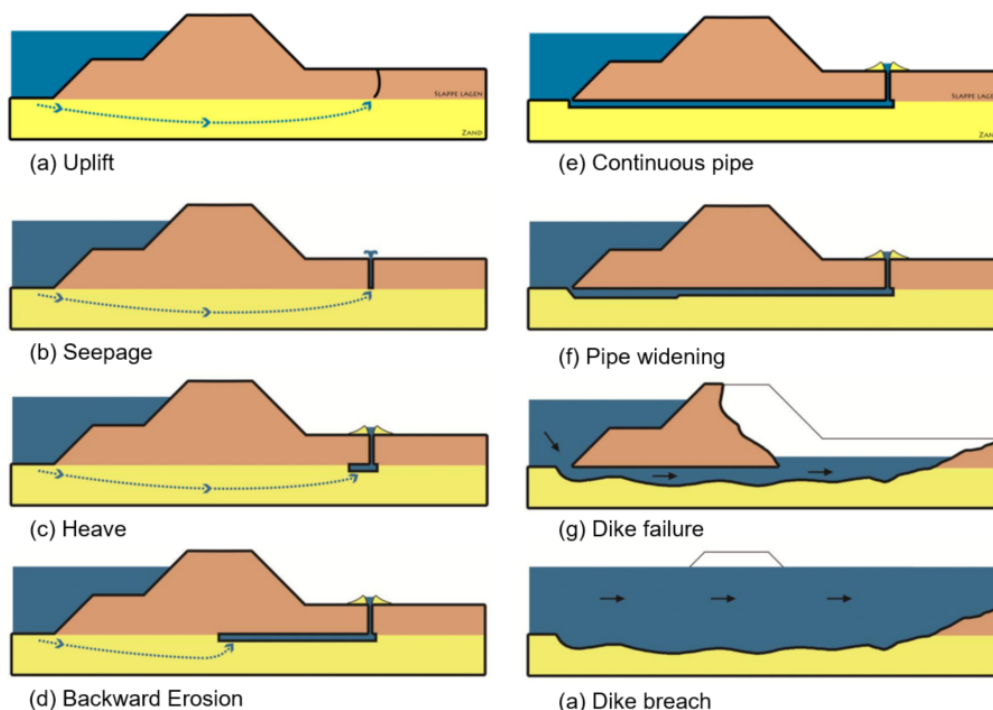(f) Pipe widening

(g) Dike failure

(a) Dike breach

Figure 2.1: The piping process in eight phases [de Bruijn, 2013, Förster et al., 2012, van Beek, 2015]

The piping process is a combination of multiple mechanisms. Figure 2.1 illustrates the piping process in eight phases. This study focusses on the first four phases distinguishing three main mechanisms: uplift, heave and backward erosion. When all three mechanisms occur we speak of piping and consider the dike failed. The driving force behind the piping mechanism is a difference between the river water level and the hydraulic head in the hinterland. The occurring pressure difference results in a horizontal groundwater flow through a permeable layer (aquifer) underneath the dike. The presence of an impermeable layer covering the permeable aquifer, the blanket layer, allows for a water pressure to develop. Once the water pressure exceeds the weight of the blanket layer, the layer is lifted. As a result ruptures occur, allowing for a concentrated vertical exit of the seepage flow. Soil is transported to the surface due to the outflow of water. Once a critical water level difference H_c is reached the erosion proceeds until a continuous pipe is formed.

In order for pipes to develop underneath a water retaining structure several conditions must be met. Primarily, the outside water level must be higher than the hydraulic head of the hinterland in order for a horizontal flow of water underneath the structure to occur. In addition, a permeable non-cohesive layer, aquifer, must be present. The susceptibility of this aquifer to erosion allows for the transport of soil. Third, an impermeable cover layer must be present to act as a roof for the pipe to prevent collapse. Piping is more likely to occur when this blanket layer is not only present underneath the dike but also in the hinterland. The presence of a blanket layer in the hinterland allows for the development of an overpressure. The overpressure results in higher local exit gradients and increases the probability of soil transport. However, piping can also occur when the blanket layer is absent in the hinterland. In that case, the exit point of the seepage flow is located at the inner toe and the pipe is solely formed underneath the dike.

Based on these conditions piping sensitive cross-sections can be identified (Figure 2.2). Figure 2.2a depicts a typical piping sensitive cross-section where all three boundary conditions are present. In this case, the location of the exit point is clear due to the presence of a ditch. In case of multiple aquifers covered by an impermeable layer, a pipe can occur at several depths as illustrated in Figure 2.2b. Despite the fact that the seepage length of the deeper aquifer is larger, piping can occur in the deeper sand layer in case the upper aquifer is not susceptible for backward erosion. This can be the case when the layer is too thin or the sand is relatively coarse. Foreland is often present in the case of river dikes as illustrated in Figure 2.2c. The presence of foreland can extend the seepage length. The extent to which, the foreland can be taken into account is determined by the presence and thickness of the blanket layer and possible existing ruptures or ditches. In addition, in practice the control area of the water board is taken into account when determining the likelihood to piping. Such legal directives are not taken into account in this research, since they do not influence the soil behaviour. A fourth scenario is the absence of a blanket layer in the hinterland as depicted in Figure 2.2d. In this case, uplift is irrelevant since the seepage flow can exit at any point. The exit point resulting in the shortest seepage length is situated at the inner to of the dike.

In the following three section the mechanisms uplift, heave and backward erosion are separately discussed. Additionally, the calculation methods related to these mechanisms are explained. The fourth and last section describes the calculation rules for the assessment of piping as applied in practice.
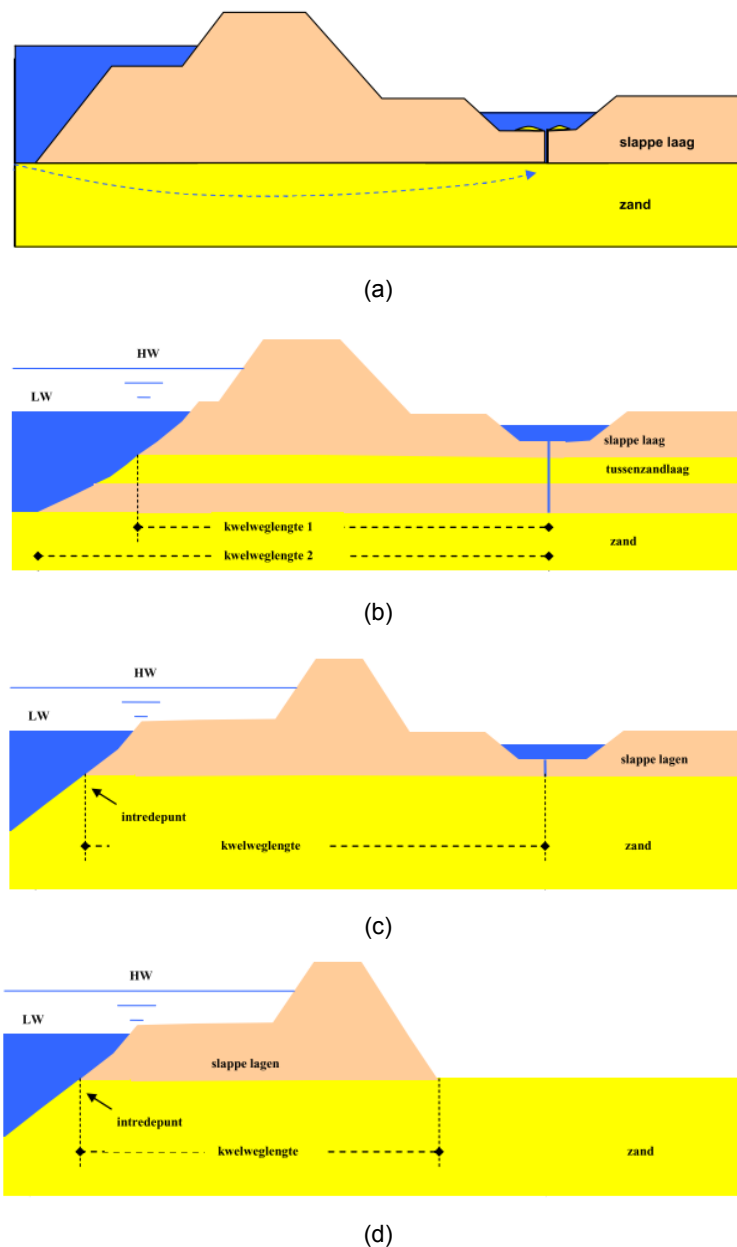
(a)

(b)

(c)

(d)

Figure 2.2: Piping sensitive cross-sections [Förster et al., 2012]

2.1. Uplift

As a result of a high river water level with respect to a lower hydraulic head in the hinterland a horizontal groundwater flow through the aquifer underneath the dike establishes. This results in an increase of the water pressure in the aquifer. The hydraulic head in the aquifer gradually develops from the outside water level to the low hydraulic head in the hinterland. This gradual development is caused by the flow resistance of the soil. The hydraulic head in the aquifer is higher than the hydraulic head in the hinterland resulting in an overpressure. In addition, the presence of a blanket layer prevents the outflow of water and escape of this pressure. The upward water pressure cannot exceed the weight of the blanket layer due to the vertical force balance. When the upward water pressure in the aquifer equals the weight of the blanket layer the blanket layer is lifted. At this point the effective stresses at the interface between the blanket layer and aquifer are zero. Consequently, the soil particles cannot withstand the water pressure and the groundwater is forced upward through the blanket layer. Ruptures occur resulting in the formation of a vertical channel allowing the free exit of water. The horizontal flow

of water underneath a structure and downstream vertical exit of this flow is called seepage. The exit location of the downstream upward water flow is called the exit point. The vertical channel acts as a kind of valve. As a result, the water pressure can suddenly escape resulting in an increase of the flow velocity and therefore the concentration of streamlines near the exit point. The potential locally decreases as a result of the pressure relief. The concentrated outflow of water is characterized by the appearance of water boils at the exit point as illustrated in Figure 2.3.

Figure 2.3: Water boil [de Bruijn, 2013]

Seepage can also occur when a natural open exit is present in the blanket layer. This can, for example, be due to previous ground investigations, roots of trees or a ditch. In this case the exit point can be situated further from the dike than is usually the case for an exit created as a result of ruptures in the blanket layer. In addition, it should be mentioned that seepage can also occur in the situation where no blanket layer is present. The upward water flow is in this case not concentrated at one exit point but spread. Figure 2.4 illustrates these different exit types.
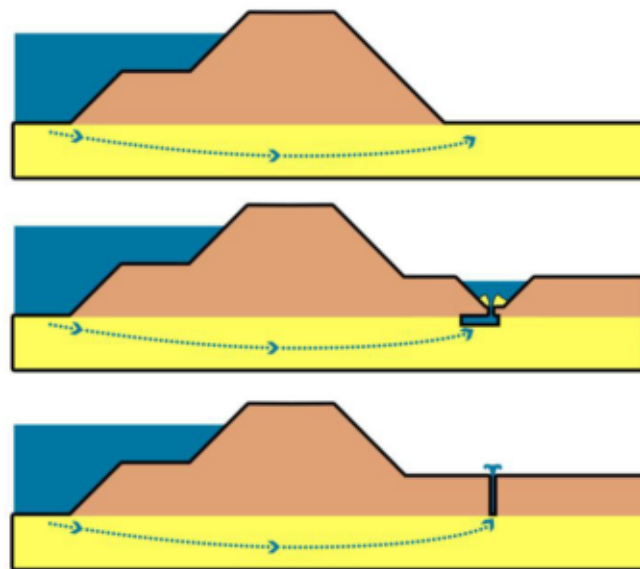

Figure 2.4: Three types of exits: plane, ditch, hole [van Beek, 2015]
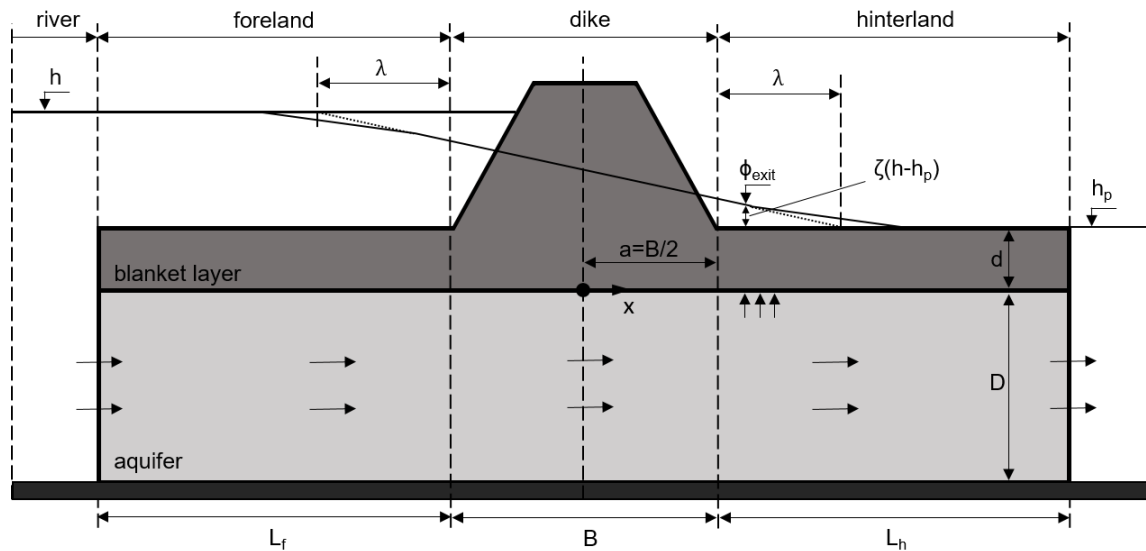
Groundwater flow model

Figure 2.5: Schematisation of analytical groundwater flow model (after [Jonkman and Schweckendiek, 2015, TAW, 2004])

The occurrence of uplift can be evaluated by means of an analytical groundwater flow model. The in Figure 2.5 presented model is based on the model used in engineering practice and presented in the Dutch guidelines [Förster et al., 2012, TAW, 1999]. The model is based on several assumptions. First, horizontal groundwater flow in the aquifer is assumed according to the law of Darcy. Second, flow through the blanket layer is assumed to be vertical. In addition, the hydraulic head at the entry point of the seepage flow is assumed to be equal to the river water level. Finally, the hydraulic head far in the hinterland is assumed to be equal to the ground level. The derivation of the formulas presented in this section is included in Appendix A. The hydraulic head at the exit point is the basis for the evaluation and referred to as the potential ϕ_{exit} [m]. The exit potential is defined as:

$$\phi_{exit} = h_p + \zeta(h - h_p) \tag{2.1}$$

where h [m] is the outside water level and h_p the phreatic level in the hinterland. The factor ζ [-] determines the extent to which damping of the outside hydraulic head occurs and thus the gradual development of the potential in the aquifer. The damping factor is derived from the flow resistance and is influenced by the geometry and thickness and permeability of the aquifer and blanket layer according to:

$$\zeta = \frac{\lambda}{L_f + B + \lambda} exp^{\frac{0.5B - x_{exit}}{\lambda}} \quad x_{exit} \geq B/2 \tag{2.2}$$

where x_{exit} [m] is the distance of the exit point from the center of the dike, B [m] is the width of the dike, L_f is the length of the foreshore and λ [m] is the leakage factor which includes the leakage through the blanket layer defined as:

$$\lambda = \sqrt{\frac{k_a D d}{k_b}} \tag{2.3}$$

where k_a and k_b [m/s] are the hydraulic conductivities of respectively the aquifer and the blanket layer and D [m] the thickness of the aquifer.

Equilibrium of the weight of the blanket layer and the upward water pressure is used to determine whether uplift will occur. Therefore, a critical potential $\phi_{c,u}$ [m] is determined to compare with the exit potential ϕ_{exit} [m]. Uplift will occur when the potential at the exit point exceeds the critical potential.

Equilibrium is reached when:

$$(\phi_{c,u} - h_a)\gamma_w = (h_g - h_a)\gamma_{sat} \tag{2.4}$$

where h_g [m] is the ground level, h_a [m] the height of the top of the aquifer, γ_{sat} [kN/m^3] the saturated volumetric weight of the blanket layer and γ_w [kN/m^3] the volumetric weight of water. Evaluation of this equilibrium results in a critical potential $\phi_{c,u}$ [m]:

$$\phi_{c,u} = h_p + d\frac{\gamma_{sat} - \gamma_w}{\gamma_w} \tag{2.5}$$

2.2. Heave

As a result of the high local flow velocity of the seepage flow sand particles are eroded and transported towards surface level. This results in the presence of fluidised sand within the exit channel. The effective stresses in the fluidised soil equal zero since the soil particles 'float' in the water. The channel is filled with a mixture of water and sand resulting in an increase of the flow resistance in the channel and thereby a decrease of the flow velocity. The erosion possibly ceases due to this increase of the flow resistance. This is the case when the flow velocity and thus the flow force is no longer sufficient to vertically transport the sand particles. In this case the water boil produces 'clean water'. In case the vertical exit gradient is large enough and reaches a critical value $i_{c,h}$ [-] this additional flow resistance will not be sufficient to stop the erosion process. The water boil will turn into a sand boil and sand is deposited outside the well. The formation of a crater ('sand volcano') can be observed as illustrated in Figure 2.7. The vertical exit gradient i [-] is dependent on the occurring potential and the thickness of the blanket layer according to:

$$i = \frac{\zeta(h - h_p)}{d} \tag{2.6}$$

Figure 2.6: Sand volcano [van Beek, 2015]

Different definitions of heave

It should be mentioned that the definition of heave and the role of heave within the piping process differs depending on the consulted source. [Förster et al., 2012],[TAW, 1999] and the former assessment guideline [MVW, 2007] define heave as the situation at which the vertical effective stresses in a sand layer equal zero as a result of vertical groundwater flow, also named fluidisation or quicksand. This situation is not considered as part of the piping process but as a separate mechanism relevant in case of vertical groundwater flow behind a structure such as a cut-off wall on the inside of a water retaining structure. In that case, the critical heave gradient is the vertical gradient at which fluidisation of the sand occurs. At the start of 2017, the new Dutch dike assessment guideline, WBI 2017, has been taken into use [RWS, 2017a,b]. This new guideline is introduced for the purpose of the fourth national dike assessment which is due in 2023. The approach towards the assessment of the likelihood to

piping has thereby changed. The guideline considers the piping process as the sequential occurrence of uplift, heave and backward erosion. The inclusion of the heave mechanism in the piping process is thereby new. Besides, heave is also still considered as a separate mechanism relevant for structures. The vertical critical gradient for heave as part of the piping process is the gradient at which the transport of sand becomes possible and a sand boil occurs. WBI 2017 applies two definitions for heave, simply stated as the fluidisation of sand and the vertical transport of sand. The latter is consistent with the definition applied in this study.

Critical heave gradient

In order to determine whether the heave mechanism occurs the vertical exit gradient i is compared to a critical vertical exit gradient $i_{c,h}$. Heave occurs when the exit gradient exceeds the critical vertical gradient. The theoretical critical vertical heave gradient equals the ratio between the buoyant weight of the soil and the volumetric weight of water [TAW, 1999]:

$$i_{c,h} = \frac{\gamma'}{\gamma_w} = \frac{(1-n)(\gamma_s - \gamma_w)}{\gamma_w} \tag{2.7}$$

where γ' [kN/m^3] is the buoyant weight of the sand particles, γ_s [kN/m^3] the volumetric weight of the soil particles and n [-] the porosity. Dependent on the porosity the critical gradient varies between 0.85 and 1.15 [TAW, 1999]. Once the critical gradient is reached the upward flow force equals the downward force as a results of the buoyant weight of the soil and the sand particles can be transported.

In the United States the engineering practice related to piping focusses entirely on the vertical critical gradient [USACE, 2000]. The safety against piping is assessed based on this vertical critical gradient. This in contrast to Dutch practice where a distinction is made between the vertical critical gradient for heave and the horizontal critical gradient for backward erosion. Both gradients are included in the assessment of the safety against piping. The theoretical vertical critical exit gradient presented in Formula 2.7 is also included in the US design guideline for dikes [USACE, 2000]. Halfway through the last century a large research into underseepage and its control has taken place in the United States. Based on the 1950 flood of the Mississippi River an empirical relation between the degree of seepage and the vertical exit gradient was established [Tyler et al., 1956], see Figure 2.7. The occurrence of sand boils indicates that the vertical critical gradient is exceeded and that piping can occur. It should be noted that the measurements related to the occurring sand boils at an exit gradient of 0.5 or lower are unreliable. An explanation for these observations is the possible reactivation of old sand boils [Tyler et al., 1956]. According to this empirical relation the critical gradient varies between 0.5 and 0.8.

The critical vertical gradients derived from the empirical relation are significantly lower than the theoretical range. Accordingly, in the United States engineering practice a more conservative value for the critical vertical gradient is applied with respect to the theoretical range. The United States design practice applies a standardized critical gradient of 0.5 [USACE, 2005]. Until recently, the Dutch engineering practice also applied a critical vertical heave gradient of 0.5. However, the definition of heave thereby deviates from the definition applied in this study as discussed in the previous section. The new Dutch guideline [RWS, 2017a,b] applies a critical vertical heave gradient of 0.5 related to heave defined as the fluidisation of sand behind a structure and a critical gradient of 0.3 for heave as part of the piping process. The latter is thereby relevant for this study.

The critical gradient of 0.3 is largely based on experiments performed by Sellmeijer (1981) to determine the head difference over the vertical channel [Koelewijn, 2008]. Within the experiments a column of sand was fluidized by a vertical flow of water in round tubes. Several experiments were conducted using smooth tubes, tubes with a sand-coating and with a clay-coating. Subsequently, the decrease of head across the tube was measured. A decrease of head results from the flow resistance in the tube. Energy dissipates as a result of this resistance causing the head to decrease. This is illustrated in Figure 2.8. The head decrease was found to correspond to 0.6 times the height of the tube. The experimental set-up is similar to a vertical exit channel. The vertical exit channel is also filled with a water-sand mixture as a result of the flow of water. The height of the channel corresponds to the thickness of the blanket layer d. The head decrease then equals 0.6d according to the experiments. In order for the fluidised sand to be transported to the surface the potential energy should exceed the

decrease of energy across the vertical channel. Thus the occurring vertical head difference over the exit channel (H_v) should be larger than the experimentally determined head decrease (0.6d):

$$H_v > 0.6d \tag{2.8}$$

The critical point is when the potential energy equals the decrease of energy. The occurring vertical head difference (ΔH_v) then equals the head decrease over the channel (0.6d). The critical vertical gradient follows from this relation:

$$H_v = 0.6d$$
$$i_{ch} = \frac{H_v}{d} = 0.6 \tag{2.9}$$

The decrease of the vertical head is equal to 0.6d when the channel is filled with fluidized sand. The current design guideline states that the flow velocity can be so large that the vertical exit channel is flushed resulting in a lower flow resistance and thus a smaller decrease of the head over the channel. Therefore, in practice a safety factor of two is applied resulting in a critical vertical heave gradient of 0.3. Considering the from the experiments resulting value of 0.6 and the empirical relation presented in Figure 2.7, it can be stated that a value of 0.3 is rather low and therefore conservative. In addition, questions arose during a study into the validation of this gradient [Koelewijn, 2008]. Although, the conclusion of this study states that the substantiation of the critical gradient is weak but that there are insufficient reasons to adapt the value, it is also suggested to use a more situation-based approach when determining the critical vertical heave gradient. Nevertheless, the current guideline [RWS, 2017a] applies a critical gradient of 0.3.
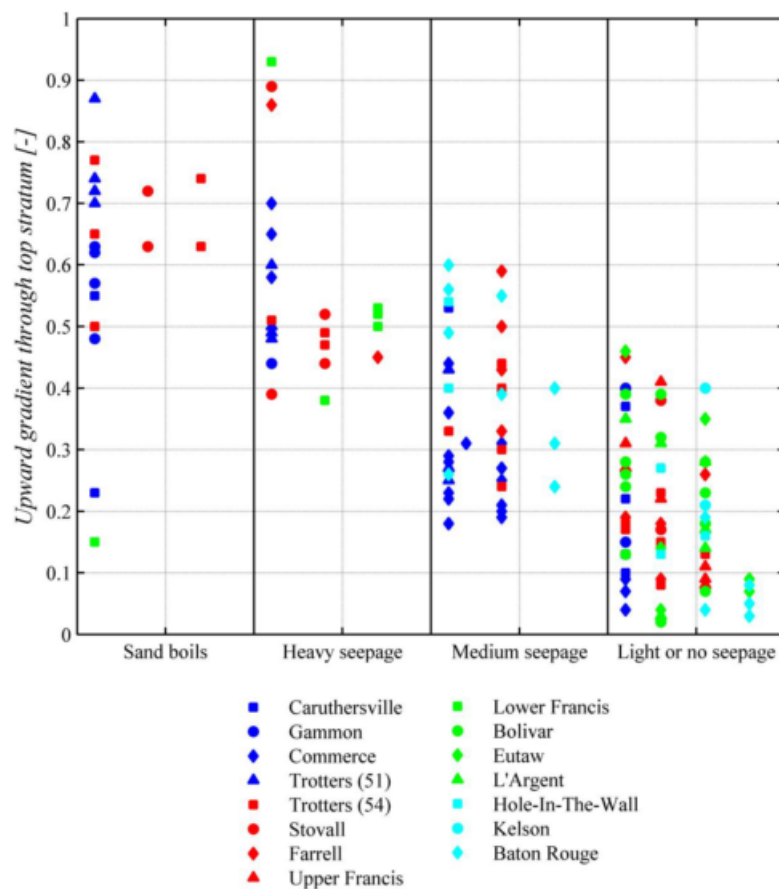
Figure 2.7: Empirical relation between the severity of seepage and the vertical exit gradient ([van Beek, 2015] modified after [Tyler et al., 1956]
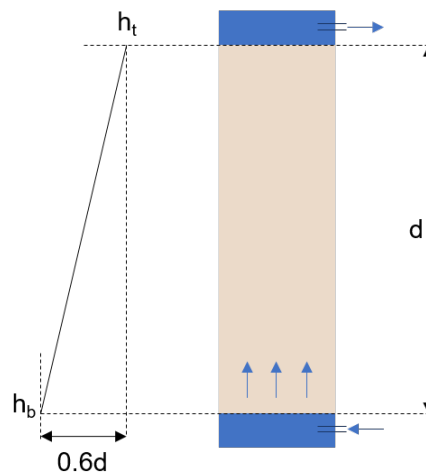
Figure 2.8: Head decrease over vertical channel

2.3. Backward erosion

Once the critical vertical heave gradient is exceeded sand is eroded. The sand particles are deposited outside the well and small horizontal pipes start to form. The formation of channels results in a local decrease of the water pressure. This can lead to equilibrium which stops the pipe formation (erosion). This phase is therefore designated as regressive backward erosion. Regressive backward erosion turns into progressive backward erosion once the hydraulic head difference further increases until a critical value is reached, the critical head difference H_c [m]. Once the critical head is reached pipe formation continues until the pipe reaches the upstream side. In this phase equilibrium is no longer possible. Theoretically, the critical vertical heave gradient is thus lower than the horizontal critical gradient. However, in practice this is not always the case. Sometimes the head required for initiation of the erosion process (heave) is higher than the critical head H_c. In that case, once the critical vertical exit gradient $i_{c,h}$ is reached the critical head H_c is also exceeded and equilibrium is not possible [van Beek, 2015, Van Beek et al., 2014].

Ultimately, the pipe formation reaches the upstream side of the dike. The water can easily flow underneath the dike and the flow accelerates. The flow force causes the diameter of the pipe to increase until the structure fails and collapses.

As mentioned the formation of horizontal channels can be observed by a local decrease of the water pressure [Förster et al., 2012, Parekh et al., 2016]. As a result of the erosion the flow resistance decreases significantly within the eroded zones. As a result the flow of water concentrates in the eroded channel causing an increase of the flow rate. At the front of the pipe (upstream side) the increased discharge flows through the still intact soil causing an increase of the flow velocity. This results in a higher head difference and thus a lower observed hydraulic head as illustrated in Figure 2.9.
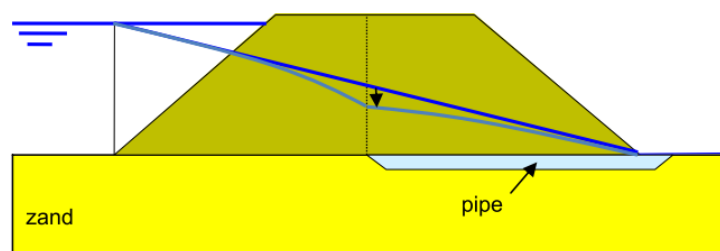

Figure 2.9: Local decrease of water pressure (light blue line) due to the formation of a horizontal pipe with respect to the initial water pressure (dark blue line) [Förster et al., 2012]

Parekh et al. (2016) show that a decrease of the water pressure over time is accompanied by the observation of sand traces and later sand boils. Growing sand boils indicate increasing erosion where progressive backward erosion can be observed by continuous sand production from the sand boils.

The erosion process in the pipe can be divided into primary erosion and secondary erosion [van Beek, 2015]. Primary erosion concerns erosion at the front of the pipe resulting in lengthening of the pipe. Secondary erosion concerns erosion of the walls of the pipe causing the pipe to deepen or widen.

Bligh and Lane
One of the early and commonly used piping prediction models is the empirical calculation rule of Bligh (1910). Bligh does not make a distinction between heave and backward erosion and assumes one critical head difference H_c [m] to evaluate piping. Due to the head difference between the river and the hinterland the groundwater percolates (creeps) through the subsoil. The travel distance of the water flow is called the creep length. The creep length is the distance between the entry and exit point and equals the seepage length L [m]. The critical head difference H_c is, according to Bligh, equal to the ratio between the seepage length L and a certain 'creep factor' C_{creep} [m] according to:

$$H_c = \frac{L}{C_{creep}}$$ (2.10)

Lane (1935) argues that the seepage length consists of vertical and horizontal parts and that the sum of both should be used in the calculation. A distinction is made between horizontal and vertical permeability. In addition, the creep factor of Bligh is replaced by a weighted creep factor including soil heterogeneity (Formula 2.11). Table 2.1 presents the creep factors according to Bligh and Lane as applied by TAW (1999). These factors are determined based on the particle gradation and include the effect of soil characteristics on the piping likelihood.

$$\Delta H_c = \frac{\left(\frac{1}{3}L_h + L_v\right)}{C_{w,creep}}$$ (2.11)

Table 2.1: Creep factors according to Bligh and Lane [TAW, 1999]

Soil type	d_{50} [μm]	C_{creep} (Bligh)	$C_{w,creep}$ (Lane)
extremely fine sand	<105		8.5
very fine sand	105 - 150	18	7
fine sand	150 - 210	15	7
coarse sand	210 - 300		6
very coarse sand	300 - 2000	12	5
fine gravel	2000 - 5600	9	4
coarse gravel	5600 - 16000		3.5
very coarse gravel	>16000	4	3

Sellmeijer
Sellmeijer (1988) developed a mathematical model for the evaluation of backward erosion. The model is based on a standard configuration as depicted in Figure 2.10. Sellmeijer's model does make a distinction between heave and backward erosion in contrast to other models such as the calculation rules of Bligh (1910) and Lane (1935). The principle of the Sellmeijer model is limit equilibrium of the sand particles at the bottom of the pipe. A critical head difference H_c [m] is determined for which this equilibrium is just ensured and the sand particles do not move. Therefore, Sellmeijer assumes that at a certain time after the occurrence of the pipe equilibrium is reached. This equilibrium can occur due to a decrease of the water pressure as a result of the formation of eroded channels as discussed in the previous section. The critical head difference is thereby dependent on the length of the pipe and occurs, for the standard configuration, when the length of the pipe equals half the seepage length (l/L = 0.5) [Sellmeijer and Koenders, 1991]. This is illustrated by Figure 2.11. The vertical axis displays the equilibrium head difference and the horizontal axis displays the ratio between the pipe length l and the seepage length L. The black parabolic line illustrates the critical head difference with increasing ratio

l/L. Above the line no equilibrium is possible and the pipe will continue to grow. If the head difference lies below the line the pipe will grow merely to a length corresponding to the present head difference and equilibrium will be reached. The maximum head is the critical head difference H_c. It can be seen that this maximum occurs at l/L = 0.5.
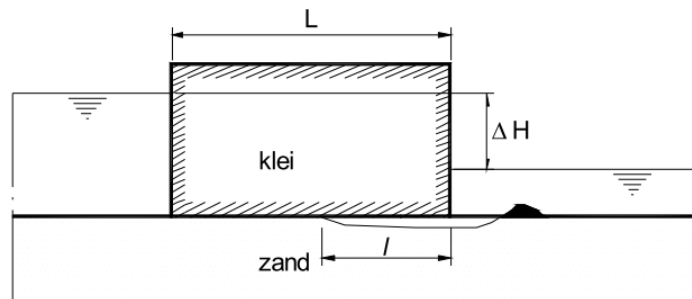

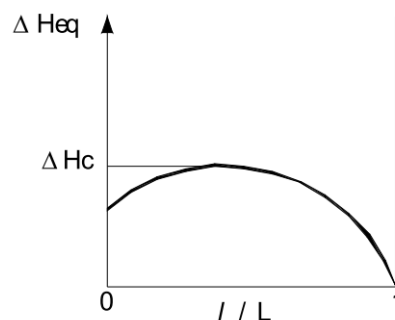Figure 2.10: Standard configuration for Sellmeijer model [Förster et al., 2012]

Figure 2.11: Critical head difference ΔH_c as a function of the ratio between pipe length l and seepage length L [Förster et al., 2012]

The Sellmeijer model includes three mechanisms: the groundwater flow through the aquifer, the flow through the pipe and the limit state equilibrium of the sand particles at the bottom of the pipe. The groundwater flow through the aquifer is regarded steady and two-dimensional and can be described by the Laplace flow equation. Sellmeijer uses the Cauchy integral formula and the theory of conformal mapping to establish the boundary conditions. The flow in the pipe as presented by Sellmeijer is depicted in Figure 2.12. The pipe flow is considered to be laminar. Sellmeijer evaluates the steady state laminar pipe flow by means of the Navier-Stokes equation obtaining a solution similar to the Poisseuille solution for pipe flow. Sellmeijer states that regarding backward erosion two pipe flow elements are particularly relevant: the continuity of flow and the shear stress (drag force) at the bottom of the pipe as a result of the pipe flow. The shear stress is influenced by the flow velocity. The limit equilibrium of the sand particles is considered based on four forces. In horizontal direction the horizontal drag force due to flow in the pipe, based on the theory of White (1940), and the horizontal seepage flow force. In vertical direction the weight of the sand particle and the vertical flow force. Limit equilibrium is associated with a critical shear strength [Sellmeijer, 1988].
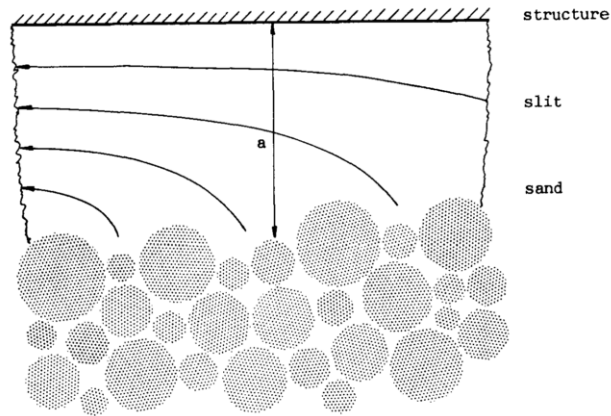
Figure 2.12: Pipe flow according to Sellmeijer (1988)

Based on the mathematical model of Sellmeijer (1988) an analytical calculation rule is derived [Sellmeijer and Koenders, 1991, Sellmeijer et al., 1989, Weijers and Sellmeijer, 1993] for a standard dike as depicted in Figure 2.13. The calculation rule is validated by means of large scale model tests [Silvis, 1991]:

$$\frac{H_c}{L} = F_R F_S F_G \qquad (2.12)$$

Where,

F_R is the resistance factor,
F_S is the scale factor,
F_G is the geometrical shape factor.
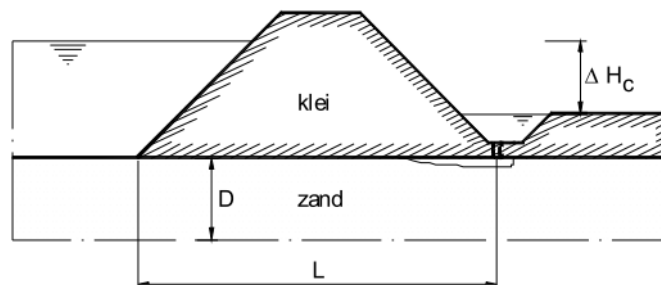
Figure 2.13: Standard dike for Sellmeijer calculation rule [Förster et al., 2012]

Based on a study by Sellmeijer (2006) the calculation rule is adapted with respect to the influence of the seepage flow forces. Once limit equilibrium is reached the smaller particles have eroded leaving the larger particles at the bottom of the pipe to stick out. The horizontal and vertical seepage flow force are only relevant when the soil particles are completely surrounded by other particles. Since, this is not the case the flow forces are considered irrelevant. Consequently, a two forces approach was selected where only the horizontal drag force and vertical weight of the sand particle are applied. This alteration was implemented in the calculation rule by means of an adjustment to the geometrical shape factor [Sellmeijer et al., 2011]. In addition, the past years many small-, medium- and large-scale experiments have been performed as part of an extensive research into the physical phenomena related to piping [van Beek et al., 2011]. The experiments showed that the theoretical influence of the sand characteristics on H_c does not correspond well with the Sellmeijer rule [Sellmeijer et al., 2011, van Beek, 2015]. A multivariate analysis on the small-scale experiments was performed. The analysis

resulted in the empirical adjustment of the calculation rule which was validated by means of the large-scale tests [Sellmeijer et al., 2011]:

$$\frac{H_c}{L} = F_R F_S F_G$$

$$F_R = \eta \left(\frac{\gamma_s}{\gamma_w} - 1 \right) \tan \theta \left(\frac{RD}{RD_m} \right)^{0.35} \left(\frac{U}{U_m} \right)^{0.13} \left(\frac{KAS}{KAS_m} \right)^{-0.02}$$

$$F_S = \frac{d_{70m}}{\sqrt[3]{\kappa L}} \left(\frac{d_{70}}{d_{70m}} \right)^{0.6}$$

$$F_G = 0.91 \left(\frac{D}{L} \right)^{\frac{0.28}{\left(\frac{D}{L} \right)^{2.8} - 1} + 0.04}$$

(2.13)

In which,

η	Whites constant	[-]
γ_s	Volumetric weight of sand grains	[kN/m^3]
γ_w	Volumetric weight of water	[kN/m^3]
θ	Bedding angle of sand	[degrees]
RD	Relative density	[-]
RD_m	Mean value relative density (72.5%)	[-]
U	Uniformity coefficient d_{60}/d_{10}	[-]
U_m	Mean value uniformity coefficient (1.81)	[-]
KAS	Measure for the angularity of grains ranging from 0 (very round) to 100 (very angular)	[-]
KAS_m	Mean value angularity (49.8%)	[-]
d_{70}	70%-fractile of the grain size distribution	[m]
d_{70m}	d_{70} reference value	[m]
κ	Intrinsic permeability ($k_a \, \nu/\gamma_w$)	[m^2]
ν	Kinematic viscosity of water at $10°C$ ($1.33 \cdot 10^{-6}$)	[Ns/m^2]
k_a	Hydraulic conductivity of aquifer	[m/s]
L	Seepage length	[m]
D	Thickness of aquifer	[m]

The resistance factor describes the limit equilibrium of the sand particles at the bottom of the pipe and includes the drag force according to the approach of White (1940). The drag force depends on the shear stress that is exerted on the grains by the flow of water. The term includes the drag force coefficient (Whites constant or coefficient of White) η [-] and the bedding angle of the sand particles θ [degrees]. The coefficient of White represents the ratio of the area of the grains over which the shear stress is divided to the total area. The bedding angle determines the degree of resistance of the sand particles against rolling. The values of the coefficient of White η [-] and the bedding angle of the sand particles θ [degrees] are standard values respectively 0.25 and 37 degrees. These values were established over time based on all experiments and researches discussed in this section. In addition, the relative density, uniformity coefficient and grain angularity are incorporated as a result of the multivariate analysis. However, the latter two have a negligible effect on the critical gradient but are included for completeness [van Beek, 2015]. Figure 2.14 illustrates the relation between the KAS-factor and grain angularity. The scale factor relates particles size and seepage size. For this the 70%-fractile of the grain size distribution d_{70} [m] is included. Smaller particles are more susceptible to erosion due to smaller weight while the larger particles have to resist the flow forces. The seepage length L [m] includes the seepage size. It should be mentioned that the scale factor is based on empirical relations concerning the particle diameter and that the effect of the particles size is currently not fully understood [Sellmeijer et al., 2011]. The geometrical shape function incorporates the influence of the shape of the geometry of the soil to the seepage flow. This influence is dependant on the ratio between the thickness and length of the sand layers. This factor is therefore dependant on the geometry. The factor

presented in Formula 2.11 is derived for a standard geometry with a constant sand layer thickness. The geometrical shape factor for a different geometry can be determined by means of the numerical program MSEEP [Sellmeijer et al., 2011].
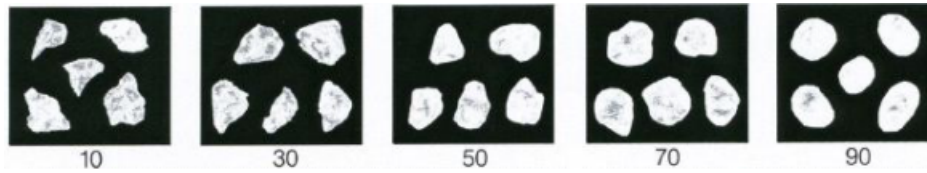

Figure 2.14: Grain angularity [van Beek et al., 2010]

The Sellmeijer calculation rule has a number of limitations with respect to practical use. The latest adaptations to the calculation rule are based purely on empirical relations. The rule may therefore be only applied within the parameters limits during testing [Sellmeijer et al., 2011]. These limits are shown in Table 2.2. Besides, the bedding angle is validated based on Delta Flume experiments [Silvis, 1991]. However, only one series of four experiments was performed. The calculation rule as presented in Formula 2.11 predicts the critical head well for fine sands. However, for coarse sand a difference of 25% percent was observed between the calculation rule outcome and the large-scale experiment [Sellmeijer et al., 2011, van Beek et al., 2011]. Additionally, it should be mentioned that only one large-scale experiment was performed with coarse sand [van Beek et al., 2011]. The Sellmeijer model assumes a homogeneous soil composition with a constant aquifer thickness. Naturally, this is not the case in practice. Van Beek (2015) did a lot of research into the Sellmeijer model and concludes that at present the Sellmeijer model is the most advanced model for predicting backward erosion. However, some limitations are mentioned. The Sellmeijer model only includes secondary erosion while the inclusion of primary erosion is essential. Besides, the Sellmeijer model assumes homogeneous conditions. Van Beek states that variations in grain size within the pipe can result in critical gradients that are almost twice as large as critical gradients observed in homogeneous soil compositions. In addition, the Sellmeijer calaculation rule is unsafe for 3D situations where the groundwater flow converges to one point. However, Van Beek states that in practice the effect of 3D flow may be less pronounced, since it is expected that in practice multiple parallel pipes will form [van Beek, 2015].

Table 2.2: Parameter limits [Sellmeijer et al., 2011]

Parameter	Minimum	Maximum	Mean
RD	50%	100%	72.5%
U	1.3	2.6	1.81
KAS	35%	70%	49.8%
d70	150 μm	430 μm	208 μm

0.3d rule

The hydraulic head difference H relevant for evaluating backward erosion is the horizontal head difference between the outside water level and the bottom of the vertical exit channel, since this is the point where the horizontal groundwater flow exits the aquifer. The head at the bottom of the exit channel is unknown. However, the head at surface level, the top of the vertical channel, is known. This head equals the hinterland water level h_p. The head difference over the vertical channel is established based on experiments [Sellmeijer, 1981] as explained in section 2.2. Since, the head at the top of the vertical channel and the head difference over the channel are known the head at the bottom of the vertical channel can be determined. The head difference at this point then equals the total hydraulic head difference over the dike (h - h_p) minus the hydraulic head difference over the vertical channel.

The experiments [Sellmeijer, 1981] discussed in section 2.2 showed that the head over the channel decreases with a factor of 0.6 times the height of the channel d as a result of the loss of energy caused by the flow resistance due to the presence of fluidised sand. In practice a safety factor of two is applied resulting in the so called 0.3d-rule [TAW, 1999]:

$$(H - 0.3d) \leq H_c \tag{2.14}$$

Since, this rule is only based on several experiments the substantiation and validation of the rule is limited. Therefore, the rule was analysed in 2009 to determine whether the use of the rule is just [Koelewijn, 2008]. Koelewijn (2008) concluded that the substantiation was weak but that there were insufficient reasons to adapt the 0.3d rule.

2.4. Assessment practice

The previous sections explained the different mechanisms of the piping process and the analytical calculation rules that apply to these mechanisms. In practice these calculation rules are not directly applied in the assessment of the dikes. A legally adopted guideline exists to provide directives for the assessment. Two main differences between theory and the assessment guideline can be identified. The first difference between the assessment practice and the calculation rules is the application of safety factors. The second difference is the use of design values for the parameters. The assessment guidelines do not use best estimate values for the parameters but slightly more conservative design values in order to incorporate extra safety. Over the years new insights and knowledge have resulted in changing guidelines. Two guidelines are of relevance in this report: the old guideline 'Voorschrift Toetsen op Veiligheid Primaire Waterkeringen (VTV2006)' [MVW, 2007] from 2006 and the new guideline 'Wettelijk Beoordelingsinstrumentarium (WBI2017)' [RWS, 2017b], introduced in 2017. The following paragraphs present the assessment rules including safety factors for both guidelines.

Former guideline
The former guideline 'Voorschrift Toetsen op Veiligheid Primaire Waterkeringen' [MVW, 2007] is based on the Technical Report on Sand Boils [TAW, 1999]. It should be noted that the guideline considers piping, including uplift and backward erosion, and heave as two separate failure mechanisms where this report designates the sequential occurrence of uplift, heave and backward erosion as one failure mechanism named piping, as discussed in section 2.2. Piping is therefore evaluated by means of an assessment of the occurrence of uplift and backward erosion.

Uplift is evaluated according to the Technical Report on Sand Boils [TAW, 1999]. A factor of safety γ is used:

$$(\phi_{exit} - h_p) \leq \frac{1}{\gamma}(\phi_{c,u} - h_p) \tag{2.15}$$

The value of the applied safety factor γ varies between 1 and 1.2 dependent on the method used to determine the occurring exit potential ϕ_{exit}. If the exit potential is determined based on the theoretical groundwater flow model as presented in this chapter the safety factor is 1.2. A lower safety factor is used when the potential is determined based on field measurements or a conservative assessment level [MVW, 2007]. Backward erosion is evaluated based on the required seepage length according to the rule of Bligh in combination with the 0.3d rule. No safety factor is used.

$$(H - 0.3d) \leq H_c = \frac{L}{C_{creep}} \tag{2.16}$$

Current guideline
The current guideline considers piping as the sequential occurrence of uplift, heave and backward erosion. Accordingly, each mechanism is assessed. Uplift and heave are assessed according to the groundwater flow model as presented in section 2.1 and backward erosion is assessed according to the calculation rule of Sellmeijer. Several safety factors are used.

The assessment criterion for uplift is:

$$(\phi_{exit} - h_p) \leq \frac{1}{\gamma_{up}\gamma_{b,u}}(\phi_{c,u} - h_p) \tag{2.17}$$

The assessment criterion for heave is:

$$i \leq \frac{1}{\gamma_{he}\gamma_{b,h}}i_{c,h} \tag{2.18}$$

The assessment criterion for backward erosion is:

$$H - 0.3d \leq \frac{1}{\gamma_{pip}\gamma_{b,p}}H_c \tag{2.19}$$

Where,

γ_{up}	Safety factor for uplift mechanism	[-]
γ_{he}	Safety factor for heave mechanism	[-]
γ_{pip}	Safety factor for backward erosion mechanism	[-]
γ_b	Schematisation factor	[-]

The safety factors for the mechanisms are based on a reliability requirement and established by means of a probabilistic method. For each dike section in the Netherlands these factors are listed in the guideline [RWS, 2017a]. The schematisation factor covers the uncertainty that results from the schematisation of the soil and determination of the parameters. The schematisation factors can be determined based on the method described in 'Technisch Rapport Grondmechanism Schematiseren'[ENW, 2012]. The schematisation factor varies between 1 and 1.3.

As mentioned is section 2.2 the critical vertical heave gradient i_{ch} is 0.3 according to the current guideline. According to the experiments of Sellmeijer (1981) the critical gradient equals 0.6. A safety factor of two has been applied to obtain a critical gradient of 0.3.

II
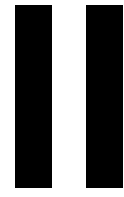
Modelling

<div style="text-align: right; font-size: 4em;">3</div>

<div style="text-align: right; font-size: 2em;">Cases</div>

This chapter introduces the cases that have been evaluated in the modelling phase. Section 3.1 introduces the research area, including information about the research locations, historic observations and the most recent safety assessment. Section 3.2 presents the schematisation of the research locations.

3.1. Research area

The area of interest for this study was the Maasvallei. The Maas is one of the large rivers in the Netherlands and has a total length of 950 kilometers. The river originates in France and runs via Belgium to the Netherlands. The Dutch part of the Maas can be divided into two parts: the part marking the border with Belgium and the Northern part which is completely situated on Dutch territory. The research area starts at the point where the Maas deviates from the Belgium border and ends near the town Mook. Roughly, the Maasvallei covers the area between Roermond and Mook as indicated by the dark blue line in Figure 3.1.
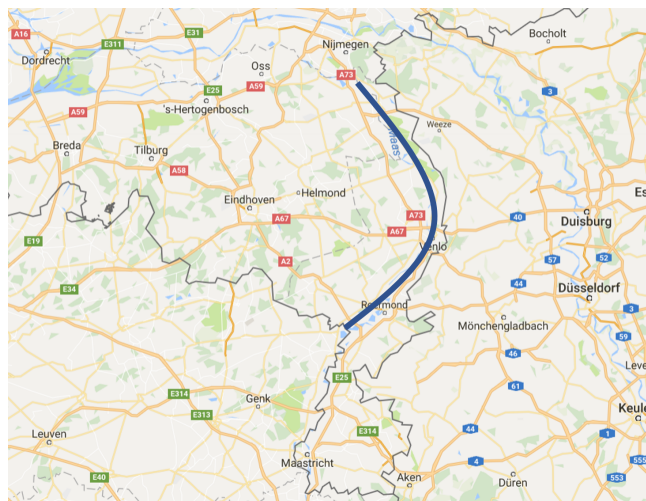
Figure 3.1: Location Maasvallei [Google, 2017]

As the name of the area suggests the part of the Maas considered in this study is situated in a valley. The surface level of the hinterland increases with increasing distance to the river. The Maasvallei dikes are thus situated on a inclined surface. As a result, a constant seepage flow towards the river is present, resulting in a lower hydraulic gradient compared to a situation with a horizontal surface level. The subsoil in the Maasvallei typically consists of a three-layered structure. First, a relatively permeable clay blanket layer followed by sand and then gravel. The permeability of the blanket layer varies within the range of 0.1 to 1 m/d, which can be considered as very high for a cover layer [Koopmans and Janssen, 2016]. The sand in the Maasvallei can be characterized as coarse with an average d_{70} of

about 250 μm. The sand layer varies greatly in thickness within the area. At some locations the sand layer is a few meters thick while at other locations the sand layer is absent. Typically, the sand layer is followed by gravel. The variability within the gravel package is very large. Often there are several layers with different permeabilities. In addition, the pores in the gravel layers can be (locally) filled with sand reducing the permeability. As a result, local zones with highly deviating permeability are present in the gravel package. The typical subsoil with a relatively permeable blanket layer, coarse sand and presence of gravel characterises the Maasvallei.

Research locations

As part of the project POV Piping four research locations were identified [Koopmans and Janssen, 2016]. The four research locations were selected based on the occurrence of the, for this area, typical three-layer soil structure as previously described. In addition, practical considerations were taken into account. In order, to select the most suitable locations for the POV piping project, available drilling's, CPT's and the control register of the water board were used. The four research locations situated near the villages Well, Beesel, Buggenum and Thorn respectively, as illustrated in Figure 3.2. At the four research locations several drilling's and CPT's were performed as part of the POV Piping project. In addition, a monitoring network was installed with piezometers and pressure sensors. Figure 3.3 indicates the exact location of the dikes. The dikes near Buggenum and Thorn are not situated directly at the river but at a side channel and small lake. The dike near Well is located further landward resulting in a large foreland.
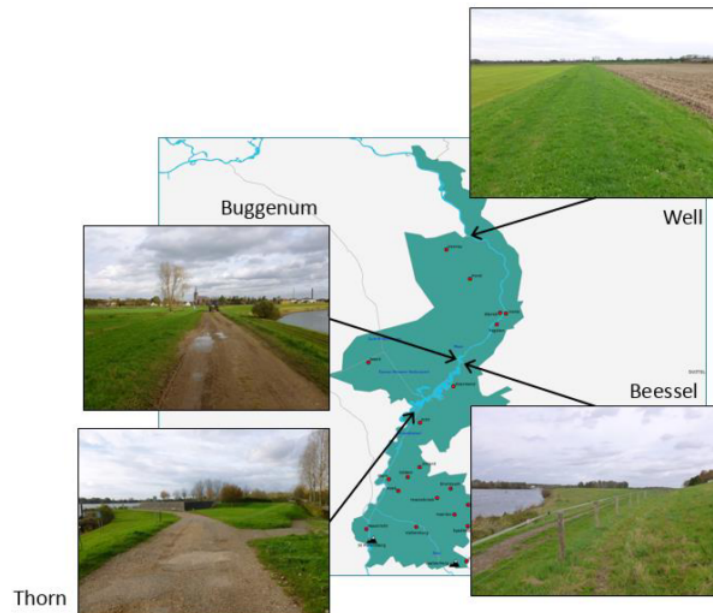
Figure 3.2: Research locations in the Maasvallei, Limburg [Koopmans and Janssen, 2016]

Figure 3.3: Location of the dike for the four research locations: a) Well b) Beesel c) Buggenum d) Thorn [Google, 2017]

Historic observations

In 1993 and 1995 extreme high water levels occurred. During those periods the primary dikes along the Maas did not yet exist. As a result of the high water levels the area flooded. After 1995, dikes were constructed to protect the area. In 2011 and 2012, again high water levels were recorded. However, there are no documented piping related observations (such as water boils or sand boils) from that period. There are two possible explanations for this absence of piping related signs. The first possibility is that the uplift and heave mechanism did not take place during the high-water periods of 2011 and 2012. A second possibility is that uplift and heave did take place but that the signs were not observed. On the one hand, this is possible due to poor inspection. The dikes along the Maas contain many manually operable retaining structures. Therefore, during high-water periods the water board is occupied with closing these structures. Limited resources are then available for inspection of the dikes. On the other hand, it is possible that the signs were difficult to observe as a result of a wet hinterland. During a high-water period the hinterland surface water level is typically high as well, causing a wet surface.

Latest Assessment

Dutch law requires the primary dikes to be assessed every twelve years. The most recent assessment was completed in 2011. The dikes along the Maas were constructed after the extreme high-water periods in 1993 and 1995 and are therefore relatively new. Originally, these dikes were not included in the legislation for water retaining structures as primary dikes. However, the dike rings in Limburg were adopted into this legislation in 2005. Therefore, the assessment of the dikes in Limburg took place for the first time, while for most other primary dikes the third assessment took place. Part of the dike section in the Maasvallei failed the piping assessment. The assessment was performed based on the former guideline 'Voorschrift Toetsen op Veiligheid Primaire Waterkeringen' [MVW, 2007] as described in section 2.4.

3.2. Schematisation

As part of the POV Piping project a lot of data was collected concerning the four selected research locations. At each location sixteen drillings were performed divided in two transects. Eight of these drillings were mechanical drillings with a depth of about six meters. The other eight were drillings by hand with a considerable smaller depth. The transects are equipped with a measurement system measuring the water levels since the end of 2014. The boreholes are located at strategic points in the foreland, at the outer toe of the dike, the inner toe of the dike and in the hinterland respectively points A, B, D and E as illustrated in Figure 3.4. The surface level at the measurement points is known. In addition, laboratory tests were performed on part of the soil samples from the boreholes. At the locations Well, Buggenum and Thorn pumping tests, additional drillings and several CPT's were conducted. Appendix B includes maps of the research locations indicating the fieldwork.
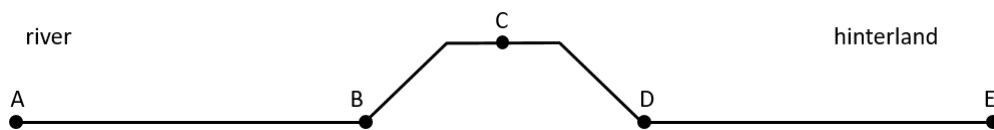
Figure 3.4: Characteristic points dike geometry

In addition to the information obtained from the POV Piping project additional sources have been used to schematize the dike cross-sections. 'Actueel Hoogtebestand Nederland' [RWS (Rijkswaterstaat)], a digital surface level map of the Netherlands, and Google Earth [Google] were used to determine the geometry of the cross-sections. 'Dinoloket' [TNO] was used to determine the composition of the deeper layers and to complement inadequacy of the POV Piping data. Dinoloket is an online database with information and data regarding the Dutch subsoil. All information and data was considered and combined resulting in a cross-section for each location. The choices and assumptions leading to the schematisation are discussed in Appendix C. All choices and assumptions were made considering the likelihood to piping. The aim was to create a realistic cross-section with the highest possible likelihood to piping. The schematisations are illustrated in Figures 3.5 to 3.8 and are also included in Appendix C.
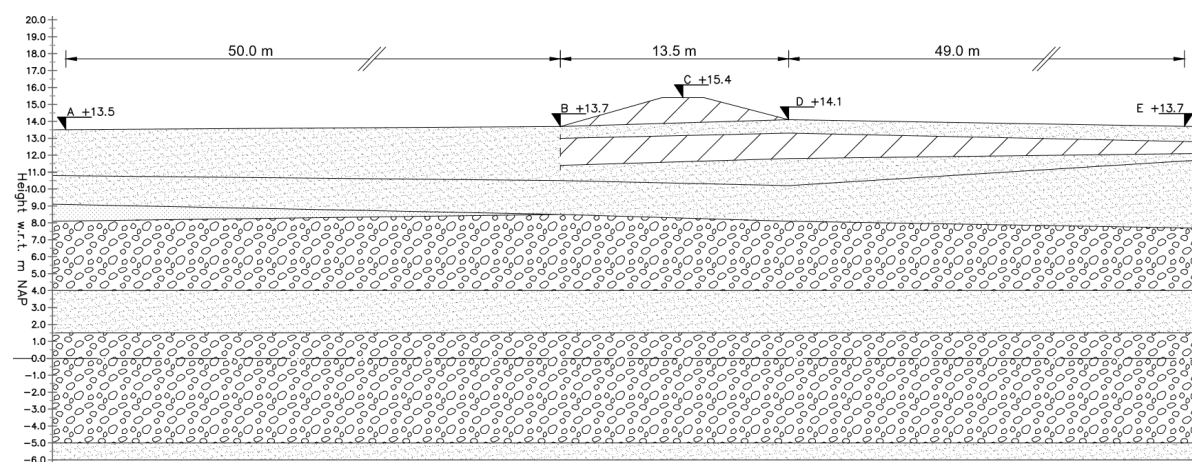
Figure 3.5: Schematisation Well
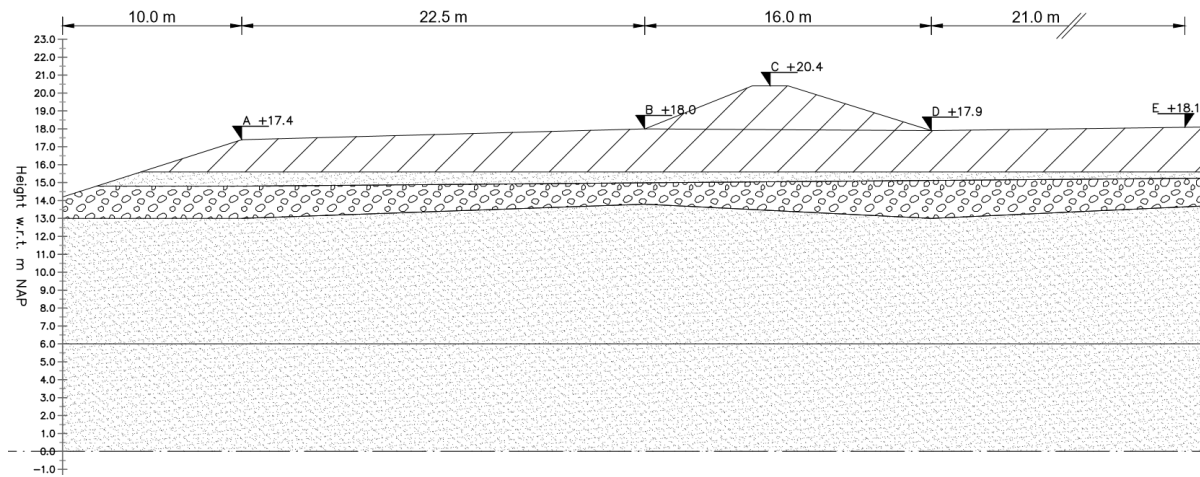
Figure 3.6: Schematisation Beesel
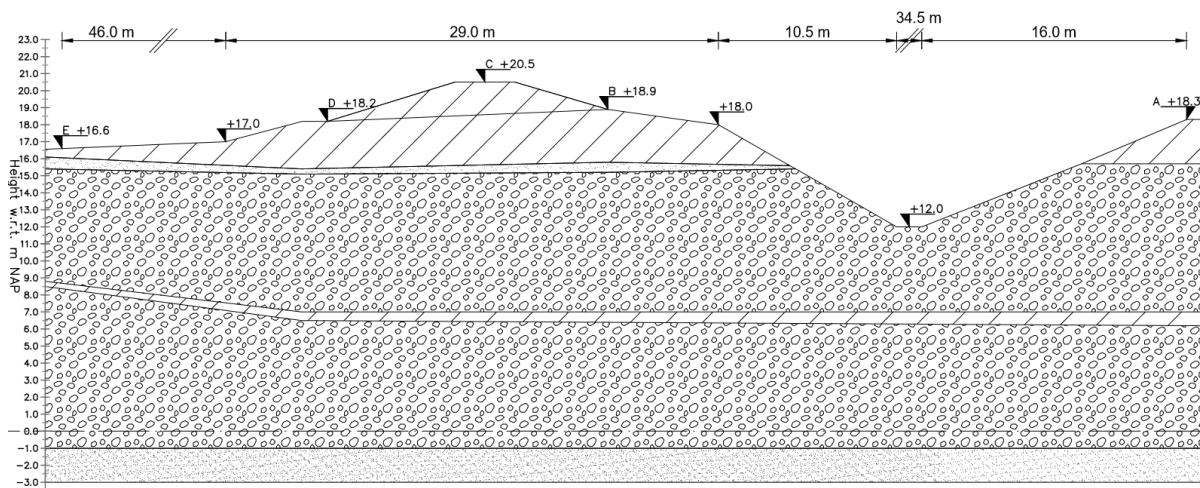
Figure 3.7: Schematisation Buggenum

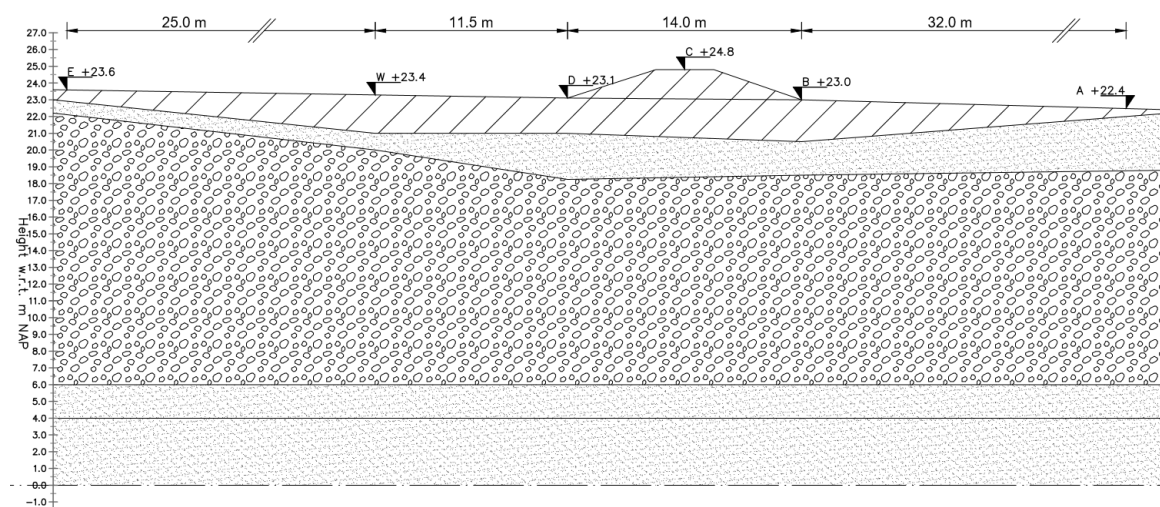

Figure 3.8: Schematisation Thorn

<div style="text-align: right; font-size: 3em;">4</div>

Analytical Analysis

In Chapter 3 the cases that have been studied in this thesis were introduced. The cases were used in two calculation phases: an analytical analysis and a numerical analysis. The first calculation phase and the topic of this chapter concerned the analytical calculations. In the first section of this chapter, section 4.1, the motivation for performing the analytical calculations is discussed. Section 4.2 explains the performed calculations. Section 4.3 describes the results of these calculations. The chapter is concluded with a critical review of the analytical calculation method in section 4.4.

4.1. Motivation

In the introduction the Maasvallei dilemma was introduced. On the one hand, several dikes in the Maasvallei were rejected in the latest assessment based on the piping criterion. On the other hand, there are no piping related observations known that confirm the past occurrence of piping in the Maasvallei. The main question of this research follows from this contradiction: Is dike-failure due to piping realistic in the Maasvallei? In order to answer that question, it is essential to understand what happened during the latest high water periods and what might happen during future high water periods. In addition, the dilemma raises the question whether the assessment method is to strict, resulting in the unnecessary rejection of dikes. Furthermore, it is relevant to understand what the effect is of the typical Maasvallei subsoil characteristics on the piping likelihood. Following these questions, three objectives regarding the analytical analysis have been determined:

A1 Hindcast of past high water events and forecast of future high water event
A2 Determining the influence of safety factors, according to the former and current assessment guideline, on calculation results
A3 Determining the parameter sensitivity

4.2. Analysis

The analytical calculations were all performed based on the analytical groundwater flow model and the calculation rule of Sellmeijer as presented in Chapter 2. In order to approximate the actual situation in the Maasvallei, realistic best estimate parameter values were used. Besides, for the first and third objective no safety factors were used. For the second objective safety factors were included, because the influence of those factors is determined. The best estimate parameter sets for each location are included in Appendix D, together with an explanation of the selection of the parameter values. The following three paragraphs explain the performed calculations for each objective.

Objective A1: Past, present and future
In order for uplift, heave or backward erosion to occur, a critical limit must be exceeded as discussed in Chapter 2. These critical limits correspond to an overall head difference for each mechanism, the critical head differences H_{crit}. These critical head differences at which uplift, heave and backward erosion occur, according to the analytical model, were determined for each research location. By means

<div style="text-align: center;">29</div>

of these critical head differences, three water level scenarios were evaluated:

- **Past**: Based on the water levels of December 1993. These Maas water levels are one of the highest recorded water levels in history.
- **Present**: Based on the high water levels of 2011. The results of this scenario could be compared with the historic observations as described in section 3.1.
- **Future**: Based on a water level prediction for the year 2075.

With respect to these scenarios it was aimed to approximate the true behaviour of the Maasvallei dikes with respect to piping. Therefore, the choice was made to select the critical vertical gradient based on the US empirical relation, as presented in section 2.2, since it reflects a great number of actual sand boil observations and does not include any safety factors. According to this empirical relation sand boils can occur for vertical gradients between 0.5 and 0.8. In order to include the complete range of vertical critical gradients, both 0.5 and 0.8 were selected to evaluate the heave mechanism.

Objective A2: Influence of safety factors
For the second objective the critical head differences were again determined, this time including safety factors according to the former and current assessment guideline as presented in section 2.4. Subsequently, the water level scenario of 1993 was re-evaluated. This analysis is similar to the 'past' scenario from the first objective, but in addition includes safety factors. By comparing the scenarios with and without safety factors, the influence of safety factors on the calculation results could be assessed. It should be noted that no safety assessment has been done, but that only the influence of safety factors has been determined. In a full safety assessment, design values should be included as well, instead of best estimate parameter values. The former guideline used Bligh to evaluate backward erosion and the current guideline uses Sellmeijer to evaluate backward erosion. For the use of Bligh a creep factor C_{creep} of 15 [-] was selected according to Table 2.1 based on the grain size of the sand. In addition, a set of safety factors was determined as presented in Table 4.1. The safety factor belonging to the former guideline γ is 1.2 as explained in section 2.3. The safety factors for the different mechanisms γ_{up}, γ_{he} and γ_{pip} come directly from the current guideline [RWS, 2017a] where the factors are listed for each dike section in the Netherlands. The schematisation factor γ_b was estimated to be 1.15. The process of determining the schematisation factors according to the 'Technisch Rapport Grondmechanisch Schematiseren [ENW, 2012] is complex. For simplicity the middle value from the range of 1 to 1.3 was selected.

Table 4.1: Used safety factors in Part B of analytical analysis [ENW, 2012, RWS, 2017a]

	Well	Beesel	Buggenum	Thorn
γ	1.2	1.2	1.2	1.2
γ_{up}	1.37	1.16	1.16	1.42
γ_{he}	1.06	0.89	0.89	1.1
γ_{pip}	1.47	1.29	1.29	1.52
$\gamma_{b,u}$	1.15	1.15	1.15	1.15
$\gamma_{b,h}$	1.15	1.15	1.15	1.15
$\gamma_{b,p}$	1.15	1.15	1.15	1.15

Objective A3: Parameter sensitivity
In order to determine the effect of the variability of the parameters a sensitivity analysis was performed. Each parameter was individually varied. The parameters that were varied are:

d thickness of the blanket layer
D thickness of the aquifer
k_b hydraulic conductivity of the blanket layer
k_a hydraulic conductivity of the aquifer
L seepage length
d_{70} the 70%-fractile of the grain size distribution

For each parameter a variation coefficient V was determined. The parameters were assumed to be normally distributed with mean value μ and standard deviation σ (=$V \cdot \mu$). The mean value is the value from the initial parameter set. The parameters were varied within a range of $\mu + 2\sigma$ and $\mu - 2\sigma$ covering in total 95% of the parameter distribution. The variation coefficients are included in Tables D.1 to D.4. For uplift the potential at the exit point ϕ_{exit} was considered to determine the influence of the different parameters. For heave the vertical exit gradient i and for backward erosion the critical head difference according to Sellmeijer H_c.

4.3. Results

In this section the results from the analytical analysis are presented. First, the results of the first objective are presented, followed by the results of the second and third objective.

4.3.1. Objective A1: Past, present and future

The results of the calculations are summarized in Figure 4.1 and Table 4.2. The figure presents graphs with on the horizontal axis the river water level h [m] and on the vertical axes the potential difference at the exit point $\Delta\phi$ [m] and the vertical gradient i [-]. The occurring exit potential difference $\Delta\phi_{exit}$ and vertical exit gradient i are depicted by respectively the blue and orange solid lines. The critical potential difference $\Delta\phi_{c,u}$ and critical vertical heave gradients (0.5 and 0.8) $i_{c,h}$ are depicted by respectively the blue and orange dashed horizontal lines. The initial river water level h_{hw} is depicted by the vertical red line. The intersections of the red line with the orange and blue lines mark the outcomes for the initial parameter set. The vertical green line depicts the critical water level h_c according to the calculation rule of Sellmeijer. This value is determined by adding the critical head difference according to Sellmeijer H_c to the hinterland ground level h_p. The critical head difference H_{crit} for uplift and heave can be deduced from the figures by looking at the intersection between respectively the blue and orange solid and dashed lines. The intersections mark the critical water levels for uplift and heave. By subtracting the hinterland ground level h_p from the resulting water level the critical head difference H_{crit} can then be determined.

An example: Figure 4.1a (Well). The blue solid and dashed line cross at a river water level h of 16 m. The hinterland ground level h_p for Well is 14 m (see Table D.1). Thus the critical head difference for uplift then equals 16-14 = 2 m.

For backward erosion the critical head difference follows directly from the calculation rule of Sellmeijer as explained in Chapter 2. The critical head differences for each mechanism are included in Table 4.2. This table is used to evaluate the three water level scenarios.

(a) Location Well

(b) Location Beesel

(c) Location Buggenum

(d) Location Thorn
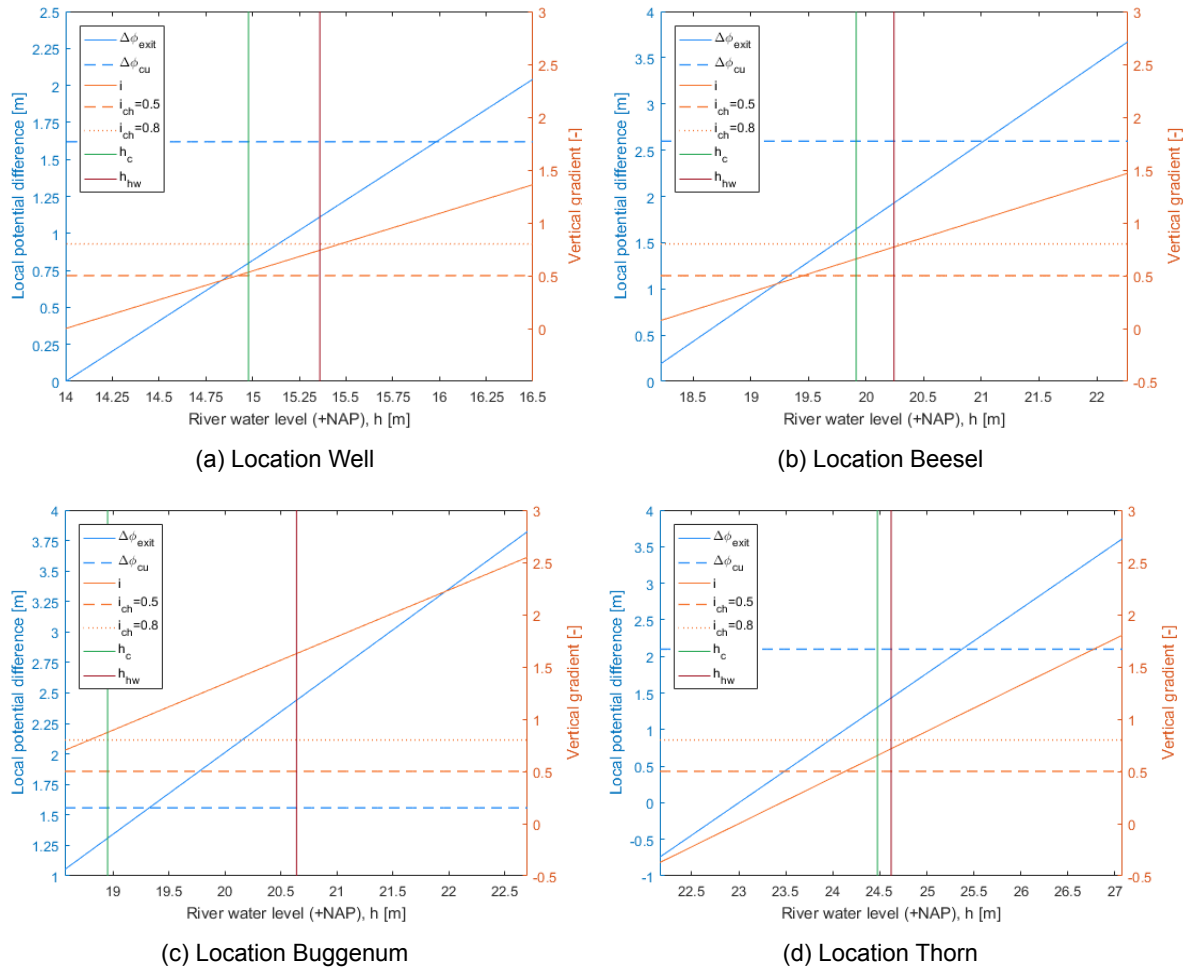
Figure 4.1: River water level h versus the potential difference and vertical heave gradient

Table 4.2: Critical head difference H_{crit} [m] per mechanism for the four research locations (actual situation without safety factors)

	Uplift	Heave (i_{ch}=0.5)	Heave (i_{ch}=0.8)	Backward erosion
Well	2	0.85	1.45	0.95
Beesel	3	1.45	2.35	1.9
Buggenum	2.3	1.1	1.8	2.1
Thorn	2.4	1.2	1.8	1.5

The following paragraphs present and discuss the results of the three water levels scenarios.

Past scenario

Table 4.3 displays the occurred head difference H [m] for each location based on the water levels from 1993 and shows whether the critical head differences for each mechanism H_{crit} [m] are exceeded by means of colours. The colour indication follows from a comparison with the values in Table 4.2. Green and red mean 'critical head not exceeded' and 'critical head exceeded' respectively. Orange indicates that the head difference differs from the critical head difference by 0.1 or less. In addition, the head differences after applying the 0.3d/0.6d rule for backward erosion are included in Table 4.3.

Table 4.3: Head difference H [m] as a result of the water levels from 1993 for each research location (Exceedance of critical head difference H_{crit} [m] (Table 4.2) is indicated by means of colours: green and red mean 'critical head not exceeded' and 'critical head exceeded' respectively. Orange indicates that the head difference H [m] differs from the critical head difference H_{crit} [m] by 0.1 m or less.)

	Uplift	Heave (i_{ch}=0.5)	Heave (i_{ch}=0.8)	Backward erosion	Backward erosion 0.3d	Backward erosion 0.6d
Well	0.8	0.8	0.8	0.8	0.35	-0.1
Beesel	2.08	2.08	2.08	2.08	1.33	0.58
Buggenum	3.53	3.53	3.53	3.53	3.08	2.63
Thorn	0.75	0.75	0.75	0.75	0.15	-0.45

Piping can only occur if the critical limits for uplift as well as heave and backward erosion are exceeded, since piping is a sequential process. Therefore, according to the calculations, only Buggenum can be considered a 'critical location' since all cells in the table are red, indicating that all critical limits are exceeded by at least 0.1 m.

Present scenario
Table 4.4 displays the occurred head difference for each location based on the water levels from 2011 and shows whether the critical values are exceeded.

Table 4.4: Head difference H [m] as a result of the water levels from 2011 for each research location (Exceedance of critical head difference H_{crit} [m] (Table 4.2) is indicated by means of colours: green and red mean 'critical head not exceeded' and 'critical head exceeded' respectively. Orange indicates that the head difference H [m] differs from the critical head difference H_{crit} [m] by 0.1 m or less.)

	Uplift	Heave (i_{ch}=0.5)	Heave (i_{ch}=0.8)	Backward erosion	Backward erosion 0.3d	Backward erosion 0.6d
Well	0.83	0.83	0.83	0.83	0.38	-0.07
Beesel	1.36	1.36	1.36	1.36	0.61	-0.14
Buggenum	2.47	2.47	2.47	2.47	2.02	1.57
Thorn	1.98	1.98	1.98	1.98	1.38	0.78

In 2011 there were dikes present in the Maasvallei. The results of this scenario are therefore comparable to actual observations. However, as discussed in section 3.1, there are no piping related observations of that period known. Yet, when we look at the table, one would expect such observations at Buggenum and possibly Thorn, since for the most part the critical limits are exceeded

Future scenario
Table 4.5 presents the head difference resulting from a prediction of the water level for 2075 and shows whether the critical values would be exceeded.

Table 4.5: Head difference H [m] as a result of the water level prediction for 2075 for each research location (Exceedance of critical head difference H_{crit} [m] (Table 4.2) is indicated by means of colours: green and red mean 'critical head not exceeded' and 'critical head exceeded' respectively. Orange indicates that the head difference H [m] differs from the critical head difference H_{crit} [m] by 0.1 m or less.)

	Uplift	Heave (i_{ch}=0.5)	Heave (i_{ch}=0.8)	Backward erosion	Backward erosion 0.3d	Backward erosion 0.6d
Well	1.63	1.63	1.63	1.63	1.18	0.73
Beesel	3.19	3.19	3.19	3.19	2.44	1.69
Buggenum	4.54	4.54	4.54	4.54	4.09	3.64
Thorn	1.38	1.38	1.38	1.38	0.78	0.18

A comparison of Table 4.5 to Table 4.3 and 4.4 shows an increase of red colouring for the future water level scenario. In addition to Buggenum, Beesel can be considered a critical location as well according to these locations. An increase of the water level causes the exceedance of more critical limits and thus an increase of the number of critical calculations.

4.3.2. Objective A2: Influence of safety factors

The calculations presented in Figure 4.1 were again performed, this time including safety factors according to the former and current guideline. Subsequently, Table 4.2 has been recreated, resulting in Table 4.6 for the former guideline and 4.8 for the current guideline. Heave was not considered in the calculations based on the former guideline since the guideline does not include heave in the assessment of piping. Table 4.7 and 4.9 display the occurred head difference for each location based on the water levels of 1993 and show for each mechanism whether the critical head differences (including safety factors) are exceeded.

Table 4.6: Critical head difference H_{crit} [m] per mechanism for the four research locations (according to former guideline including safety factors)

[m]	Uplift	Backward erosion
Well	1.65	0.9
Beesel	2.53	2.97
Buggenum	1.93	1.93
Thorn	1.98	2

Table 4.7: Head difference H [m] as a result of the water levels of 1993 for each research location (Exceedance of critical head difference H_{crit} [m] (according to former guideline, Table 4.6) is indicated by means of colours: green and red mean 'critical head not exceeded' and 'critical head exceeded' respectively. Orange indicates that the head difference H [m] differs from the critical head difference H_{crit} [m] by 0.1 m or less.)

	Uplift	Backward erosion 0.3d
Well	0.8	0.35
Beesel	2.08	1.33
Buggenum	3.53	3.08
Thorn	0.75	0.15

Table 4.8: Critical head difference H_{crit} [m] per mechanism for the four research locations (according to current guideline including safety factors)

	Uplift	Heave	Backward erosion
Well	1.27	0.45	0.56
Beesel	2.27	0.83	1.29
Buggenum	1.75	0.67	1.32
Thorn	1.43	0.55	0.84

Table 4.9: Head difference H [m] as a result of the water levels of 1993 for each research location (Exceedance of critical head difference H_{crit} [m] (current guideline, Table 4.8) is indicated by means of colours: green and red mean 'critical head not exceeded' and 'critical head exceeded' respectively. Orange indicates that the head difference H [m] differs from the critical head difference H_{crit} [m] by 0.1 m or less.)

	Uplift	Heave (i_{ch} =0.3)	Backward erosion 0.3d
Well	0.8	0.8	0.35
Beesel	2.08	2.08	1.33
Buggenum	3.53	3.53	3.08
Thorn	0.75	0.75	0.15

By comparing Table 4.2 with Table 4.8 and 4.6 it can be seen that the safety factors have a significant influence on the critical head differences. However, by comparing Table 4.7 and 4.9 to Table 4.3, it can be seen that for uplift and backward erosion the inclusion of safety factors does not have an effect on the colouring. Despite the differences in the critical limits, there is no difference in whether or not these

are exceeded. On the other hand, for heave there is a big difference in the colouring between Table 4.9 and Table 4.3. This is not surprising since a lower critical heave gradient of 0.3 was used.

4.3.3. Objective A3: Parameter sensitivity

The results of the sensitivity analysis are displayed in Figure 4.2 which presents tornado plots that give insight into the parameter sensitivity for the different mechanisms for the research location near Buggenum. The tornado plots for the research locations near Well, Beesel and Thorn (Figures D.5, D.6 and D.7) are included in Appendix D, because they are similar to Figure 4.2 and show the same results with respect to the parameter sensitivity. For uplift and heave two plots were constructed, one including the outside water level h and one without, in order to give a better insight into the sensitivity of the other parameters.

Figure 4.2 shows that the outside water level has by far the greatest influence on the piping likelihood. For uplift, the difference between the influence of the other parameters is small. Furthermore, it stands out that the influence of the hydraulic conductivity of the aquifer k_a, the aquifer thickness D and the blanket layer thickness d are equal for the uplift mechanism. The same holds for the hydraulic conductivity of the aquifer k_a and the aquifer thickness D regarding heave. This can be explained by the used calculation rules and the variation coefficient V, which is equal for the three parameters. For uplift, the parameters k_a, D and d are incorporated in Formula 2.3 in equal way. Variation within equal ranges therefore leads to equal influence on the result. For heave, both Formula 2.3 and 2.5 are of importance. Out of the three parameters k_a, D and d, only d is also incorporated in Formula 2.5. Therefore, the influence of d varies with respect to the influence of k_a and D. The result is that the thickness of the blanket layer d has the greatest influence on heave (with the exception of h). Regarding backward erosion the seepage length has the greatest influence.

It can be stated that the most influential parameters are the water level h, the seepage length L and the blanket layer thickness d. The seepage length and blanket layer thickness are parameters that are related to the geometry, where the water level is a boundary condition. In practice this boundary condition is predetermined based on a normative assessment water level. In addition, a distinction can be made between the blanket layer thickness and the seepage length based on the uncertainty of these parameters. The seepage length can be determined with reasonable certainty for a dike cross section. On the other hand, the thickness of the blanket layer can not be determined with certainty for every point in the hinterland. The uncertainty for d is therefore greater than for L. Differences between the real situation and a model are therefore more likely to occur for the blanket layer thickness than for the seepage length. Thus, the blanket layer thickness is not only of importance because of its high sensitivity but also because of the great uncertainty. This makes the blanket layer thickness a crucial parameter.

In addition, Figure 4.2 clearly shows that decreasing the parameters has a greater influence than increasing the parameters. Depending on the parameter, this effect is positive or negative with respect to the likelihood to piping. This is the case for all three mechanisms. This can be explained by means of Figure 4.3, which shows a decreasing gradient i with increasing blanket layer thickness d. The gradient of this line decreases with increasing layer thickness. The influence of a parameter decreases towards the critical value. When this critical value is reached, increasing the parameter value further hardly contributes to the resistance against the three mechanisms. Graphs similar to Figure 4.3 were created for all parameters and all four locations. These graphs are included in Appendix D.

(a)

(b)

(c)

(d)

(e)
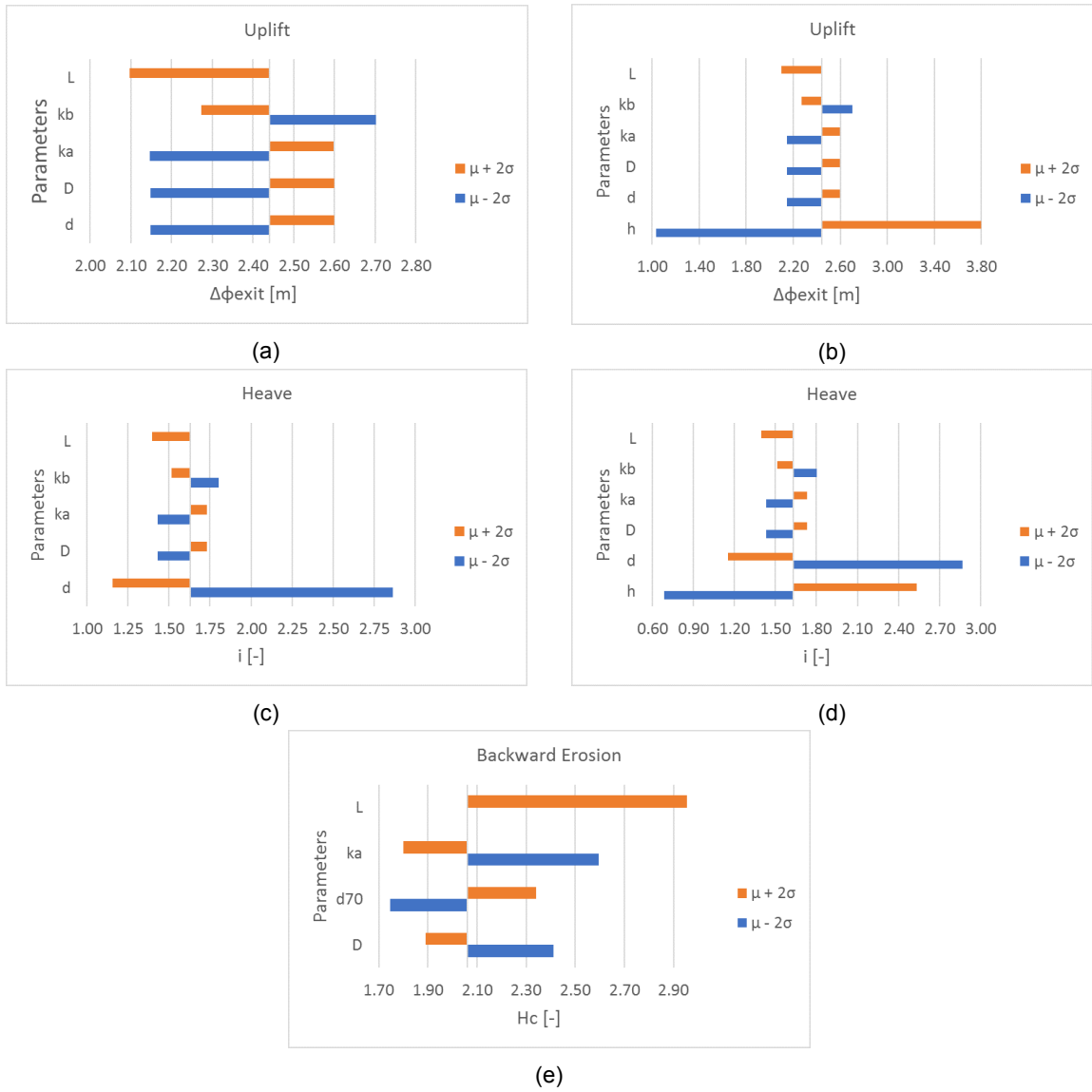
Figure 4.2: Parameter sensitivity per mechanism for the research location near Buggenum
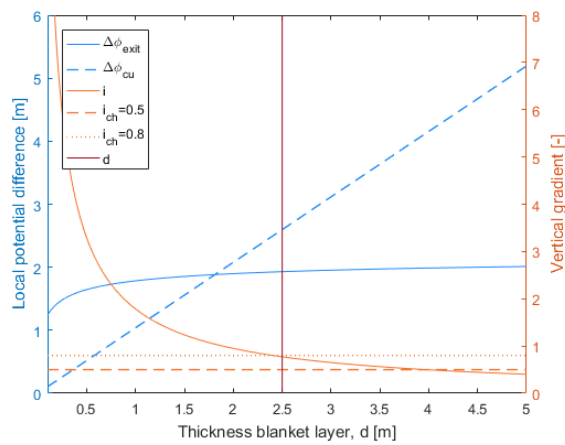
Figure 4.3: Blanket layer thickness d versus the potential difference and vertical heave gradient for the location near Beesel. Reproduction of Figure D.2a with a larger range of d

4.4. Review of analytical model

Figure 2.6 presented the schematisation of a dike that serves as a basis for the analytical groundwater flow model used within this analytical analysis to evaluate uplift and heave. This schematisation largely corresponds to the in Figure 2.13 presented standard dike for the Sellmeijer calculation rule. Both assume a two-layer system with a top layer and an aquifer. These layers are assumed perfectly horizontal with constant thickness, homogeneous properties and without irregularities. As a result, the groundwater flow is assumed to be perfectly horizontal in the aquifer and vertical in the blanket layer. Additionally, Sellmeijer assumes a completely impermeable blanket layer and thus no leakage. However, in reality, the subsoil consists of multiple layers that do not have a constant thickness and are in some cases non-continuous. In addition, the layers are very heterogeneous and contain multiple irregularities.

For the analytical analysis, one aquifer was selected that actually consists of multiple sand and gravel layers. Therefore, a weighted average of the permeabilities of the sand and gravel layers was calculated to reach one single permeability for the aquifer. The aquifer was assumed to be homogeneous. However, in reality this aquifer is a combination of multiple layers each individually influencing the groundwater flow. In addition, the model does not include time dependency. In reality, a high water level must have a certain duration to allow for the development of a continuous pipe. Besides, the analytical model is based on a 2D situation. Possible convergence of the groundwater flow is therefore not considered.

In conclusion, a number of deficiencies regarding the analytical model could be identified. These relate to the assumptions underlying the model where the actual situation differs. The model incorrectly assumes:

- the presence of only two layers (aquifer and blanket layer),
- continuous layers,
- layers with constant thickness,
- homogeneous layers,
- a 2D situation,
- a time-independent situation,
- perfect horizontal groundwater flow in the aquifer,
- perfect vertical leakage through the blanket layer (groundwater flow model),
- an impermeable blanket layer and thus no leakage (Sellmeijer only).

In addition, Table 2.2 presented that the use of the Sellmeijer calculation rule is bound to certain parameter ranges. The parameters that have been used in the analytical analysis lie within this range and, according to [Sellmeijer et al., 2011], the Sellmeijer calculation rule could therefore be used. However, as discussed in section 2.3, the Sellmeijer calculation rule does not perfectly predict the critical gradients for coarse sand. The sand found in the Maasvallei is relatively coarse. In addition, Sellmeijer does not include the full erosion process. Only primary erosion is included in the calculation rule.

In response to the presented deficiencies of the analytical model, the following questions regarding the applicability of the model could be asked:

- To what extent does the groundwater flow model correctly predicts the exit potentials in the Maasvallei?
- To what extent is the Sellmeijer calculation rule applicable for the Maasvallei?

These questions have been addressed in the second calculation phase, the numerical analysis as presented in the next chapter, Chapter 5.

<div align="right">

5

</div>

Numerical Analysis

The previous chapter explained the first calculation phase of this study, the analytical analysis. After the analytical analysis a numerical analysis has been performed. This chapter explains the numerical analysis and presents its results. The first section, section 5.1, explains the motivation and objectives of the numerical analysis. Section 5.2 describes the modelling process and resulting numerical model. Section 5.3 discusses the performed calculations and section 5.4 presents the results. The chapter is concluded with section 5.5, which gives a critical review of the numerical model.

5.1. Motivation
The previous chapter was concluded with two questions related to the validity of the analytical model:

- To what extent does the analytical groundwater flow model correctly predicts the exit potential?
- To what extent is the Sellmeijer calculation rule applicable for the Maasvallei?

These questions arose from the many assumptions underlying the analytical model. Most of these assumptions are not required for a numerical model. Because, a numerical model allows for the construction of complex geometries, there is no limitation to the number of layers, the location of the layers or the thickness. Consequently, an unlimited amount of layers can be constructed with varying thickness and irregularities such as a local absence of the layer. The previously used analytical model only allowed one single water level without a specified time horizon. However, with a numerical model it is possible to simulate a high-water period with a certain time duration. Therefore, time dependent groundwater flow can be modelled instead of solely a stationary situation. In both an analytical as a numerical model, the layers are assumed homogeneous. However, in fact, ground layers are never fully homogeneous. In a numerical analysis, this can partly be overcome by simulating multiple smaller layers. Nonetheless, these smaller layers are still homogeneous.

The above results in a model with a great level of detail. Because eof that, it can be said that a numerical model is reasonably truthful. A numerical model therefore offers the possibility to evaluate and validate the analytical model.

The evaluation of the analytical model by means of a numerical model corresponds to sub-question 3 presented in the introduction of this report: Which models are suitable for the evaluation of piping? In addition, after the literature review and analytical analysis, sub-question 2 was not fully answered: What is the sensitivity of model components on the piping likelihood? Based on these remaining research question, two objectives for the numerical analysis have been identified:

N1 Determining the effect of model components (layering and soil characteristics) on the likelihood to piping
N2 Validation of the analytical groundwater flow model and the Sellmeijer calculation rule

5.2. Modelling

For the numerical analysis, one model was used, applied in two numerical finite element programs, PlaxFlow and D-Geo Flow. The model has been set-up and calibrated by means of PlaxFlow and was subsequently adopted in D-Geo Flow. Both PlaxFlow and D-Geo Flow can be used to model groundwater flow. D-Geo Flow is a new program released during this research. In addition to PlaxFlow, D-Geo Flow contains an erosion module. Therefore it is possible to model both groundwater flow and backward erosion.

The selected research location for the model was Buggenum. From the analytical calculations presented in Chapter 4, it followed that Buggenum is a critical location with respect to piping. In addition, a lot of measurements, field and lab tests were available for this location. Therefore, this location was selected. Besides the model of Buggenum, it has been attempted to create a numerical model of the other three research locations. These modelling attempts provide insight into the complexity of the creation of a realistic numerical model. A description and evaluation of these modelling attempts is therefore included in Appendix E.

The numerical analysis aimed to provide insight into the actual behaviour of the Maasvallei dikes with respect to piping. To achieve this, safety factors were disregarded. Accordingly, best estimate parameter values and a water level scenario representing actual behaviour were used. The used water levels correspond to the level of winter 1993.

This section first briefly discusses the theory behind PlaxFlow and D-Geo Flow. Subsequently, the development and resulting numerical model is described.

5.2.1. PlaxFlow and D-Geo Flow

PlaxFlow and D-Geo Flow are numerical finite element software applications. This section explains the relevant theory behind the models.

PlaxFlow

PlaxFlow is the groundwater flow module of the finite element software Plaxis. The groundwater flow is described by Darcy's law. The numerical model used in this thesis consists of two dimensions, x and y. Darcy's law for two dimensions is given by the following two equations [Plaxis, 2016]

$$q_x = \frac{k_x}{\rho_w g} \frac{\partial p}{\partial x} \tag{5.1}$$

$$q_y = \frac{k_y}{\rho_w g} \left(\frac{\partial p}{\partial y} - \rho_w g \right) \tag{5.2}$$

In which,

q	specific discharge	[m/s]
k	hydraulic conductivity	[m/s]
ρ_w	density of water	[kg/m^3]
g	gravitational acceleration	[m/s^2]
p	pore pressure	[N/m^2]

D-Geo Flow

D-Geo Flow, like Plaxis, is a numerical finite element program. D-Geo Flow is a groundwater flow program that, in addition, contains a module that allows the erosion of a pipe to be modelled based on the theory of Sellmeijer. D-Geo Flow was released halfway 2017. De version used in this study is therefore a first version. This study was one of the first projects in which D-Geo Flow was used. Therefore, some caution is desirable when interpreting the results. The model of Sellmeijer is based on three components: the groundwater flow through the subsoil, the pipe flow and equilibrium in the pipe. The first mechanism is incorporated by means of Darcy's law as is the case for PlaxFlow [Deltares, 2017, van Esch et al., 2012].

The pipe flow is modelled by means of the law of conservation of mass and the Poiseuille flow theory assuming a horizontal pipe. The Poiseuille theory describes flow in a channel assuming laminar flow of an incompressible fluid. As a horizontal flow is assumed, the formulation concerns only one dimension. The pipe flow is incorporated by means of the following formula's [Deltares, 2017, van Esch et al., 2012]:

$$\frac{dq}{dx} + s = 0 \tag{5.3}$$

$$q = -\frac{a^3}{12\mu}\frac{dp}{dx} \tag{5.4}$$

In which,

q	specific discharge	[m/s]
s	source term used to couple the aquifer flow to the pipe flow	[m/s]
a	height of the pipe	[m]
μ	dynamic viscosity	[kg/s]
p	pore pressure	[N/m^2]

The third component is the pipe equilibrium. In D-Geo Flow the pipe path is manually specified. Subsequently, the pipe is divided into several elements that are in series. The calculation is performed element by element. When a critical point is reached, an element is activated. This process is illustrated by Figure 5.1. The graphs present the height of the pipe a as a function of the local horizontal gradient dh/dx. The dark blue line represents the limit equilibrium condition. Below the line there is a limit state equilibrium, the grains do not move. Above the line there is no equilibrium and erosion can take place. The calculation starts at the first element. During the calculation the height of the element, and thus the pipe, is increased stepwise. By increasing the element height the permeability of the element increases leading to a decrease of the local horizontal gradient as explained in Chapter 2. At a certain height the element becomes unstable corresponding to the first point where the red line intersects the dark blue line in the left figure. When the elements changes from stable to unstable the element is activated and 'opened' completely. The calculation continues with the second element an so on. If for a certain element the maximum pipe height is reached and the element is still stable, the pipe growth stagnates. This is depicted by the right figure. The head difference is then not sufficient to result in a continuous pipe [Deltares, 2017, van Esch et al., 2012].
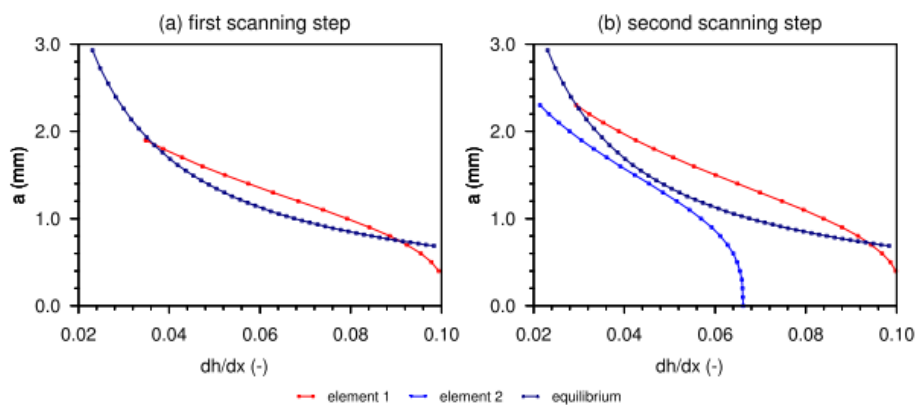
Figure 5.1: Graphical presentation of element activation in D-Geo Flow [Deltares, 2017]

5.2.2. Numerical model

The modelling process consisted of four steps. First, the geometry was constructed and the materials and parameters were assigned. Second, the model was calibrated based on mean values of the field measurements, the stationary calibration. The third step was the non-stationary calibration including time-dependent boundary conditions. In the fourth step, a high-water period was incorporated. For this purpose, the response of the outer boundary to the change in river water level was determined.

All steps are separately explained. As mentioned, the model development including calibration was done by means of PlaxFlow. Subsequently, the model was adopted in D-Geo Flow. Therefore, some adaptations to the model had to be made. The last paragraph describes these adaptations.

step 1: geometry and parameters
The initial geometry and parameters were determined based on the available data and the schematisations as presented in section 3.2. With respect to the schematisations, the geometry was further expanded with deeper layers. Besides, a value for the hydraulic conductivity was selected for each layer based on the available soil information as described in section 3.2.

step 2: stationary calibration
After construction of the initial model, the model needed to be calibrated to ensure that the model calculations corresponded to the actual measured potentials. The first calibration step involved the stationary calibration. A stationary calibration implies that the potential at the measurement points resulting from a numerical model must correspond to the average value of the field measurements. Data from 2015 and 2016 was used for this purpose, both for the water level of the Maas and the field measurement points. A maximum difference between the modelled and measured potentials of 0.05 m was allowed. In order to minimize the difference to a maximum of 0.05 adjustments were made to the hydraulic conductivity of the soil layers. Figure 3.4 illustrates the characteristic points in a dike geometry. Measurements of the potential at points A, B, D and E were available for the calibration of the numerical model.

step 3: non-stationary calibration
The second calibration step was the non-stationary calibration. For that purpose, time-dependent boundary conditions were used instead of one mean value. A short period in which the water level of the Maas deviates from the average value and returns to that average after a period of at least ten days was therefore selected. The measurements at point A and E within that same period were used as boundary conditions. Flow functions were incorporated to include the varying river water level and boundary conditions over time. A flow function is a table containing the time steps and the corresponding potential difference. Subsequently, the calculated potentials at points A, B, D and E resulting from the numerical model were compared to the measurements from the selected period. Again, in order to minimize the difference between the modelled and measured values of the potential adjustments were made to the hydraulic conductivity of the soil layers. During the two calibration phases several adjustments to the hydraulic permeability of the soil layers were done. The second gravel layer was splitted into three parts to include a present low permeable gravel zone. In addition, the hydraulic conductivities of the upper gravel layers and the silt layer were adapted. Figure 5.2 presents the final geometry including the resulting values of the hydraulic conductivity of the soil layers.

step 4: high-water simulation
Once the stationary and non-stationary calibration were completed a period of high-water could be simulated. Naturally, a high-water level is not reached instantaneously. Therefore, a high-water peak was generated based on an interpolation tool from the water board in Limburg. This tool predicts the water levels at a certain location along the Maas based on flow rate data from the Maas near the village Borgharen. In order to properly simulate the period of high-water, the response of the hinterland boundary, point E, to the river water fluctuations was determined. In order to determine the response of the potential at point E, the highest peaks of the Maas water level during the period of 2015-2016 and the corresponding peaks of the measurements of point E were selected. A relationship between the river water level and the boundary condition could be derived from the extent to which the potential at point E moves with the fluctuation of the river level. As mentioned, the used maximum water level to generate the high-water peak corresponds to the level of winter 1993. For Buggenum, the maximum water level equals 20.53 m + NAP. Figure 5.3 illustrates the generated high-water peak and the corresponding peak for the boundary at point E based on the 1993 water level. The fluctuating river water level and boundary conditions were included in the model by means of flow functions as discussed in the previous step.
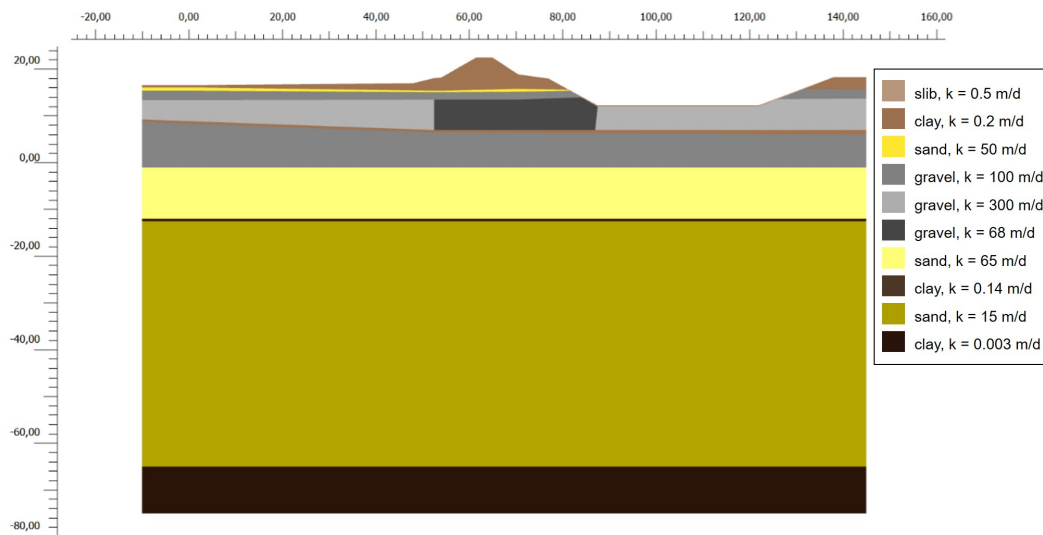
Figure 5.2: Geometry of calibrated numerical model of Buggenum including hydraulic conductivity of the layers
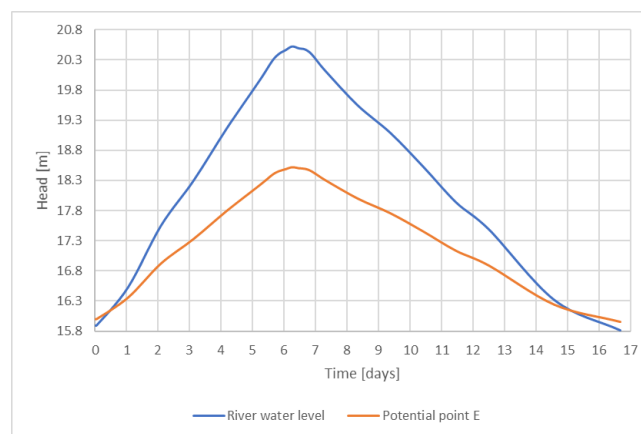
Figure 5.3: High-water peak for river water level and hinterland boundary (point E)

Adaptations in D-Geo Flow

In D-Geo Flow the sand layer below the blanket layer, the piping sensitive layer, must be a perfect horizontal layer with equal thickness. Therefore, the sand layer in the model was adapted to a horizontal layer with a thickness of 40 cm. Consequently, the blanket layer thickness in the far hinterland increased and the thickness of the first gravel layer slightly changed. In addition, the small silt layer was extended to the top of the dike to overcome modelling problems related to very small layering.

5.3. Analysis

This section explains the performed calculations of the numerical analysis per objective.

Objective N1: Effect of model components

The effect of model components (layering and soil characteristics) to the piping likelihood has been studied by means of a variation study with respect to the original model as depicted in Figure 5.4. A total of 23 model variations has been studied related to the geometry and the permeability of the layers:

- **Model variations 1a - 2b:** Influence of the permeability of the blanket layer and sand layer
- **Model variations 3a - 3i:** Influence of the permeability and composition of the upper gravel layers
- **Model variations 4a - 4d:** Influence of first clay layer (aquifer thickness)
- **Model variations 5a - 6b:** Influence of the thickness of the blanket layer and sand layer

Table 5.1 gives an overview of all model variations. The second column contains a description of the model variations. The descriptions refer to the layer numbering in Figure 5.4. Appendix E includes Figures E.2 to E.18 illustrating the geometries of the model variations 3a to 6b. For the other model variations no illustration of the geometry was included, because the description of these variations is clear without an illustration.
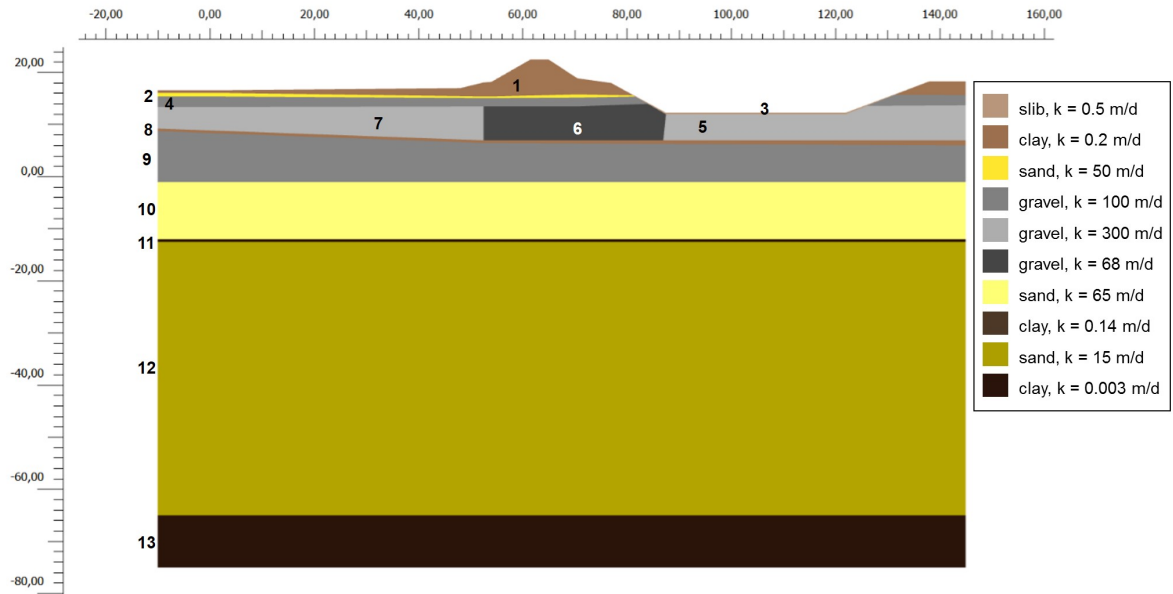
Figure 5.4: Geometry of calibrated numerical model of Buggenum with layer numbering

Table 5.1: Overview of the model variations for the numerical model of Buggenum

Model variations	Description	Figure
1a	Hydraulic conductivity blanket layer (layer 1), k_b = 0.1 m/d	
1b	Hydraulic conductivity blanket layer (layer 1), k_b = 0.3 m/d	
1c	Hydraulic conductivity blanket layer (layer 1), k_b = 0.5 m/d	
1d	Hydraulic conductivity blanket layer (layer 1), k_b = 1 m/d	
2a	Hydraulic conductivity first sand layer (layer 2) = 40 m/d	
2b	Hydraulic conductivity first sand layer (layer 2) = 60 m/d	
3a	Hydraulic conductivity second gravel layer (layers 5 and 7) equal to hydraulic conductivity of first gravel layer (layer 4), 100 m/d	E.2
3b	Hydraulic conductivity first gravel layer (layer 4) equal to hydraulic conductivity of second gravel layer (layers 5 and 7), 300 m/d	E.3
3c	Hydraulic conductivity of left part of second gravel layer (layer 7) = 68 m/d, middle and right part (layers 6 and 5) 300 m/d	E.4
3d	Hydraulic conductivity of right part of second gravel layer (layer 5) = 68 m/d, middle and left part (layers 6 and 7) 300 m/d	E.5
3e	All gravel above first clay layer (layers 4, 5, 6 and 7) hydraulic conductivity of 100 m/d	E.6
3f	All gravel above first clay layer (layers 4, 5, 6 and 7) hydraulic conductivity of 300 m/d	E.7
3g	All gravel above first clay layer (layers 4, 5, 6 and 7) hydraulic conductivity of 68 m/d	E.8
3h	Gravel pocket (k=100 m/d) in sand layer (layer 2) left of exit point	E.9
3i	Pocket of low permeable gravel (k=68 m/d) in first gravel layer (layer 4) below exit point	E.10
4a	First clay layer (layer 8) replaced by gravel with hydraulic conductivity of 100 m/d	E.11
4b	Local absence of first clay layer (layer 8), 20 m, in foreland	E.12
4c	Local absence of first clay layer (layer 8), 20 m, below dike	E.13
4d	Local absence of first clay layer (layr 8), 20 m, hinterland	E.14
5a	Increased thickness of first sand layer (layer 2) by replacing first gravel layer (layer 4) with sand	E.15
5b	Increased thickness of first sand layer (layer 2) with 1 m	E.16
6a	Decreased blanket layer (layer 1) thickness with 0.5 m	E.17
6b	Increased blanket layer (layer 1) thickness with 0.5 m	E.18

Objective N2: Validation of analytical model
The validation of the analytical model is divided into two parts:

1. *Validation of the analytical groundwater flow model*
   The analytical groundwater flow model has been validated by means of a comparison of the analytical and the numerical (PlaxFlow) groundwater flow models based on the exit potential and flow pattern.

2. *Validation of the calculation rule of Sellmeijer*
   The calculation rule of Sellmeijer has been validated by means of a comparison of the analytical calculation rule and the numerical model implemented in D-Geo Flow based on the critical head difference H_c. The difference between the analytical and numerical method has been explained based on the findings from the variation study and an evaluation of the model input.

5.4. Results

This section presents and discusses the results of the numerical analysis. First the results of N1 are presented followed by the results of N2.

5.4.1. Objective N1: Effect of model components

Table 5.3 gives an overview of the model variations and their resulting potentials at the exit point at the time when the river water level reached its maximum value of 20.53 m + NAP. Additionally, the potential resulting from the initial model is included, 18.92 m + NAP. The table also shows the difference in exit potential between the original model and the different variations. A complete evaluation of the groundwater flow pattern of all model variations is included in Appendix E.

The variation of the hydraulic conductivity of the blanket layer k_b had great effect on the exit potential as shown by the potential differences of variations 1a to 1d. The higher the permeability the lower the exit potential. On the other hand, the variation of the hydraulic conductivity of the sand layer (layer 2) had no effect on the exit potential (model variations 2a and b). The same holds for the thickness of the blanket layer d and sand layer (model variations 5a to 6b). The variation of the blanket layer thickness had great effect on the exit potential, in particular a reduction of the thickness. The smaller the blanket layer the smaller the exit potential. However, the variation of the thickness of the sand layer had no effect on the exit potential. In addition, the (local) increase of the aquifer thickness D had an effect on the exit potential (model variations 4a to 4d). The larger the aquifer thickness the higher the exit potential. When the aquifer thickness is only locally increased (model variation 4b to 4d), the location of this increase is important. A local increase in the hinterland (near exit point, variation 4d) has the greatest effect on the exit potential.

From model variations 3a to 3i it followed that layering and variation in permeability (horizontal and vertical) within the aquifer have great effect on the exit potential. A distinction can be made between the model variations with varying specific geometry (horizontal zones with varying permeability) resulting in non-horizontal flow line patterns (model variations 3a, 3b, 3c and 3d) and model variations with horizontal flow lines and varying vertical permeability (model variations 3e, 3f and 3g). The first category shows the effect of the flow pattern (location of zones) and the second category shows the effect of the overall permeability of the aquifer to the exit potential.

The impact of the model variations on the exit potential is summarized in Table 5.2. The results are combined into the five most influential model components. The table indicates which variations correspond to which category. The variations that had no effect on the exit potential are not included. For two categories the exit potential of the original model provided a lower boundary for the exit potential. The blanket layer properties (permeability and thickness) have the greatest impact on the potential. The second most influential component is the specific geometry of the aquifer. Zones with highly varying permeability cause deviations of the flow lines which influence the potential significantly. The overall permeability of the aquifer and the aquifer thickness are of influence, but significantly less than the blanket layer properties and the specific geometry of the aquifer.

Table 5.2: The effect of model components on the exit potential summarized in five categories based on the results of the variation study

model component	specification	variations	exit potential range [m + NAP]	potential difference [m]
hydraulic conductivity blanket layer, k_b	range from 0.1 to 1 m/d	1a - 1d	19.02 - 18.39	0.63
blanket layer thickness, d	range from 1 to 2 m	6a, 6b	18.19 - 18.98	0.79
aquifer thickness, D	range from 8 to 27 m	original model, 4a - 4d	18.92 - 19.09	0.17
specific geometry aquifer	horizontal zones with highly varying permeability	original model, 3a - 3d	18.92 - 19.47	0.55
permeability aquifer	horizontal flow lines	3e - 3h	19.08 - 19.25	0.17

Table 5.3: Overview of maximum potential underneath the blanket layer for each model variation

Model variation	Maximum exit potential [m + NAP]	Difference w.r.t. original model
original model	18.92	
1a	19.02	0.10
1b	18.83	-0.09
1c	18.68	-0.24
1d	18.39	-0.53
2a	18.92	0.00
2b	18.92	0.00
3a	19.06	0.14
3b	18.98	0.06
3c	19.47	0.55
3d	19.16	0.24
3e	19.14	0.22
3f	19.25	0.33
3g	19.08	0.16
3h	18.92	0.00
3i	18.92	0.00
4a	19.09	0.17
4b	18.92	0.00
4c	18.98	0.06
4d	19.04	0.12
5a	18.89	-0.03
5b	18.94	0.02
6a	18.19	-0.73
6b	18.98	0.06

5.4.2. Objective N2: Validation of analytical model

The following two paragraphs present the results for the validation of the analytical groundwater flow model and the calculation rule of Sellmeijer separately.

Analytical groundwater flow model

The exit potential that followed from analytical calculations is 19.32 m + NAP. The numerical model resulted in an exit potential of 18.92 m + NAP. This is significantly lower than the analytical potential, but still higher than the critical potential which equals 18.64 m + NAP. The relatively low numerical exit potential can be explained by evaluating the groundwater flow pattern (Figure 5.5) and the analytical groundwater flow model assumptions.

Figure 5.5 illustrates the groundwater flow of the numerical model. The colouring indicates the flow velocity. The lighter the color the higher the flow velocity. The figure shows that the groundwater, to a large extent, enters the aquifer via the first gravel layer (layer 4). This appears from the higher flow rate in the part below the dike of layer 4 relative to layer 6. At the inner toe of the dike, the water flows downwards into the left part of the second gravel layer (layer 7). This is explained by the difference in permeability. The middle part of the second gravel layer (layer 6) is relatively impermeable (68 m/d), while the left part (layer 7) is highly permeable (300 m/d). Past the inner toe the groundwater is no longer 'forced' to flow through the relative small upper gravel layer (layer 4), but instead can flow through the deeper second gravel layer (layer 7) which has a larger thickness and permeability. Due to this sudden transition in the permeability, the water at the inner toe seems to be 'pulled down'. It can be concluded that this specific geometry of the aquifer results in a deviation of the flow lines with respect to a perfect horizontal flow. As shown by the variation study (objective N1), this deviation has a large influence on the potential. The analytical groundwater flow model is based on the assumption of perfect horizontal aquifer flow as described in section 4.4. It is therefore not surprising that the analytical potential differs from the numerical result.
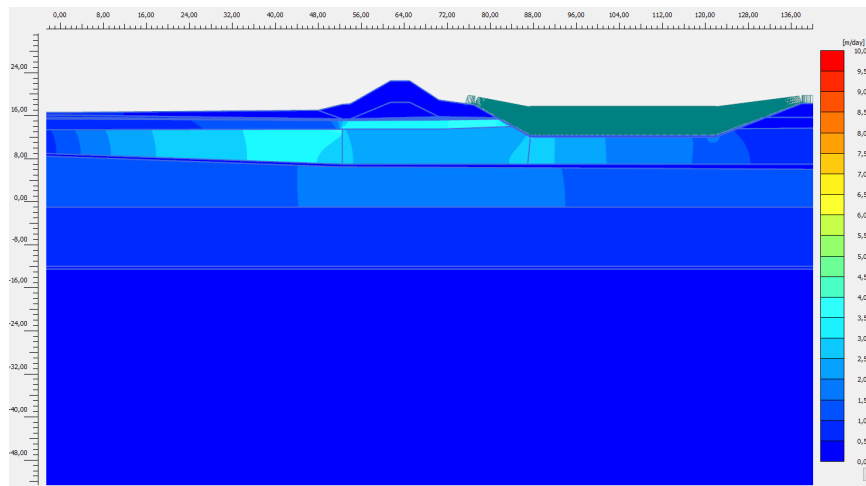
Figure 5.5: Graphical presentation of the groundwater flow |q| [m/d] of the numerical model of Buggenum at the maximum river water level of 20.53 m + NAP

Sellmeijer calculation rule

For the evaluation of the Sellmeijer calculation rule, the numerical model has been implemented in D-Geo Flow in order to model the development of a pipe and determine the critical head difference H_c. The pipe path was manually specified at the top of the sand layer between the river and the exit point at two meter from the inner toe, resulting in a total pipe length of 35.3 m. The water level of 1993 was applied which equals 20.53 m + NAP. For that water level, the numerical calculation resulted in the development of a continuous pipe. Thus, according to the numerical calculations, the development of a continuous pipe can occur at the location near Buggenum under the hydraulic circumstances of 1993, once uplift and heave have taken place. The critical head difference H_c was reached at a pipe length of 6.45 m and equalled 3.3 m. This is illustrated by Figure 5.6 which depicts the head difference with respect to the pipe length. The outside water level at the critical point was 20.3 m + NAP, almost the maximum level of 20.53 m + NAP. Figure 5.7 illustrates the model at the critical point. The pipe and hydraulic head are displayed.

The critical head resulting from the analytical calculation rule of Sellmeijer is 2.45 m. The difference between the numerical and analytical value is significant, 0.85 m. In addition, the ratio between pipe length and seepage length l/L differs greatly from the theoretical maximum. Figure 2.11 showed that the theoretical maximum head difference, and thus the critical head difference, corresponds to l/L equal to 0.5. In this case the ratio is 0.18 (6.45/35.3). The difference between the analytical calculation rule of Sellmeijer and the numerical model concerns the dike configuration. The calculation rule of Sellmeijer is based on a standard and greatly simplified geometry according to the assumptions previously described in section 4.4, while the more realistic geometry of the numerical model deviates from this standard configuration. The difference in critical head H_c between the calculation rule and the numerical model is most likely caused by this difference in model configuration.
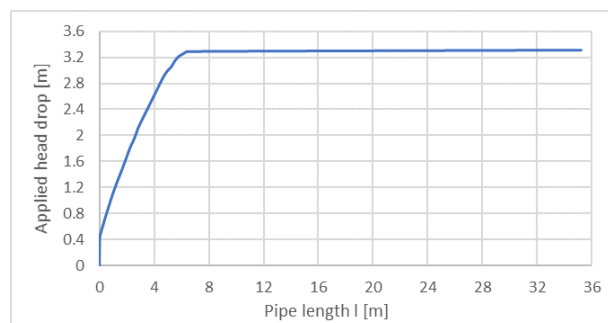
Figure 5.6: Applied head difference H versus pipe length for the numerical model of Buggenum implemented in D-Geo Flow, with a maximum water level of 20.53 m + NAP corresponding to the hydraulic circumstance of 1993
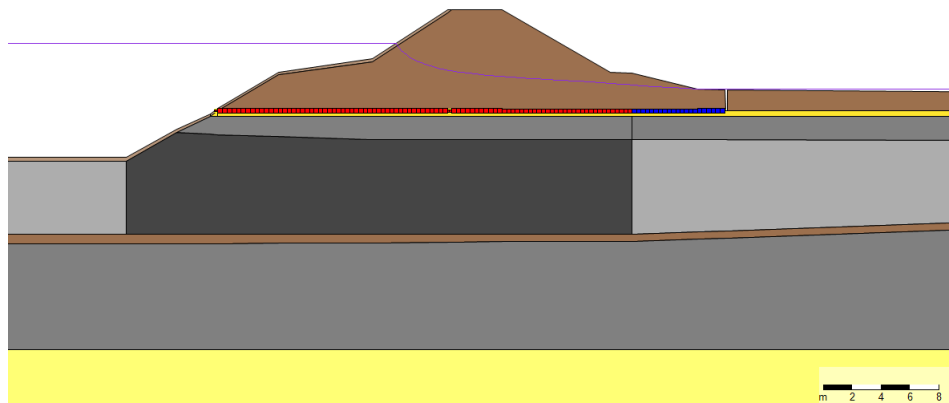
Figure 5.7: Picture of numerical model in D-Geo Flow at critical point (right before development of continuous pipe)

5.5. Review of numerical model

Following the numerical analysis, a number of discussion points regarding this analysis has been identified. The points concern the field measurement data, the software D-Geo Flow and the dimensions of the model.

Field measurements

The numerical model has been calibrated by means of potential measurements of a two-year period. However, the water level on the Maas during that period did not deviate significant from the normal circumstances. A relation between the river water level and the hinterland potential was deduced from these measurements. It is possible that this relation is different under more extreme hydraulic circumstances. Nonetheless, the calibrated model has been used to model a high-water wave. It is questionable whether the model is completely correct under high-water circumstances.

D-Geo Flow

In the numerical analysis, the new groundwater flow and erosion software D-Geo Flow was used. During this research the first version of D-Geo Flow was released. This first version is developed and validated by means of simple geometries. It is not yet completely clear whether the software provides complete accurate results for more complex models. In addition, the software possibly still contains minor faults and incorrect features that will have to be eliminated during the first usage phase. Additionally, it has been found that the results are dependent on the coarseness of the calculation grid. An adaptation of the grid coarseness results in small variations of the resulting critical head difference. In addition, the result is dependent on whether a steady-state or transient calculation is performed. The difference is a few centimeters. Furthermore, the outflow of the groundwater must be a free outflow according to the Sellmeijer model. This means that no blanket layer is present at the exit point. However, in reality the vertical exit channel is filled with fluidised sand. This possibly effects the potential at the bottom of the exit channel and thus the critical head difference.

2D versus 3D

The numerical analysis has been performed by means of a two-dimensional model. In D-Geo Flow the pipe is therefore modelled as a perfect horizontal straight line. However, in reality the pipe can also deviate in the third dimension. This coincides with the flow path, which also deviates in three dimensions. In the numerical analysis it was found that the potential is influenced by the deviation of the flow lines. Naturally, this is not limited to two dimensions and also applies to deviations in the third dimension.

III
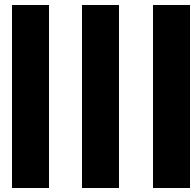
Conclusion

6

Discussion, conclusion and recommendations

Chapter 6 is the final chapter of this thesis. The chapter contains the discussion, conclusion and recommendations. Section 6.1 presents the discussion in which the calculation results, relevant literature and used models are evaluated and discussed. Section 6.2 presents the conclusion of this thesis. The final section, section 6.3, presents recommendations for further research following from the discussion and conclusion.

6.1. Discussion

The results of the analytical analysis (Chapter 4) and the numerical analysis (Chapter 5) were already briefly discussed in the separate chapters. This section presents a more elaborate discussion related to all results. The discussion is divided into several paragraphs, each addressing a main component of this research.

Water level scenarios and observations
Piping is the sequential occurrence of uplift, heave and backward erosion. A continuous pipe can only be formed if the critical limits for all three mechanisms are exceeded and thus when all three mechanisms have occurred. The hindcast of past high water events showed that in 1993 and 2011, water levels have occurred at which (part of) the critical limits are exceeded. For one of the four research locations (location near Buggenum) this concerned all critical limits. Therefore, this location can be marked as a critical location with respect to dike-failure as a result of piping.

Nonetheless, during the high water period of 2011 no piping related signs such as sand boils were observed. Therefore, the question remains whether uplift, heave and backward erosion have taken place in 2011. Or in other words, are the calculation results wrong or were the signs missed? According to the calculations based on the water level from 2011, the critical limit for uplift (critical exit potential) at Buggenum was exceeded by only 0.17 m. It is therefore possible that favourable conditions such as a higher blanket layer permeability have resulted in a real potential that was lower than this calculation suggests. However, it is hard to imagine that this was the case along the entire dike ring, but it is conceivable that the blanket layer was only lifted at one or a few locations. This can then easily be missed when inspecting the dikes. Besides, there is no information about the thoroughness of the dike inspection during that period in 2011.

Influence of model components
The effect of model components such as layering and soil characteristics has been studied in both the analytical and numerical analysis. Both analysis have shown that the blanket layer properties have the greatest influence on the potential compared with other model components. The analytical analysis showed only the importance of the blanket layer thickness. The numerical analysis showed that both the permeability and thickness of the blanket layer are of great importance. This difference can be

explained by the range in which the permeability has been varied in both analysis. In the analytical analysis, the permeability has been varied between 0.1 and 0.3 m/d while in the numerical analysis the for the Maasvallei realistic range of 0.1 to 1 m/d has been used. Since the range of 0.1 to 1 m/d is realistic for the Maasvallei, it can be stated that both the permeability and the thickness of the blanket layer play an important role with respect to piping. However, there is an important difference between both parameters. The blanket layer permeability affects only the occurring potential, but not the critical potential. This means that when the permeability increases the potential decreases and thus the risk of uplift, as the critical potential remains the same. In contrast, the thickness of the blanket layer has an effect on both the exit potential and the critical potential. When the thickness of the blanket layer decreases, the exit potential also decreases. However, the critical potential decreases even more, resulting in an increase of the likelihood to uplift. Thus, for both parameters, a decrease results in an increase of the likelihood to uplift. In addition, the thickness of the blanket layer is not only important for the potential but also for the vertical exit gradient. The greater the thickness of the blanket layer, the smaller the vertical gradient and thus the likelihood of heave.

The hydraulic conductivity of the blanket layer in the Maasvallei typically varies between 0.1 and 1 m/d. The mean characteristic value then lies around 0.5 m/d. In the assessment practice a material factor is applied to determine a safe design value. A design value is often significantly lower than the characteristic mean value. This means that it is possible that, for example, a design value of 0.2 m/d is selected while in reality the hydraulic conductivity of the blanket lies between 0.5 and 1 m/d. Extensive soil investigation can result in a better estimation of the permeability and thus a smaller range of possible values. This results in a more realistic estimate.

In addition to the blanket layer properties, it has been shown that, the specific geometry of the aquifer is also of great importance for the piping likelihood. A strong horizontal variation of the permeability in addition to vertical variation can result in deviating flow lines with respect to a standard horizontal flow path. When the groundwater flow in the aquifer deviates from a perfect horizontal flow path, the potential underneath the blanket layer is influenced. The subsoil in the Maasvallei typically contains gravel layers. Some (parts) of the gravel layers contain sand reducing the permeability and causing high variability. The numerical model of Buggenum showed such variations that caused deviations in the flow path which resulted in a reduction of the exit potential. However, the numerical model showed that the opposite, a deviating flow path resulting in a higher exit potential, is also possible. A deviation in the specific geometry of the aquifer can be very local. It is therefore possible that piping is a very local problem.

Models
Several assumptions underlie the analytical groundwater flow model and the analytical calculation rule of Sellmeijer in order to schematize reality in a simplified manner. In Section 4.4 these assumptions were elaborately discussed. In summary, the analytical schematisation is based on a two-layer system (aquifer and blanket layer) with perfectly horizontal continuous and homogeneous layers. It is assumed that the groundwater flow in the aquifer is perfectly horizontal. In addition, the analytical groundwater flow model assumes that the flow through the blanket layer (leakage) is vertical. Sellmeijer, assumes a complete impermeable blanket layer and thus no leakage.

The flow path assumed in the analytical methods possibly differs from the real flow path as a result of these underlying assumptions. In reality, the flow is often not perfectly horizontal and vertical, but will follow curved and mostly smooth lines. In the numerical variation study it has been shown that the shape of the flow lines has a significant effect on the occurring potential. When the real flow lines in the aquifer deviate significantly from a horizontal flow path, the analytical potential will most likely differ from the actual potential. This explains the difference in exit potential between the analytical (19.32 m + NAP) and numerical (18.92 m + NAP) solution.

The calculation rule of Sellmeijer resulted in a critical head difference H_c of 2.45 m. The numerical model implemented in D-Geo Flow resulted in a critical head difference of 3.3 m. The explanation for this difference can also be attributed to the difference in schematisation of the groundwater flow between the analytical rule and the numerical model. The calculation rule of Sellmeijer as presented

in formula 2.13 is based on a standard dike configuration according to the assumptions as described above. The geometrical shape function F_G incorporates the influence of the aquifer geometry to the groundwater flow by means of a fit parameter. This is the factor 0.91 in the geometrical shape function (see formula 2.13). This factor is only correct for a standard dike configuration. For other geometries the factor should be redetermined by means of numerical methods as explained in section 2.3. For the analytical calculations in this study, the standard factor of 0.91 is used, which explains the difference in H_c between calculation rule and numerical model. Assuming that the critical head difference H_c resulting from the numerical model of Buggenum (3.3 m) is realistic, this would mean that the fit parameter of the shape factor is 1.23 instead of 0.91. The assessment guideline also uses the standard calculation rule with a fit factor of 0.91. It can be questioned whether this results in a realistic evaluation of backward erosion for other dike configurations.

In addition, during the development of D-Geo Flow it was found that for a standard dike, the calculation rule with the fit factor of 0.91 results in slightly lower values for H_c than a numerical model. The calculation rule is therefore conservative with respect to a numerical model. It was stated that the calculation rule of Sellmeijer provides lower bound values for H_c [van Esch et al., 2012].

The majority of the assumptions underlying the analytical methods does not apply to a numerical model, as discussed in detail in section 5.1. A numerical schematisation is based on a much greater level of detail than the analytical schematisation. Nonetheless, it is important to recognize that the numerical model is a simplified schematisation of reality, but due to the high level of detail it can be said that a numerical model is a very reasonable approximation of reality. In this study, a numerical model has therefore been regarded as reasonably truthful.

However, the used numerical model (and numerical software) also contains some questionable components. D-Geo Flow is a new finite element software, developed and validated based on simple geometries. As discussed in the review of the numerical model it is not yet completely clear whether the software provides accurate results for more complex soil conditions. Therefore, some caution is required with respect to the interpretation of the results. In addition, the accuracy of the numerical model with respect to the groundwater flow during high water can be doubted. The numerical model has been validated based on measurement data of normal hydraulic conditions. Ideally, measurements of a high water period are used to ensure that the groundwater flow during extreme hydraulic conditions is modelled well. Furthermore, both the numerical and analytical model assume a two-dimensional situation. By assuming this, the variability of the geometry and soil properties in the longitudinal direction of the dike is not included. This is in accordance with the assessment practice. However, deviations of the groundwater flow and pipe development in the longitudinal direction most likely have an influence on the exit potential and critical head H_c.

Assessment

With respect to the assessment practice two components have been studied in this thesis: the safety factors and the critical vertical heave gradient. With respect to the safety factors, the analytical analysis showed that the safety factors significantly influence the critical limits, but that this does not lead to a change in whether or not these limits are exceeded in comparison with the calculations without safety factors. In practice an assessment is performed using safety factors and, in addition, design parameter values by means of a material factor as previously discussed. The use of safety factors in combination with design values might lead to a change in whether or not the critical limits are exceeded.

In addition, the analytical analysis showed that for the hydraulic circumstances of 2011, the critical limits for uplift and heave were exceeded at the research location near Buggenum. Nevertheless, no sand boils were observed during that period. This may indicate that the actual critical vertical gradient $i_{c,h}$ is higher than the critical gradient used in the calculations (0.5 and 0.8). According to the empirical relation established after the 1950 flood of the Mississippi River, the critical vertical gradient varies between 0.5 and 0.8 [Tyler et al., 1956]. In addition, experiments performed by Sellmeijer (1981) resulted in a value for the critical vertical heave gradient of 0.6. The theoretical critical vertical gradient even results in higher values, depending on the porosity, of 0.85 to 1.15 [TAW, 1999]. Nonetheless, in practice a significantly lower value of 0.3 is applied for the critical vertical gradient. This value is based on the

above mentioned experiments of Sellmeijer. A safety factor of two is applied resulting in an assessment value of 0.3.

In addition to the critical vertical gradient, the occurring vertical gradient as applied in the assessment guideline can also be questioned. The occurring vertical gradient i that is used for the assessment is based on the critical exit potential $\phi_{c,u}$ for which uplift occurs. However, the exit potential slightly decreases after uplift has taken place due to a local pressure relief. This means that the exit potential after uplift is smaller than the critical exit potential. Possibly, the locally decreased pressure slightly increases again due to the flow resistance caused by the presence of sand and water in the exit channel. It is possible that the pressure stabilises at constant outflow. Nonetheless, given the fact that the exit channel continues to function as a valve, it is likely that the pressure will locally remain lower than the critical potential. However, in the assessment rule the critical exit potential is used to evaluate heave. This raises the question whether the assessment rule is based on a too high exit potential and thus a too high vertical exit gradient.

6.2. Conclusion

This section presents the conclusions of the report by answering the research questions. First the answers to the sub-questions are presented. Subsequently, the main question is answered: Is dike-failure due to piping realistic in the Maasvallei?

6.2.1. Sub research questions

The conclusions of the sub questions are separately presented according to the order as presented in the introduction of this report.

What are the processes leading to piping?

Piping is an internal erosion mechanism creating hollow spaces (pipes) underneath the dike as a result of the transport of soil particles due to seepage. The complete piping process is a combination of the occurrence of three main mechanisms: uplift, heave and backward erosion. As a result of a high river water level with respect to a lower hydraulic head in the hinterland a horizontal groundwater flow through the aquifer underneath the dike establishes. This results in an increase of the water pressure in the aquifer. The hydraulic head in the aquifer is higher than the hydraulic head in the hinterland resulting in an overpressure. In addition, the presence of a blanket layer prevents the outflow of water and escape of this pressure. The upward water pressure cannot exceed the weight of the blanket layer due to the vertical force balance. When the upward water pressure in the aquifer equals the weight of the blanket layer the blanket layer is therefore lifted. At this point the effective stresses at the interface between the blanket layer and aquifer are zero. Consequently, the soil particles cannot withstand the water pressure and the groundwater is forced upward through the blanket layer. Ruptures occur resulting in the formation of a vertical channel allowing the free exit of water.

As a result of the high local flow velocity of the seepage flow, sand particles are eroded and transported through the vertical channel towards surface level. This results in the presence of fluidised sand in the channel leading to an increase of the flow resistance and thus a decrease of the flow velocity. The erosion possibly ceases if the flow velocity is not sufficient to overcome this resistance. Once the head difference is large enough and the vertical exit gradient reaches a critical value $i_{c,h}$ [-] this additional flow resistance will not be sufficient to stop the erosion process. This vertical erosion process is called heave.

Once the critical vertical heave gradient is exceeded sand is eroded. The sand particles are deposited outside the well and small horizontal pipes start to form. The formation of channels results in a local decrease of the water pressure. This can lead to equilibrium which stops the pipe formation (erosion). This phase is therefore designated as regressive backward erosion. Regressive backward erosion turns into progressive backward erosion once the hydraulic head difference further increases until a critical value is reached, the critical head difference H_c [m]. Once the critical head is reached pipe formation continues until the pipe reaches the upstream side.

What is the sensitivity of model components (layering and soil characteristics) on the piping likelihood?
In this study it was found that two model components in particular have great effect on the piping likelihood: the blanket layer properties and the specific geometry of the aquifer.

The most important component is the blanket layer; the thickness as well as the hydraulic conductivity of the blanket layer are of importance. For both, a low parameter value results in a high piping likelihood. Not only do the properties have a large influence on the piping likelihood, they also have a high spatial variability. It is impossible to determine exactly the value of the blanket layer parameters for a complete dike cross-section. Additionally, the range of values for the hydraulic conductivity of the blanket layer in the Maasvallei is large, 0.1 to 1 m/d. This large range of possible values creates additional uncertainty regarding the permeability. Therefore, it is preferable, to perform more soil investigation for critical locations in order to narrow the parameter range.

The second most important model component is the specific geometry of the aquifer. By specific geometry, local variations in the hydraulic conductivity creating zones are meant. The zones with highly varying permeability cause the deviation of flow lines with respect to a horizontal flow path. This has a great effect on the potential underneath the blanket layer. Due to the presence of gravel with highly variable permeability in the Maasvallei, this phenomenon is very relevant for that area. For critical locations it is recommendable to use a numerical groundwater flow model in order to more accurately determine the groundwater flow path and thus the potential in the aquifer.

Which models are suitable for the evaluation of uplift, heave and backward erosion?
In this study three models have been used and evaluated: the analytical groundwater flow model for the evaluation of uplift and heave, the calculation rule of Sellmeijer for the evaluation of backward erosion and a numerical model implemented in the finite element software PlaxFlow and D-Geo Flow.

In this study, a numerical model has been regarded as reasonably truthful because of the high level of detail of the schematisation. However, a lot of information is required in order to create an accurate numerical model, such as field measurements of the hydraulic levels, preferable during high water, and sufficient soil investigation. In addition, the calibration of a numerical model is time consuming. Therefore, it is not realistic to always use a numerical model instead of the analytical model in every day engineering practice. However, the use of numerical modelling in the assessment practice for critical locations with respect to piping is recommended.

The analytical groundwater flow model and calculation rule of Sellmeijer are a simplification of reality based on several assumptions. Both models consider the groundwater flow in the aquifer as perfectly horizontal. In addition, the analytical groundwater flow model assumes that the flow through the blanket layer (leakage) is completely vertical. Sellmeijer assumes a complete impermeable blanket layer and thus no leakage. In reality, the groundwater flow is not perfectly horizontal or vertical, but mostly follows a curved and smooth path. This study has shown that deviations of the flow path have a great effect on the potential in the aquifer. It can be concluded that when the groundwater flow shows strong deviations with respect to a horizontal flow path, the potential resulting from the analytical groundwater flow model will most likely differ from the actual potential. This can result in both a conservative and likelihood of piping.

The analytical calculation rule of Sellmeijer is based on a standard dike configuration according to the assumptions as previously described. The geometrical shape function F_G incorporates the influence of the geometry to the groundwater flow by means of a fit parameter. The standard fit parameter is 0.91 and corresponds to the standard configuration. From the calculations it followed that the critical head difference H_c according to the analytical calculation rule deviates from the critical head difference following form a numerical model when the numerical schematisation of the geometry differs from the standard dike configuration. This difference in H_c can be significant, 0.85 m for the numerical model used in this study. Assuming that the numerical model results in a realistic value for H_c, it can be stated that the analytical calculation rule of Sellmeijer results in a critical head difference that deviates from the realistic value if the actual geometry significantly differs from the standard dike configuration. In order

to better match the calculation rule to reality, the fit factor from the geometrical shape function (0.91 for the standard calculation rule) can be redetermined for a specific geometry by means of a numerical model.

For critical locations, it is advisable to verify to what extent the analytical schematisation of the ground-water flow differs from the actual situation. Besides, it should be verified if the calculation rule of Sellmeijer matches the actual situation or whether the fit factor should be redetermined.

Does the assessment method match the actual situation in the Maasvallei?
Two aspects of the assessment method have been evaluated: the safety factors and the critical vertical heave gradient.

The assessment guideline applies safety factors to incorporate extra safety in the assessment. Evaluation of the safety factors has shown that the influence of the factors on whether or not the critical limit is exceeded, is small.

The assessment guideline applies a critical vertical gradient of 0.3 for the evaluation of heave. Past experiments and observational studies [Sellmeijer, 1981, Tyler et al., 1956] have shown that the critical vertical heave gradient varies between 0.5 and 0.8. In addition, within this study it has been shown that the lack of observations of sand boils in the Maasvallei indicates that the actual critical vertical gradient in this area possibly exceeds 0.5 and possibly even 0.8. In that case the critical vertical gradient would come close to the theoretical range of 0.85 to 1.15 [TAW, 1999]. Although it is not completely clear, the critical gradient of 0.3 as applied in the assessment practice seems to be conservative with respect to the dikes in the Maasvallei. In addition, the question was raised whether the potential used to determine the occurring vertical gradient in the assessment of heave is too high. The guideline uses the critical potential while the potential after uplift decreases with respect to the critical potential due to a local pressure release.

What is the effect of a future increase of the water level on the likelihood to piping?
A future increase of the water level will result in a larger head difference between the outside and inside of the dike. Consequently, the head in the aquifer increases as well, causing higher potentials resulting in a higher piping likelihood. This study showed that the number of critical locations in the Maasvallei with respect to piping will increase in the future.

6.2.2. Main research question
In the most recent safety assessment of the Dutch dikes many of the dikes in the Maasvallei were found to be unsafe against piping. However, the lack of early signs of piping during recent high-water periods contradicts this rejection. The question arose whether the rejection of the Maasvallei dikes has been just. To answer that, more insight into the piping likelihood in the Maasvallei area is needed. The question central in this report:

Is dike-failure due to piping realistic in the Maasvallei?

According to this study, water levels have occurred in the past (1993 and 2011) for which (part of) the critical limits for uplift, heave and backward erosion were exceeded. When all three critical limits are exceeded a location is assumed to be a 'critical location' with respect to piping. Out of the four research locations (Well, Beesel, Buggenum and Thorn), only one meets the criterion of a critical location (Buggenum). This study also showed that the number of critical locations in the Maasvallei will increase in the future as a result of the expected rise of the river water level.

Although the calculations suggest that the critical limits were exceeded during past high-water periods, the dilemma remains that there are no piping related observations to support those results and the outcome of the latest assessment. It is therefore not possible to verify whether the dikes rejected during the latest assessment are indeed critical locations with respect to piping.

With respect to the current assessment practice four main conclusions were presented in this chapter:

- The exit potential following from the analytical groundwater flow model possibly deviates with respect to the actual value when the groundwater flow deviates from a standard horizontal flow path.
- The analytical calculation rule of Sellmeijer results in a critical head difference that possibly deviates from the realistic value if the actual geometry significantly differs from the standard dike configuration.
- The safety factors have a limited influence on whether or not the critical limits are exceeded.
- The critical limit for heave (0.3) seems to be conservative.

In order to prevent that dikes are not correctly assessed and unnecessarily rejected in the coming safety assessment, it is important to take these points into account for critical locations. Hence, it should be verified whether the analytical groundwater flow model and the calculation rule of Sellmeijer reflect the real situation.

The calculations in this study support the outcome of the most recent safety assessment. Based on this, it can be stated that dike-failure due to piping is realistic in the Maasvallei. However, only future observations can prove whether this is actually correct.

6.3. Recommendations

Following the research described in this report, some recommendations for further research could be made. The recommendations include five topics: the critical heave gradient, measurement data, field observations, the permeability of the blanket layer and the software D-Geo Flow.

Critical heave gradient

In this research it became clear that the critical heave gradient has a major influence on the evaluation of the heave mechanism. Experiments and observations ([Sellmeijer, 1981, Tyler et al., 1956]) have shown that values between 0.5 and 0.8 are realistic with respect to this gradient. However, the Dutch assessment practice uses a lower value of 0.3. In this study it has been concluded that this value seems to be conservative. In addition, Koelewijn (2008) addressed that the substantiation for the use of 0.3 is limited. It is therefore recommended that more (experimental) research into the critical gradient is conducted.

Measurements and observations

At the end of 2014 many piezometers were installed at the research locations in the Maasvallei as part of the POV Piping project. During the subsequent years, a lot of data has been accumulated. However, there has been no high-water during that period. In order to be able to properly study the groundwater flow during high-water, measurement data of a high-water period is required. It is therefore recommended to continue the measurements until a high-water period has occurred. In addition, it is also important that the dikes are thoroughly inspected during the next high water period, especially for the critical locations regarding piping. This way it can mostly be ruled out that important signs are missed.

Blanket layer permeability

This study has shown that the blanket layer permeability is one of the most influential model components with respect to the piping likelihood. Typically, the hydraulic conductivity of the blanket layer in the Maasvallei varies between 0.1 and 1 m/d. This relatively large range results in a high uncertainty with respect to the exit potential. It is therefore relevant to be able to better predict the blanket layer hydraulic conductivity. A more precise (local) estimate of this parameter can prevent that too conservative values are selected and used in the dike assessments. It is therefore recommended to further investigate the hydraulic conductivity of the top soil layer in the Maasvallei area.

D-Geo Flow

The version of the numerical finite element software D-Geo Flow that has been used in this study is a first version. This first version is developed and validated by means of simple geometries. It is not yet completely clear whether the software provides complete accurate results for more complex models. In

addition, the software possibly still contains minor faults and incorrect features. However, D-Geo Flow is currently the only numerical tool that is able to model the development of a pipe in addition to the groundwater flow. For that reason, D-Geo Flow could be a useful tool in the daily engineering practice. Hence, it is essential that the software can handle complex models. To achieve that, D-Geo Flow will need to be further developed and validated in the near future. It is then recommended to study more realistic cases by means of D-Geo Flow.

Bibliography

W.G. Bligh. Dams, barrages and weirs on porous foundations. Engineering News, 64(Dec):708, 1910.

H.T.J. de Bruijn. Het pipingproces in stripvorm. Technical report, Deltares, 2013.

Deltares. D-Geo Flow User Manual. Technical report, Deltares, Delft, 2017.

ENW. Technisch Rapport Grondmechanisch Schematiseren bij Dijken. Technical report, Expertisenetwerk Waterveiligheid, 2012.

U. Förster, G. Van den Ham, E. Calle, and G. Kruse. Onderzoeksrapport Zandmeevoerende Wellen. Technical report, Rijkswaterstaat Water, Verkeer en Leefomgeving, 2012.

Google. Google Earth.

Google. Google Maps, 2017. URL `google.nl/maps`.

S.N. Jonkman and T. Schweckendiek. Flood Defences Lecture Notes CIE5314. Delft University of Technology, 2015.

A.R. Koelewijn. Evaluatie 0,3d-regel. Technical report, Deltares, 2008.

R. Koopmans. Plan van aanpak POV Piping verkenning Heterogeniteit. Technical report, Arcadis, 2016.

R. Koopmans and W. Janssen. POV Piping - Invloed leem- en grindlagen. Technical report, Arcadis, 2016.

E.W. Lane. Security from underseepage: Masonary dams ond earth foundations. Trans. Am. Soc. Civ. Eng., 100:1235 – 1272, 1935.

MVW. Voorschrift Toetsen op Veiligheid Primaire Waterkeringen. Technical report, Ministerie van Verkeer en Waterstaat, 2007.

M.L. Parekh, W. Kanning, C. Bocovich, M.A. Mooney, and A.R. Koelewijn. Backward Erosion Monitored by Spatial–Temporal Pore Pressure Changes during Field Experiments. Journal of Geotechnical and Geoenvironmental Engineering, 142, 2016.

Plaxis. PLAXIS Scientific Manual. Technical report, 2016.

RWS. Handreiking ontwerpen met overstromingskansen. Technical report, Rijkswaterstaat Water, Verkeer en Leefomgeving, 2017a.

RWS. Schematiseringshandleiding piping. Technical report, Rijkswaterstaat, Water Verkeer en Leefomgeving, 2017b.

RWS (Rijkswaterstaat). Actueel Hoogtebestand Nederland - AHN Viewer (online). URL `https://ahn.arcgisonline.nl/ahnviewer/{#}`.

H. Sellmeijer. On the mechanism of piping under impervious structures. PhD thesis, Delft University of Technology, 1988.

H. Sellmeijer, J. López de la Cruz, V.M. van Beek, and H. Knoeff. Fine-tuning of the backward erosion piping model through small-scale, medium-scale and IJkdijk experiments. European Journal of Environmental and Civil Engineering, 15:1139–1154, 2011.

J.B. Sellmeijer. Piping due to flow towards ditches and holes. In Proceedings Euromech 143, Delft, 1981.

J.B. Sellmeijer. Numerical computation of seepage erosion below dams (piping). In Third International Conference on Scour and Erosion, pages 596–601, 2006.

J.B. Sellmeijer and M.A. Koenders. A mathematical model for piping. Applied Mathematical Modelling, 15:646 – 651, 1991.

J.B. Sellmeijer, E.O.F. Calle, and J.W. Sip. Influence of aquifer thickness on piping below dikes and dams. In Proceedings of International symposium on analytical evaluation of dam related safety problems, pages 357 – 366, 1989.

F Silvis. Verificatie Piping Model: Proeven in de Deltagoot - Evaluatierapport. Technical report, Grondmechanica Delft, Delft, 1991.

TAW. Technical Report on Sand Boils (Piping). Technical report, Technische Adviescommissie voor de Waterkeringen, 1999.

TAW. Technisch Rapport Waterspanningen bij dijken. Technical Report september, Technische Adviescommissie voor de Waterkeringen, 2004.

TNO. DINOloket - Ondergrondmodellen. URL `https://www.dinoloket.nl/ondergrondmodellen`.

M. C. Tyler, A. Casagrande, S.J. Buchanan, K. E. Fields, W. Wells, W. J. Turnbull, C. I. Mansur, J. B. Eustis, and H. N. Fisk. Investigation of underseepage and its control, Lower Mississippi /River Levees. I(October):498, 1956.

USACE. Design and Construction of Levees - EM 1110-2-1913. Technical report, U.S. Army Corps of Engineers, 2000.

USACE. Design Guidance for Levee Underseepage. Technical report, U.S. Army Corps of Engineering, 2005.

Vera M. van Beek, Han Knoeff, and Hans Sellmeijer. Observations on the process of backward erosion piping in small-, medium- and full-scale experiments. European Journal of Environmental and Civil Engineering, 15(8):1115–1137, 2011.

V.M. van Beek. Backward Erosion Piping - Initiation and Progression. PhD thesis, Delft University of Technology, 2015.

V.M. van Beek, J.G. Knoeff, J. Rietdijk, J.B. Sellmeijer, and J. Lopez De La Cruz. Influence of sand characteristics and scale on the piping process - experiments and multivariate analysis. 2010.

V.M. Van Beek, A Bezuijen, J.B. Sellmeijer, and F.B.J. Barends. Initiation of backward erosion piping in uniform sands. Géotechnique, 64(12):927–941, 2014.

J M van Esch, J B Sellmeijer, and D. Stolle. Modelling transient Groundwater Flow and Piping under Dikes and Dams. 3rd International Symposium on Computational Geomechanics (ComGeo III), (1): 1–27, 2012.

O. Van Loon. POV Piping - PlaxFlow berekeningen voor de Maasvallei. Technical Report December, Arcadis, 2016.

J.B.A Weijers and J.B. Sellmeijer. A new model to deal with the piping mechanism. In Brauns, Schuler, and Heibaum, editors, Filters in geotechnical and hydraulic engineering: proceedings of the first International conference "Geo-filters', pages 349 – 355. Balkema, Rotterdam, 1993.

C.M. White. The Equilibrium of Grains on the Bed of a Stream. In Proceedings of the Royal Society of Londen. Series A, Mathematical and Physical Sciences, volume 174, pages 322–338. Royal Society, 1940.

A
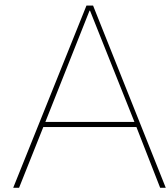
Groundwater Flow Model
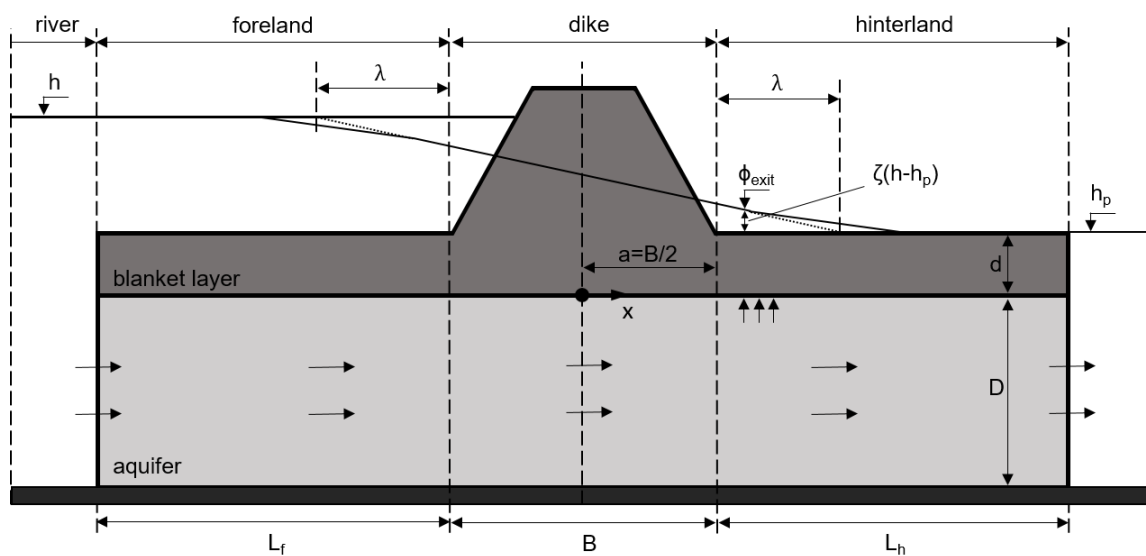
Figure A.1: Groundwater flow model (after [Jonkman and Schweckendiek, 2015, TAW, 2004])

Parameters and assumptions

h	River water level	[m]
h_p	Water level in hinterland (ground level)	[m]
h_a	Height of the top of the aquifer	[m]
h_g	Ground level	[m]
d	Thickness of blanket layer	[m]
D	Thickness of aquifer	[D]
L_f	Length of foreland	[m]
B	Dike width	[m]
L_h	Length of hinterland	[m]
ϕ_{exit}	Potential at exit point	[m]
$\phi_{c,u}$	Critical potential	[m]
$\Delta\phi$	Difference between potential and polder water level	[m]
k_a	Hydraulic conductivity of the aquifer	[m/d]
k_b	Hydraulic conductivity of the blanket layer	[m/d]
γ_w	Unit weight of water	[kN/m^3]
γ_{sat}	Saturated unit weight of the blanket layer	[kN/m^3]

The model is based on several assumptions:
- The groundwater flow in the aquifer is assumed horizontal
- The groundwater flow through the blanket layer is assumed vertical (leakage)
- The hydraulic head at the entry point is assumed equal to the river water level h
- The hydraulic head far in the hinterland is assumed equal to the polder level h_p
- The polder level h_p is assumed equal to the ground level h_g

Occurring potential

The flow resistances in the foreland, hinterland and underneath the dike are characterized as:

$$W_f = \frac{\lambda_f}{k_a D} tanh \frac{L_f}{\lambda_f} \tag{A.1}$$

$$W_h = \frac{\lambda_h}{k_a D} tanh \frac{L_h}{\lambda_h} \tag{A.2}$$

$$W_f = \frac{B}{k_a D} \tag{A.3}$$

The properties of the blanket layer are assumed to be equal in the foreland and hinterland. Therefore, $\lambda_f = \lambda_h = \lambda$. λ is the leakage factor which accounts for the leakage through the blanket layer.

$$\lambda = \sqrt{k_a D c} \tag{A.4}$$

where, c is the resistance factor of the blanket layer defined as:

$$c = \frac{d}{k_b} \tag{A.5}$$

The leakage factor λ then becomes:

$$\lambda = \sqrt{\frac{k_a D d}{k_b}} \tag{A.6}$$

The total resistance is:

$$\Sigma W = W_f + W_d + W_h \tag{A.7}$$

The for piping relevant exit point is located in the hinterland. Therefore, only the mathematical formulation of the potential in the hinterland is explained. Based on the above presented formulations the potential at the inner toe of the dike can be determined according to the following formula.

$$\phi(B/2) = h_p + (h - h_p)\frac{W_h}{\Sigma W} = h_p + (h - h_p)\frac{\lambda tanh\frac{L_h}{\lambda}}{\lambda tanh\frac{L_f}{\lambda} + B + \lambda tanh\frac{L_h}{\lambda}} \tag{A.8}$$

The development of the potential in the hinterland is given by:

$$\phi(x) = h_p + (\phi(B/2) - h_p)\frac{sinh\frac{\frac{B}{2}+L_h-x_{exit}}{\lambda}}{sinh\frac{L_h}{\lambda}} \tag{A.9}$$

Two simplifications can be applied to simplify Formula A.9:

1. In case of a continuous blanket layer in the hinterland, $\frac{L_f}{\lambda}$ and $\frac{L_h}{\lambda}$ > 1.8 - 2, the resistance factor of the hinterland can be approximated by $W_h \approx \frac{\lambda}{k_a D}$. The development of the potential can be approximated by:

$$\phi(x) \approx h_p + (\phi(B/2) - h_p)exp^{\frac{\frac{B}{2}-x_{exit}}{\lambda}} \tag{A.10}$$

2. In case of a finite blanket layer in the foreland, $\frac{L_f}{\lambda}$ and $\frac{L_h}{\lambda}$ < 0.5, the resistance factor of the foreland can be approximated by $W_f \approx \frac{L_f}{k_a D}$.

These simplifications are assumed to be valid for the situation in the Maasvallei. Combining the simplifications and the formulation presented in formula A.8 results in a usable formulation for the development of the potential in the hinterland, Formula A.12.

$$\phi(B/2) = h_p + (h - h_p)\frac{\frac{\lambda}{k_a D}}{\frac{L_f}{k_a D} + \frac{B}{k_a D} + \frac{\lambda}{k_a D}} = h_p + (h - h_p)\frac{\lambda}{L_f + B + \lambda} \tag{A.11}$$

$$\phi(x) = h_p + (h - h_p)\frac{\lambda}{L_f + b + \lambda}exp^{\frac{\frac{B}{2} - xexit}{\lambda}} \tag{A.12}$$

Critical potential

The critical potential is reached when the upward water pressure in the aquifer equals the weight of the blanket layer. At that point the effective stress at the interface between the aquifer and the blanket layer equals zero. Assuming a phreatic water level in the hinterland equal to ground level, the critical point is described as:

$$\begin{aligned}
(\phi_{c,u} - h_a)\gamma_w &= (h_g - h_a)\gamma_{sat} \\
(\Delta\phi_{c,u} + d)\gamma_w &= d\gamma_{sat} \\
\gamma_w\Delta\phi_{c,u} &= d\gamma_{sat} - d\gamma_w \\
\Delta\phi_{c,u} &= d\frac{\gamma_{sat} - \gamma_w}{\gamma_w} \\
\phi_{c,u} &= h_p + d\frac{\gamma_{sat} - \gamma_w}{\gamma_w}
\end{aligned} \tag{A.13}$$

B

Overview soil investigation
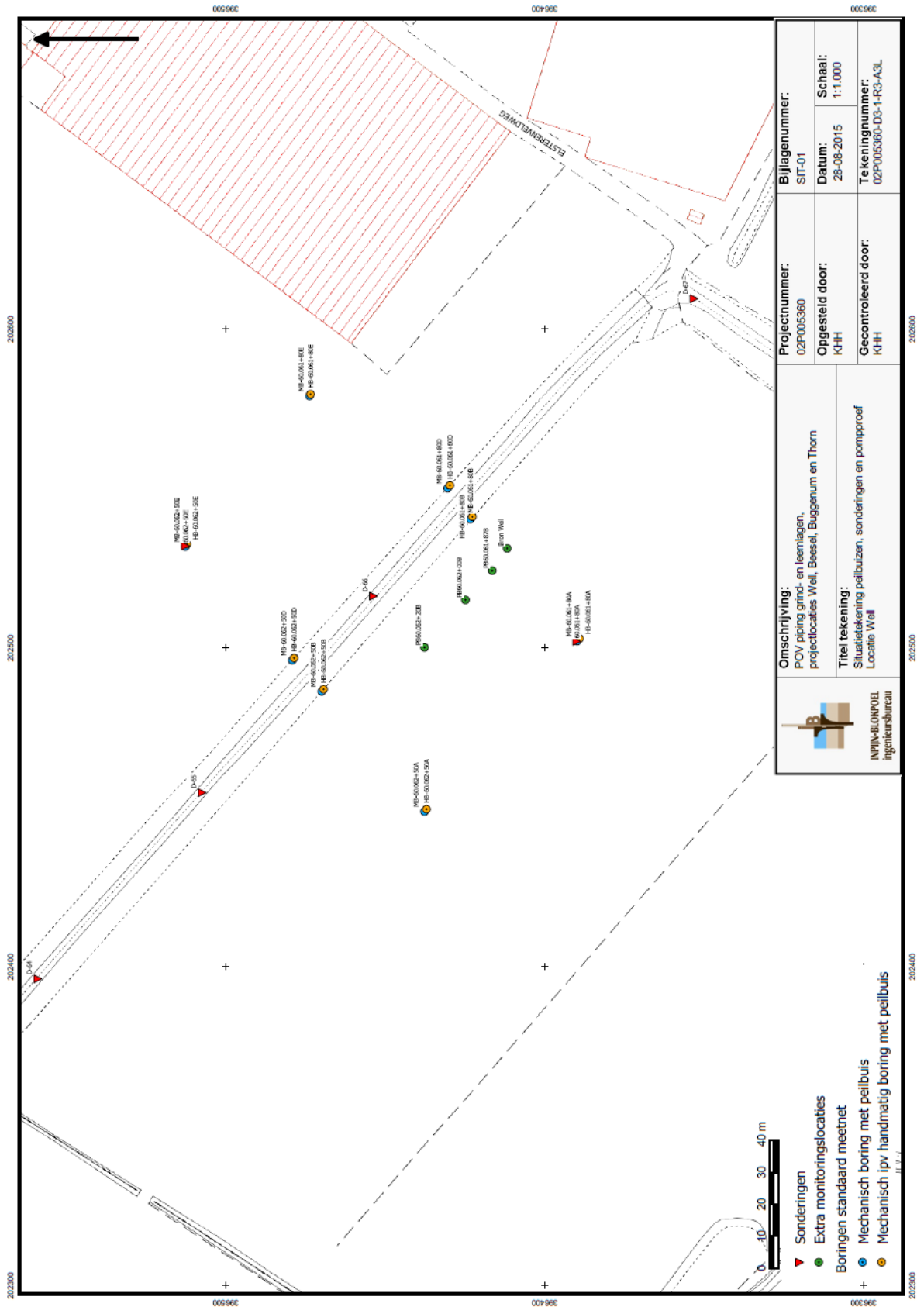
Figure B.1: Soil investigation Well

benaming	x-coord	y-coord	maaiveld [	kpb [NAP]	Uitvoering
MB-75.030+50A	196329.03	359997.37	18.43	18.4	mechanisch boren
MB-75.030+50B	196273.47	360026.27	18.81	19.04	mechanisch boren
HB-75.030+50B	196272.97	360025.26	18.81	19.01	handboren
MB-75.030+50D	196257.53	360033.95	18.3	18.52	mechanisch boren
HB-75.030+50D	196257.06	360033.03	18.3	18.53	handboren
MB-75.030+50E	196213.42	360056.89	16.77	17.03	mechanisch boren
HB-75.030+50E	196212.82	360056.09	16.77	16.95	handboren
Mb-75.030+85A	196344.89	360015.85	18.32	18.31	mechanisch boren
HB-75.030+85B	196288.2	360052.53	18.91	19.12	handboren
MB-75.030+85D	196287.57	360051.55	18.91	19.15	mechanisch boren
HB-75.030+85D	196272.17	360060.53	18.1	18.33	mechanisch boren
MB-75.030+85D	196271.68	360059.67	18.1	18.29	handboren
MB-75.030+85E	196227.95	360084.93	16.58	16.84	mechanisch boren
HB-75.030+85E	196227.24	360083.98	16.58	16.6	handboren

Figure B.2: Soil investigation Beesel
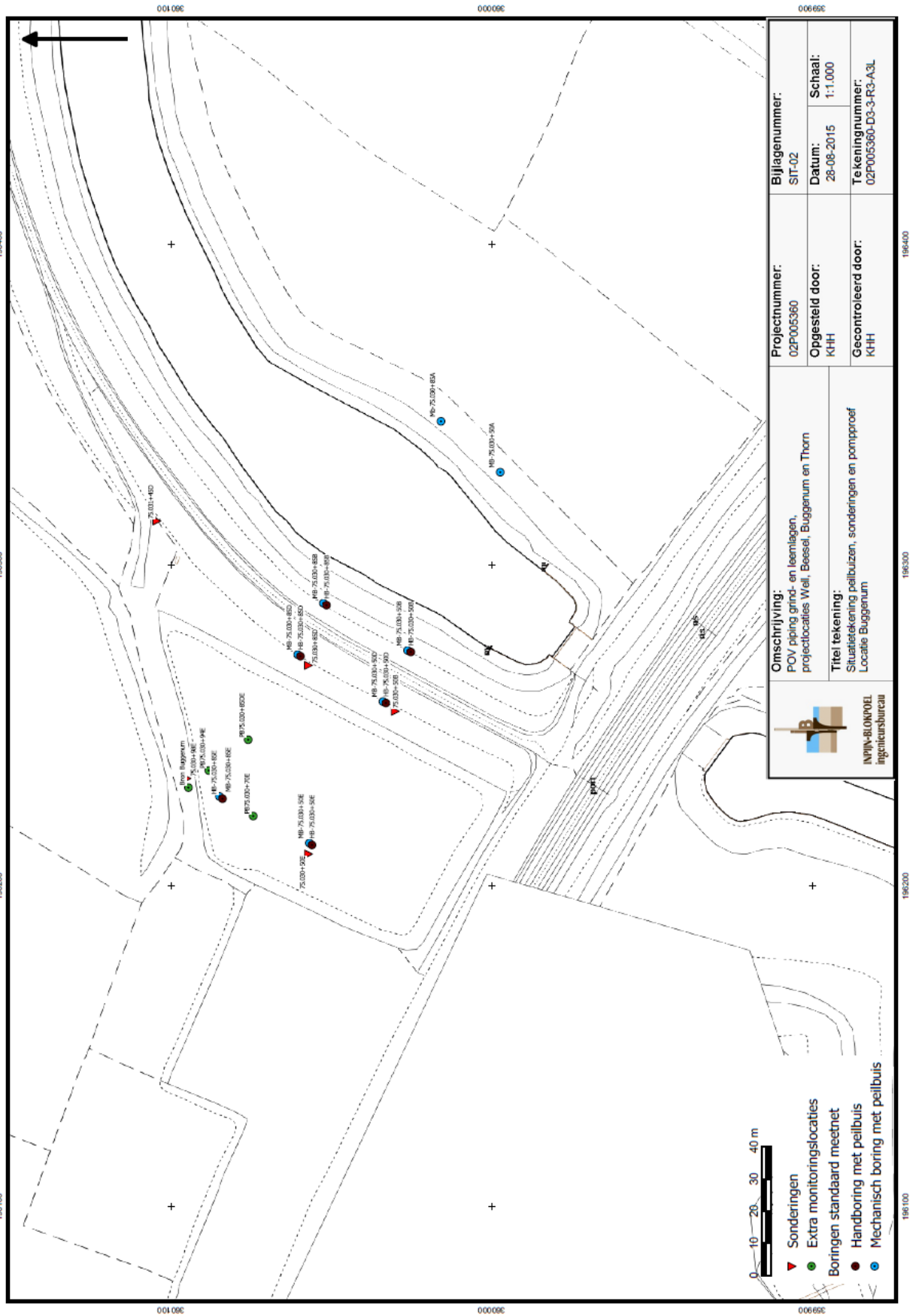
Figure B.3: Soil investigation Buggenum

Figure B.4: Soil investigation Thorn

C
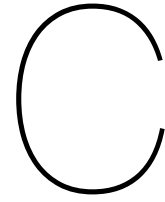
Schematisations Research Locations

Location Well

The drillings were performed in two transects referred to as transect 60.061+80 and 60.062+50 indicating the location along the dike ring. The schematisation was based on transect 60.062+50 because of the presence of clay in the cover layer. At transect 60.061+80 the cover layer solely exists of sand. At point B a clay layer of 1.5 m thickness is present. This clay layer is absent at point A. Due to the uncertainty with regard to the presence of this layer between point A and B, the assumption was made that the clay layer ends at point B. An extension of the clay layer towards point A would lead to an increase of the leakage length resulting in a decrease of the exit gradient and thereby a decrease of the likelihood to piping. The base of the first gravel layer was assumed at +4 m NAP based on the CPT at point E and the drilling performed at the well of the pumping test. This drilling is considerably deeper than the drillings at the transects. The thickness of the fine sand layer following the first gravel layer was also based on the CPT at point E and the drilling at the well. The fine sand layer is followed by a second gravel layer. The base of this layer was based on the CPT at point E and a deep drilling from Dinoloket. The drilling has a distance of 377 m with respect to point E. The CPT at point E ends at -6 m NAP indicating gravel. The drilling from Dinoloket showed the transition from the Kiezeloöliet formation to the formation of Breda at about -5 m NAP. Due to the absence of the end of the gravel layer on the CPT data it was assumed that the transition to the formation of Breda marks the base of the gravel layer. The first and second gravel layer and the fine sand layer were assumed horizontal due to a lack of information concerning the exact depths at the other points. The schematised cross-section of Well is depicted in Figure C.1.

Location Beesel

In contrast to the other locations limited information was available for the location near Beesel. The performed site investigation related to the POV Piping project only concerned the two transects with sixteen drillings. The transects are referred to as 73.035+50 and 73.036+50. The schematisation was based on transect 73.035+50 because of the presence of a clay layer in the hinterland. This layer is absent at transect 73.036+50. The presence of a clay layer in the hinterland allows for a pressure to develop and prevents diffused exit of the seepage flow. However, the sand layer at transect 73.035 is very thin with a complete absence at point B. On the other hand, the drillings at transect 73.036+50 showed a thick layer of sand. Therefore, the thickness of the sand layer was assumed larger than observed. The top and bottom of the layer between point A and E were connected ensuring a continues sand layer. It was assumed that such a soil composition is likely to occur. The schematised cross-section of Beesel is depicted in Figure C.2.

Location Buggenum

The geometry of Buggenum is different with respect to the other locations. Point A is situated on the other side of the water instead of in the foreland. Besides, a berm on both the inner side and outer side of the dike is present. The transects equipped with a measurement system are referred to as transect 75.030+85 and 75.030+50. The schematisation used in this study was adopted from the earlier work

which concerns the numerical modelling of the groundwater flow for this location [Van Loon, 2016]. The schematisation was based on transect 75.030+85 because of the central position in the dike ring. Exact information concerning the depth of the channel was absent. Therefore, the bottom of the channel was assumed at +12 NAP. The thickness of the soil layers was based on both the drillings and the results of the pumping test. The results of the pumping test deviate from the drillings, in particular with respect to the thickness of the sand layer. The selected thickness lies in between the two values. The schematised cross-section of Buggenum is depicted in Figure C.3.

Location Thorn

The drillings were performed in two transects referred to as transect 79.037 and 79.037+50. The schematisation used in this study was adopted from the work of Van Loon (2016). The schematisation was based on transect 79.037 because of the central position in the dike ring. The drillings showed several gravel pockets in the sand layer. The local presence of these gravel pockets decreases the likelihood to piping and were therefore disregarded in the schematisation. It was assumed that a soil composition without the local presence of gravel is likely to occur. The schematised cross-section of Thorn is depicted in Figure C.4.
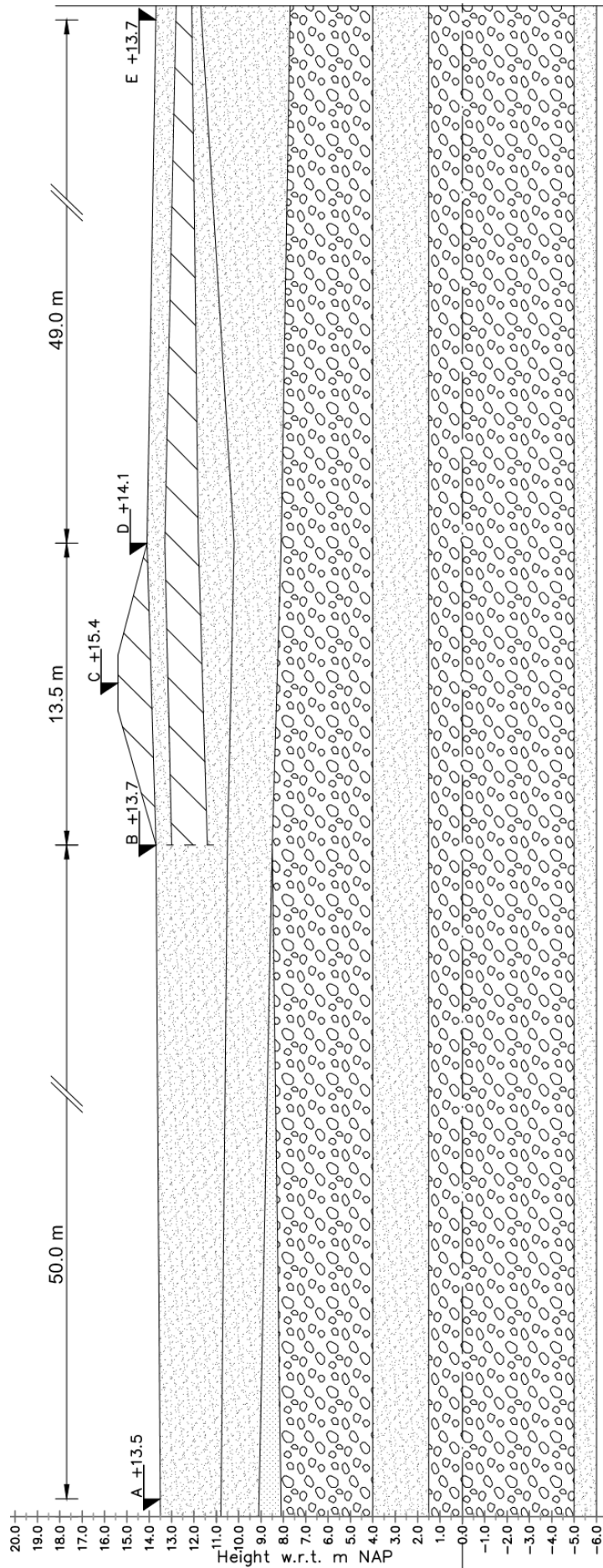
Figure C.1: Schematisation Well
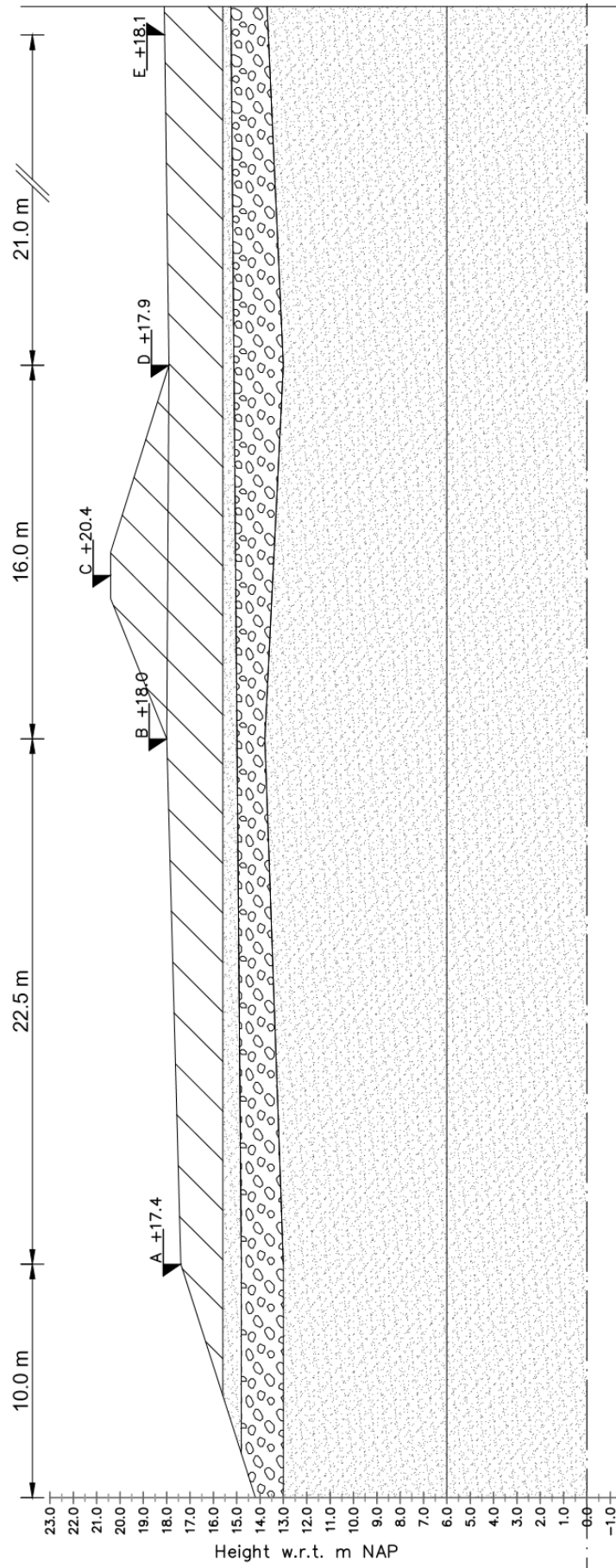
Figure C.2: Schematisation Beesel
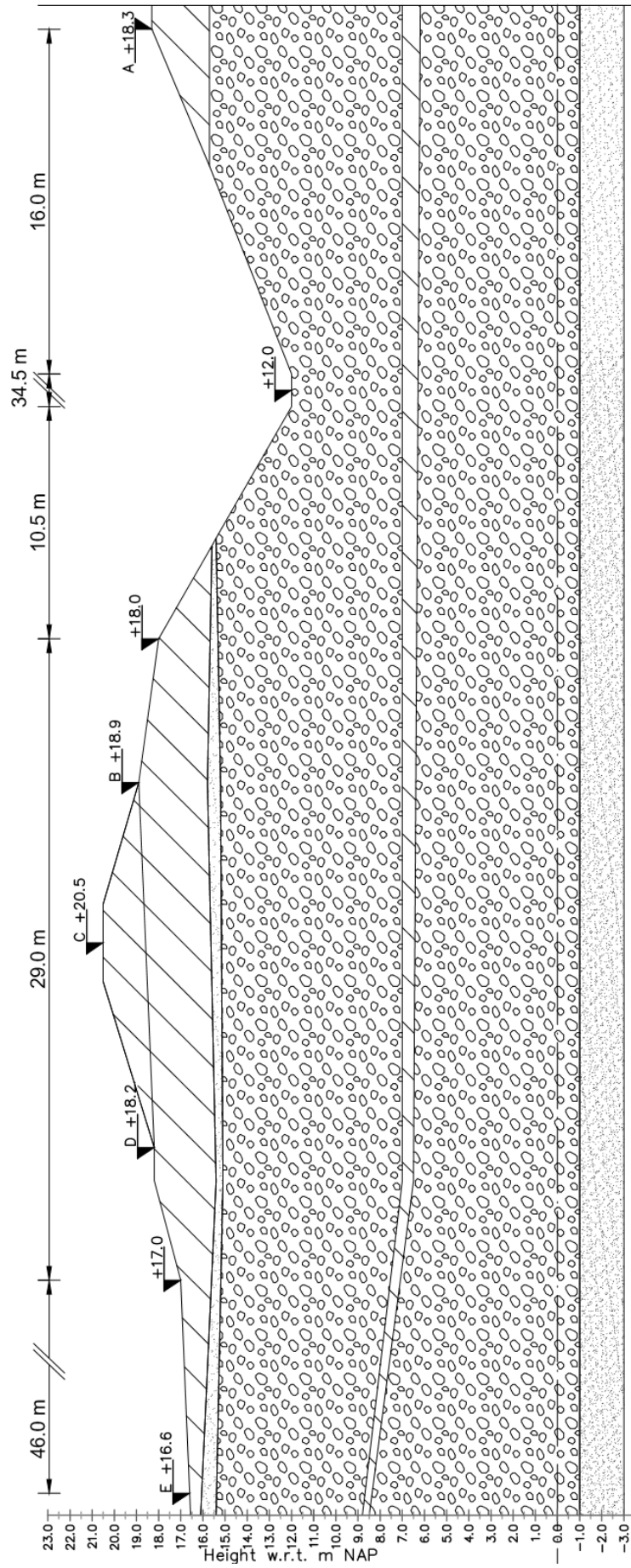
Figure C.3: Schematisation Buggenum
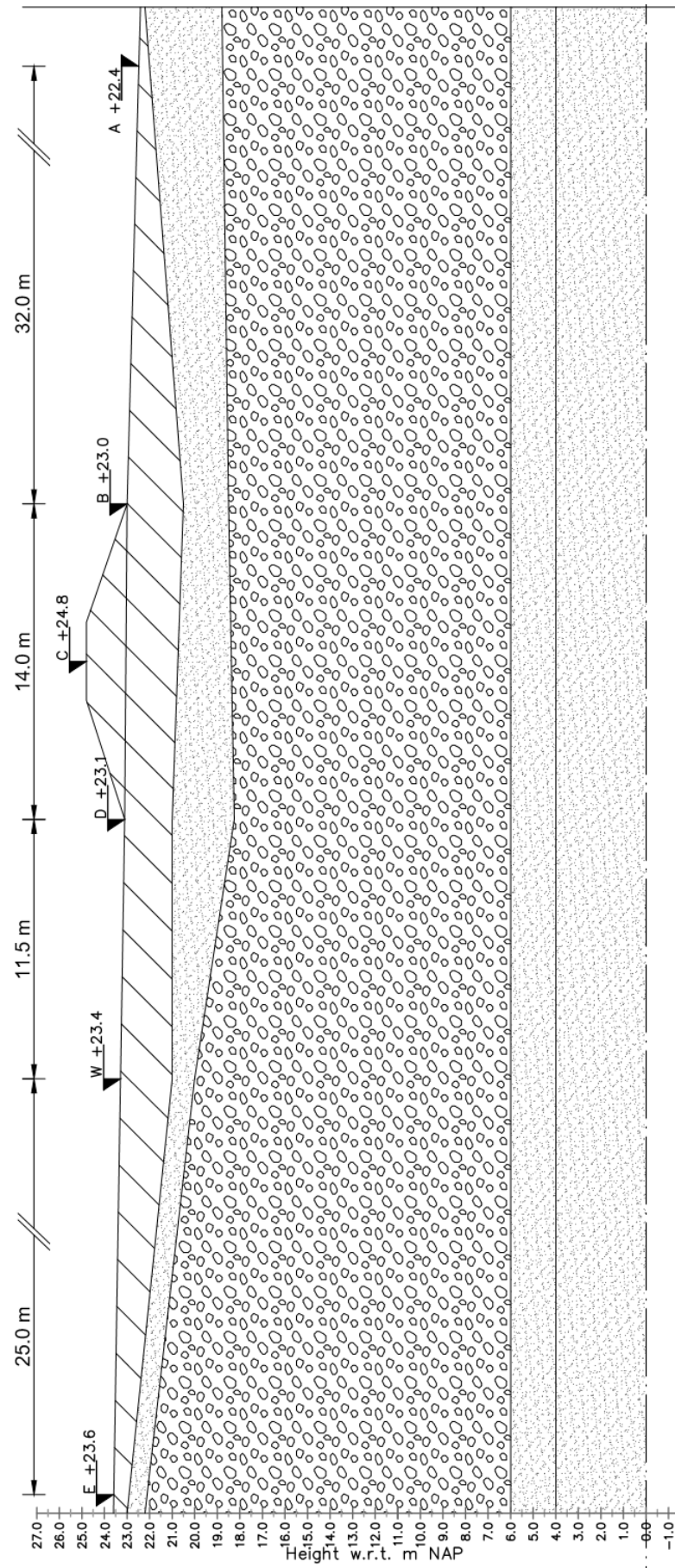
Figure C.4: Schematisation Thorn

<div style="text-align: right; font-size: 4em;">D</div>
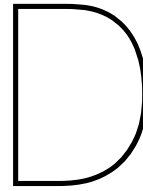
Appendix Analytical Analysis

This appendix corresponds to Chapter 4, the Analytical Analysis. The first section discusses the parameter selection and presents the initial parameter sets of the analytical calculations. The second section includes graphs that resulted from the sensitivity analysis.

D.1. Parameters

For the analytical analysis an initial set of parameters was selected based on best estimates for each research location. The initial parameter values were selected based on the available information as discussed in Chapter 3. The parameters for each locations are included in Tables D.1 to D.4.

The hinterland water level was chosen to be equal to ground level. The thickness of the blanket layer was based on the schematisations. The thickness of the blanket layer below the dike and directly behind the dike was considered and a representative average thickness was selected. The selected thickness of the aquifer depended on the presence of a deep impermeable or semi impermeable layer. In case such a layer was not present in the deeper subsoil an aquifer thickness of 100 m was assumed. The width of the dike followed directly from the schematisation. A possible present berm was included in the dike width. The included foreland length was based on the thickness of the blanket layer in the foreland. In the case of the location near Well the presence of the top clay layer cannot be guaranteed due to the fact that the drilling at point A does not contain clay. Therefore the foreland length was assumed to be zero. At the location near Beesel a continuous thick clay layer is present in the foreland. Therefore, the complete foreshore length was included. In Buggenum the thickness of the blanket layer was considered to thin to include the foreland. For the location near Thorn, half of the foreshore length was included based on sufficient thickness of the blanket layer. In all cases a blanket layer thickness of 1.5 m was considered sufficient. In practice the extent to which the foreland length is included depends also on the control area of the water board. As mentioned, such legal directives are not taken into account in this study. In all four cases the exit point was assumed at the inner toe of the dike. Within the analytical model the thickness of the blanket layer is considered continuous. Local deviations resulting in a smaller blanket layer thickness are not taken into account. Therefore, the exit point was chosen at the inner toe since this resulted in the smallest seepage length and thus the highest possibility for piping. The hydraulic conductivity of the aquifer, hydraulic conductivity of the blanket layer and the saturated volumetric weight of the blanket layer were selected based on test results available from the POV Piping project. The hydraulic conductivity of the aquifer was based on a weighted average of the permeabilities of the upper sand and gravel layers. In the case of the location near Beesel no test results were available. Therefore, Dinoloket [TNO] was used and an average value corresponding to the hydraulic conductivity at the other locations was selected. For all four locations a hydraulic conductivity of the blanket layer of 0.2 m/d was chosen. This value was initially established in the POV Piping project. During this study, the value was reconsidered based on new information. At that time, it was concluded that 0.5 is a more realistic value for the hydraulic conductivity of the blanket layer in the Maasvallei. The porosity of the aquifer was assumed to be 0.35. The constant of White, bedding angle of sand, kinematic viscosity of water and the d_{70} reference value were standard values derived from

<div style="text-align: center;">79</div>

literature [Förster et al., 2012, RWS, 2017b, Sellmeijer et al., 2011, TAW, 1999, van Beek, 2015]. The 70%-fractile of the grain size distribution was for all four locations 250 μm, which was established in the POV Piping project based on test results. This value corresponded to the grain size at the top of the aquifer. For the locations near Well and Buggenum a relative density was determined. Therefore, the cone resistance at the top of the sand layer was assessed. The outside water level used as a starting point in the initial parameter set was based on a water level scenario considering the current climate conditions and a return period of 50 years. The variation coefficient for d_{70} was adapted from the Dutch guideline [RWS, 2017b]. The other variation coefficient were based on a logic common range of values.

Table D.1: Parameters Well

parameter	symbol	unity	value	variation coeff.
outside water level	h	m + NAP	15.36	0.05
hinterland water level	h_p	m + NAP	14	
volumetric weight of water	γ_w	kN/m^3	9.81	
thickness blanket layer	d	m	1.5	0.25
thickness aquifer	D	m	7.5	0.25
dike width	B	m	13.5	
length foreland	L_f	m	0	0.25
exit point	x_{exit}	m	6.75	
hydraulic conductivity aquifer	k_a	m/d	64.4	0.25
hydraulic conductivity blanket layer	k_b	m/d	0.2	0.25
saturated volumetric weight blanket layer	γ_{sat}	kN/m^3	20.4	
volumetric weight sand grains	γ_s	kN/m^3	26	
aquifer porosity	n	-	0.35	
White's constant	η	-	0.25	
bedding angle sand	θ	degrees	37	
kinematic viscosity of water	ν	m^2/s	$1.33 \cdot 10^{-6}$	
70%-fractile grain size distribution of sand	d_{70}	μm	250	0.12
d_{70} reference value	d_{70m}	μm	208	
mean relative density	RD_m	%	72.5	
cone resistance at top sand layer (at 2.1 m depth)	q_c	MPa	8	

Table D.2: Parameters Beesel

parameter	symbol	unity	value	variation coeff.
outside water level	h	m + NAP	20.24	0.05
hinterland water level	h_p	m + NAP	18	
volumetric weight of water	γ_w	kN/m^3	9.81	
thickness blanket layer	d	m	2.5	0.25
thickness aquifer	D	m	100	0.25
dike width	B	m	16	
length foreland	L_f	m	28.5	0.25
exit point	x_{exit}	m	8	
hydraulic conductivity aquifer	k_a	m/d	60	0.25
hydraulic conductivity blanket layer	k_b	m/d	0.2	0.25
saturated volumetric weight blanket layer	γ_{sat}	kN/m^3	20	
volumetric weight sand grains	γ_s	kN/m^3	26	
aquifer porosity	n	-	0.35	
White's constant	η	-	0.25	
bedding angle sand	θ	degrees	37	
kinematic viscosity of water	ν	m^2/s	$1.33 \cdot 10^{-6}$	
70%-fractile grain size distribution of sand	d_{70}	μm	250	0.12
d_{70} reference value	d_{70m}	μm	208	

Table D.3: Parameters Buggenum

parameter	symbol	unity	value	variation coeff.
outside water level	h	m + NAP	20.64	0.05
hinterland water level	h_p	m + NAP	17	
volumetric weight of water	γ_w	kN/m^3	9.81	
thickness blanket layer	d	m	1.5	0.25
thickness aquifer	D	m	8	0.25
dike width	B	m	29	
length foreland	L_f	m	0	0.25
exit point	x_{exit}	m	14.5	
hydraulic conductivity aquifer	k_a	m/d	58.22	0.25
hydraulic conductivity blanket layer	k_b	m/d	0.2	0.25
saturated volumetric weight blanket layer	γ_{sat}	kN/m^3	20	
volumetric weight sand grains	γ_s	kN/m^3	26	
aquifer porosity	n	-	0.35	
White's constant	η	-	0.25	
bedding angle sand	θ	degrees	37	
kinematic viscosity of water	ν	m^2/s	$1.33 \cdot 10^{-6}$	
70%-fractile grain size distribution of sand	d_{70}	μm	250	0.12
d_{70} reference value	d_{70m}	μm	208	
mean relative density	RD_m	%	72.5	
cone resistance at top sand layer (at 2.55 m depth)	q_c	MPa	13	

Table D.4: Parameters Thorn

parameter	symbol	unity	value	variation coeff.
outside water level	h	m + NAP	24.62	0.05
hinterland water level	h_p	m + NAP	23	
volumetric weight of water	γ_w	kN/m^3	9.81	
thickness blanket layer	d	m	2	0.25
thickness aquifer	D	m	88	0.25
dike width	B	m	14	
length foreland	L_f	m	16	0.25
exit point	x_{exit}	m	7	
hydraulic conductivity aquifer	k_a	m/d	60	0.25
hydraulic conductivity blanket layer	k_b	m/d	0.2	0.25
saturated volumetric weight blanket layer	γ_{sat}	kN/m^3	20.1	
volumetric weight sand grains	γ_s	kN/m^3	26	
aquifer porosity	n	-	0.35	
White's constant	η	-	0.25	
bedding angle sand	θ	degrees	37	
kinematic viscosity of water	ν	m^2/s	$1.33 \cdot 10^{-6}$	
70%-fractile grain size distribution of sand	d_{70}	μm	250	0.12
d_{70} reference value	d_{70m}	μm	208	

D.2. Graphs sensitivity analysis

Figures D.1 to D.4 present graphs in which the varying parameter values are plotted against the resulting gradients for each mechanism. On the horizontal axis the individual parameters are plotted. The range of values was determined by means of the variation coefficient. On the vertical axes the potential difference $\Delta\phi$, vertical gradient i and in some cases the overall hydraulic head difference H are plotted. The solid blue line indicates the potential difference at the exit point $\Delta\phi_{exit}$ and the dashed blue line indicates the critical exit potential $\Delta\phi_{c,u}$. The solid orange line indicates the vertical gradient at the exit point i and the dashed orange lines indicates the critical vertical heave gradients (0.5 and 0.8) $i_{c,h}$. The solid green line indicates the critical horizontal head difference according to Sellmeijer H_c

and the dashed green line indicates the occurring head difference H. In addition, a vertical solid red line indicates the initial (mean) parameter value.

Figure D.5, D.6 and D.7 show tornado plots for the research locations near Well, Beesel and Thorn respectively. The tornado plot of Buggenum is included in Chapter 4.
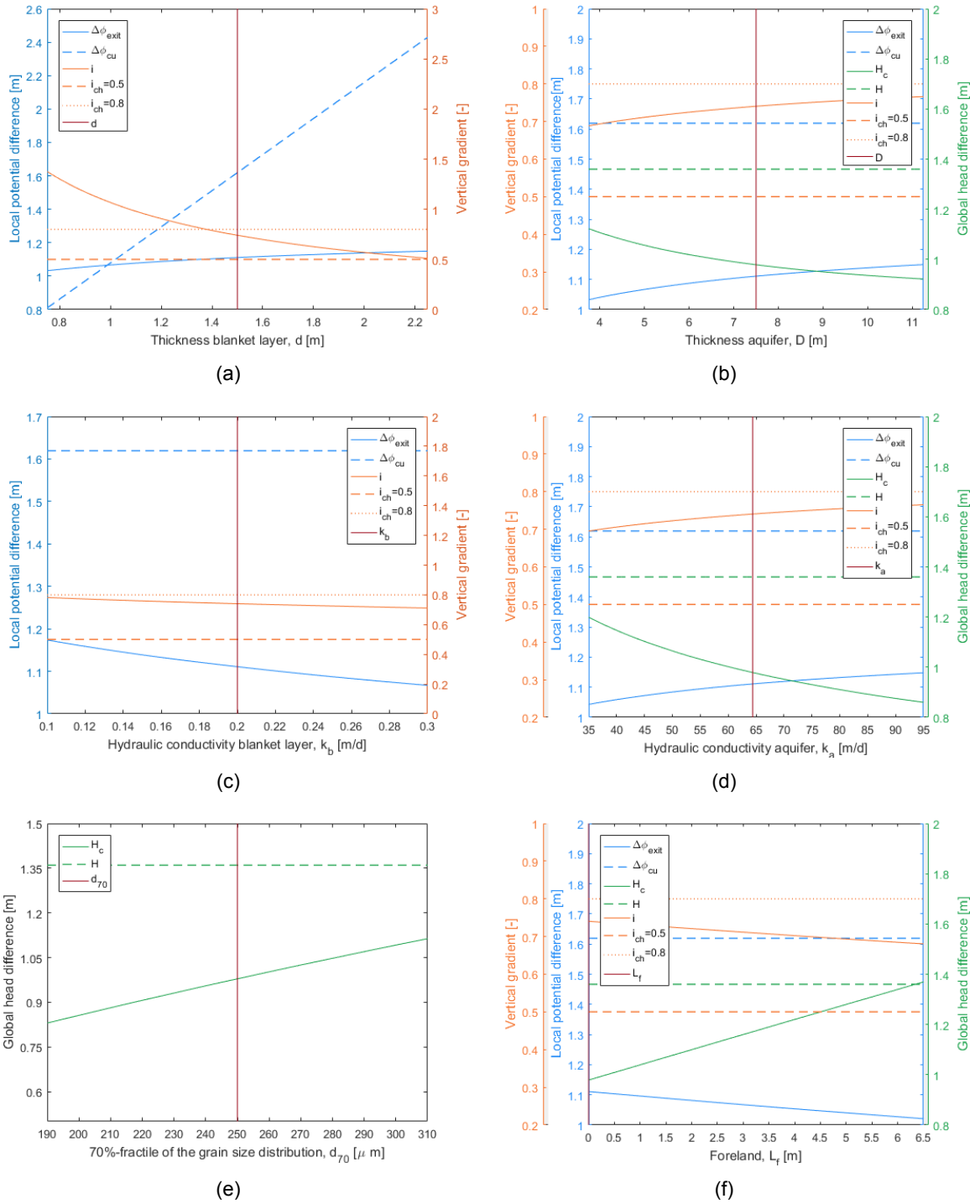
Figure D.1: Influence of parameter variation on exit potential, exit gradient en critical hydraulic head for the research location near Well
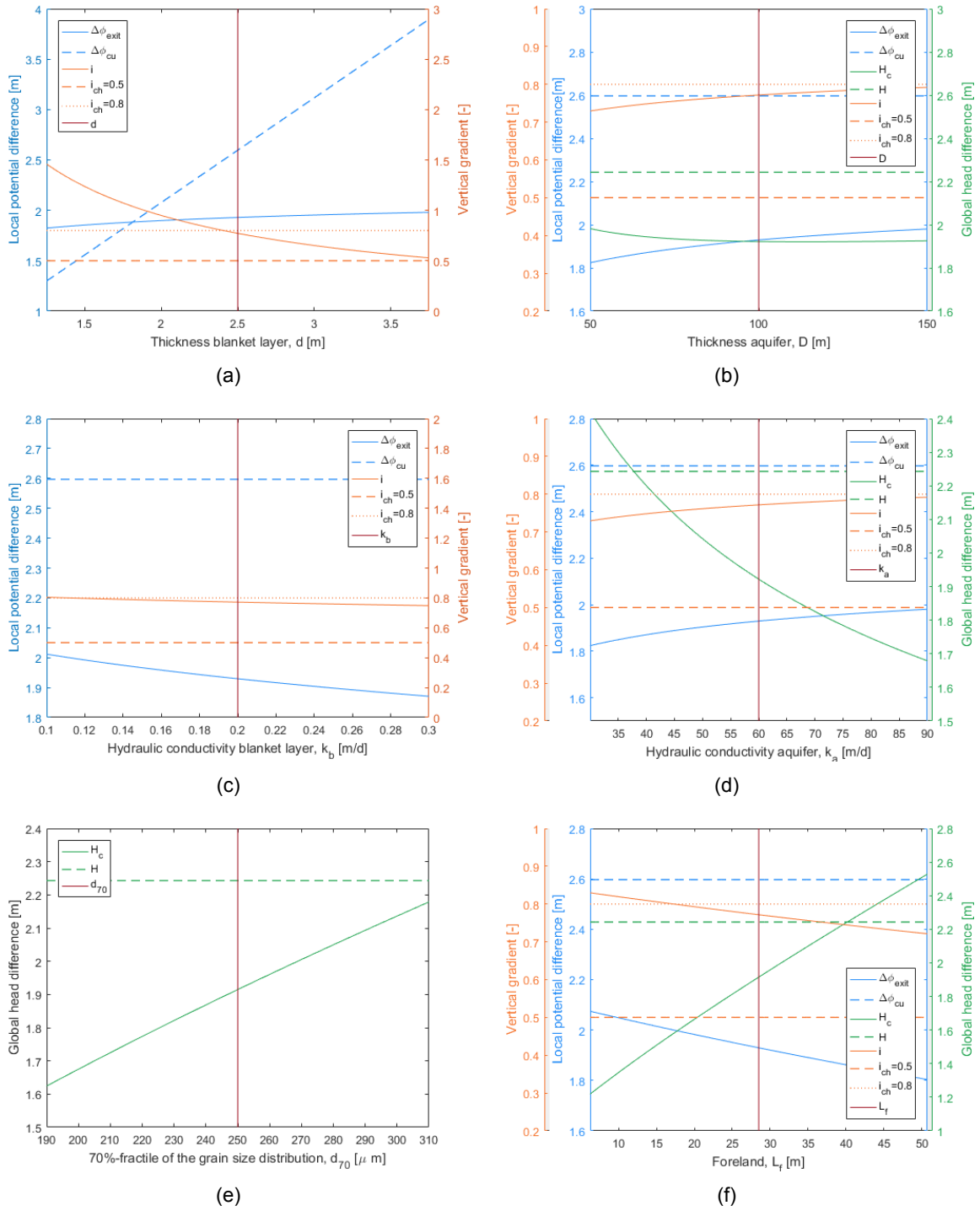
Figure D.2: Influence of parameter variation on exit potential, exit gradient en critical hydraulic head for the research location near Beesel

(a)

(b)

(c)

(d)

(e)

(f)
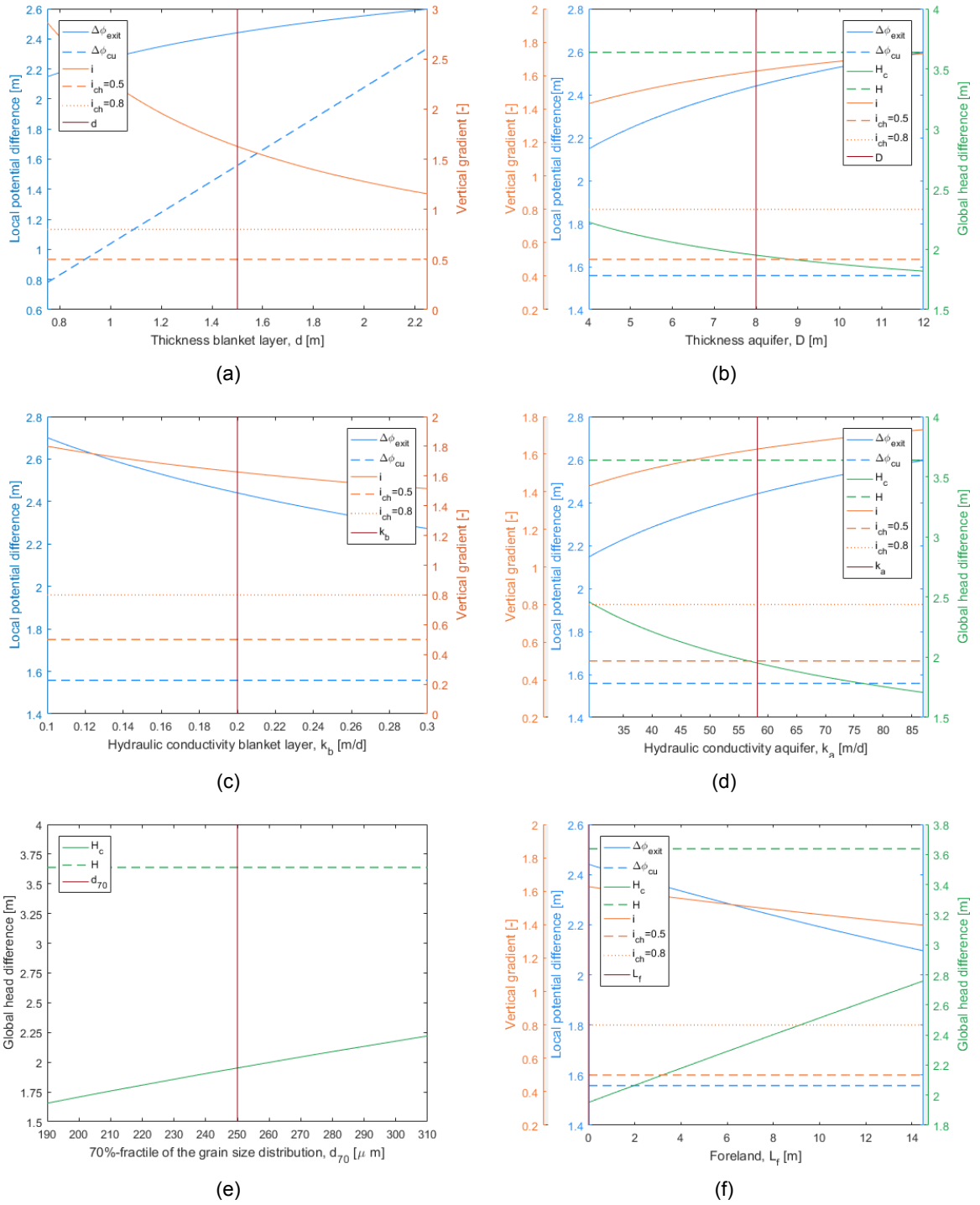
Figure D.3: Influence of parameter variation on exit potential, exit gradient en critical hydraulic head for the research location near Buggenum
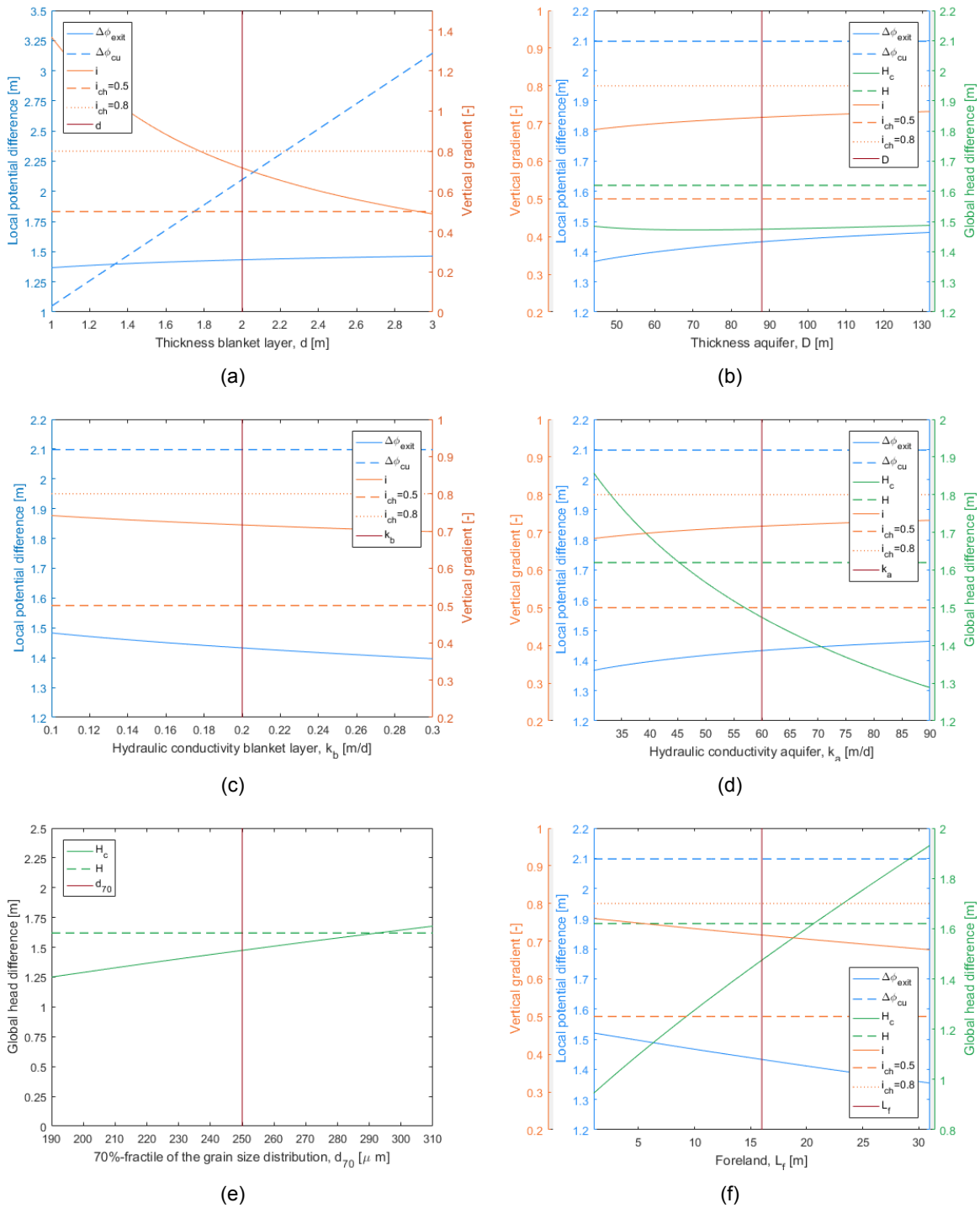
Figure D.4: Influence of parameter variation on exit potential, exit gradient en critical hydraulic head for the research location near Thorn

(a)

(b)

(c)

(d)

(e)
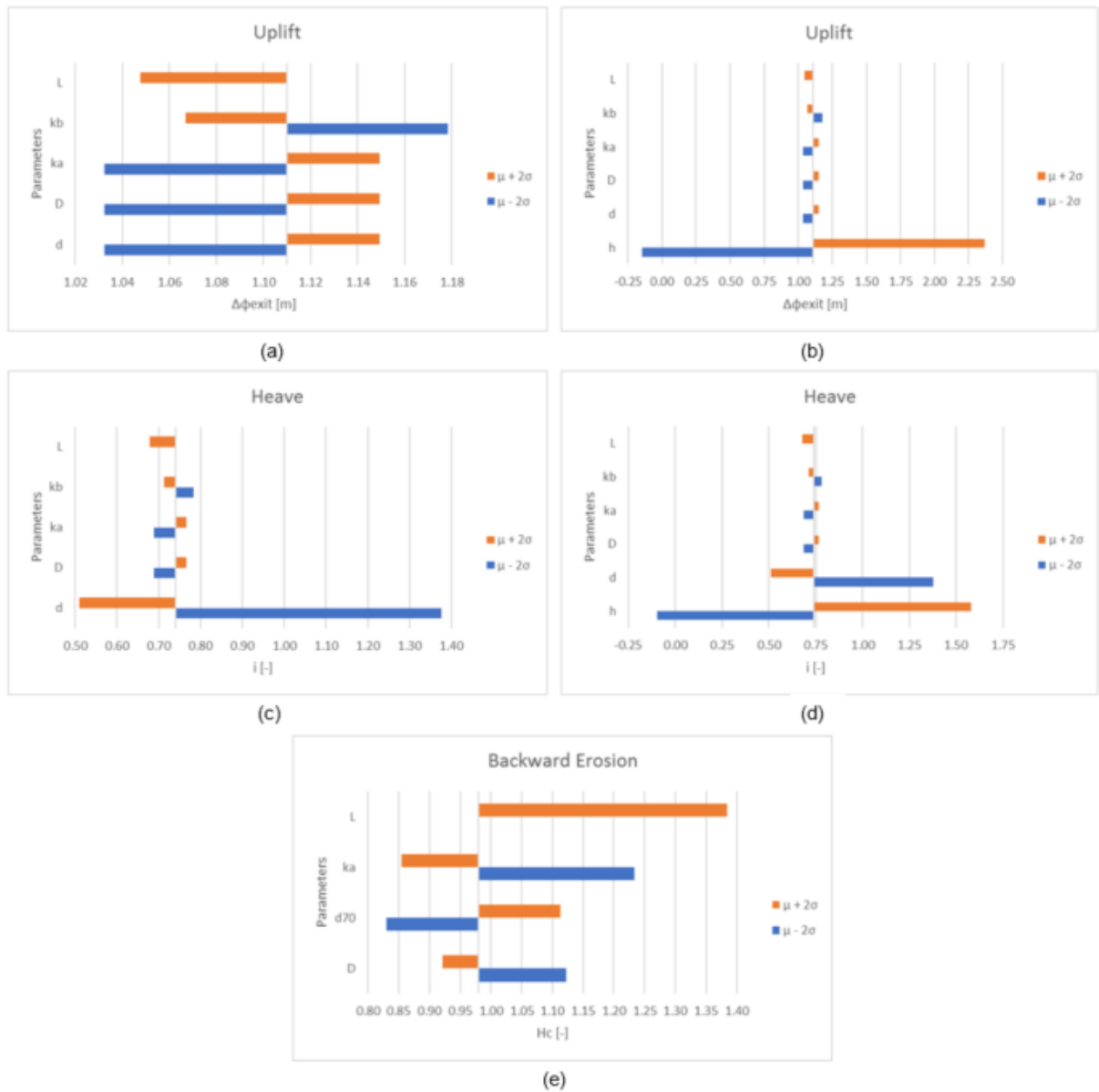
Figure D.5: Parameter sensitivity for the research location near Well
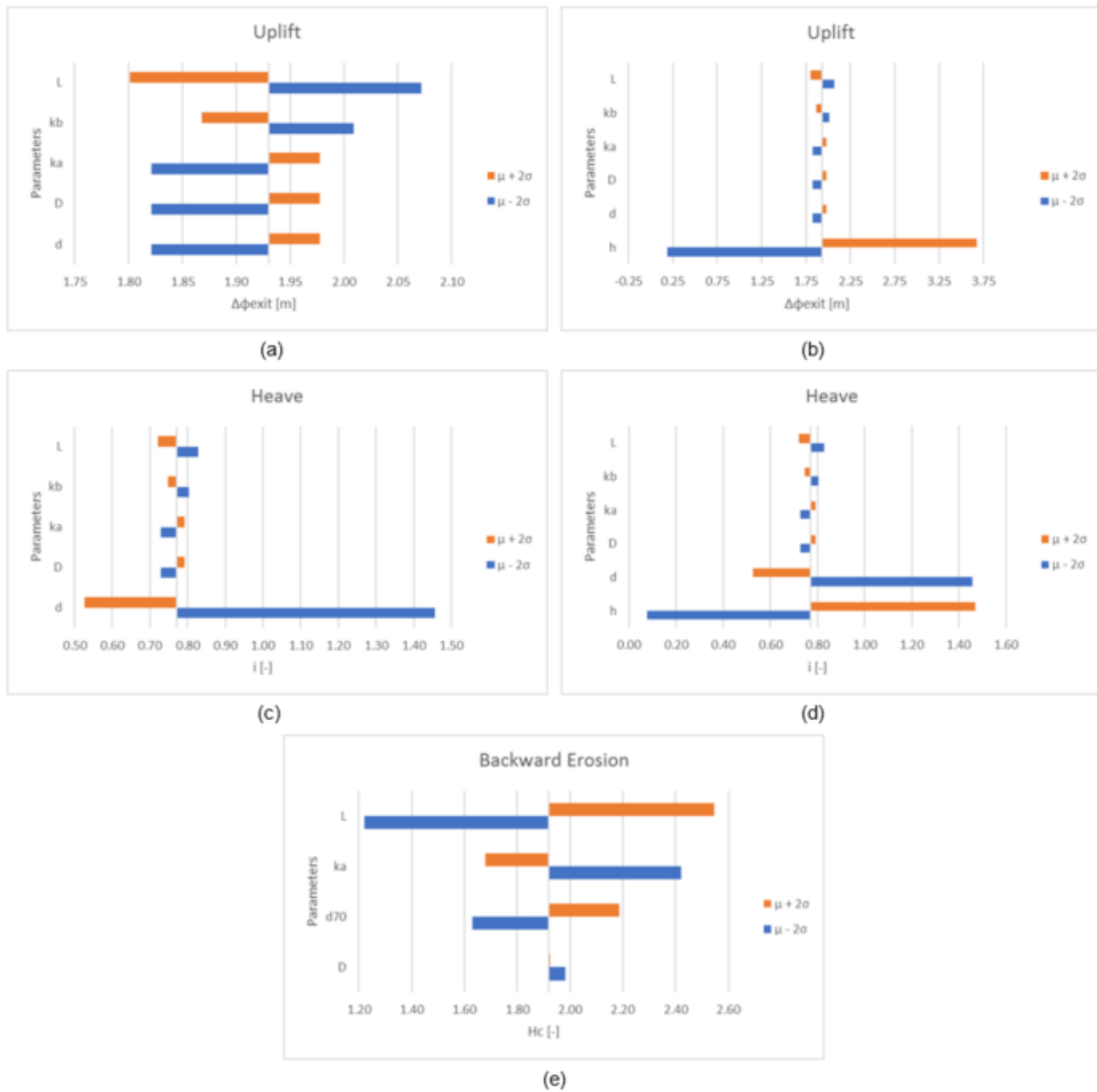
Figure D.6: Parameter sensitivity for the research location near Beesel
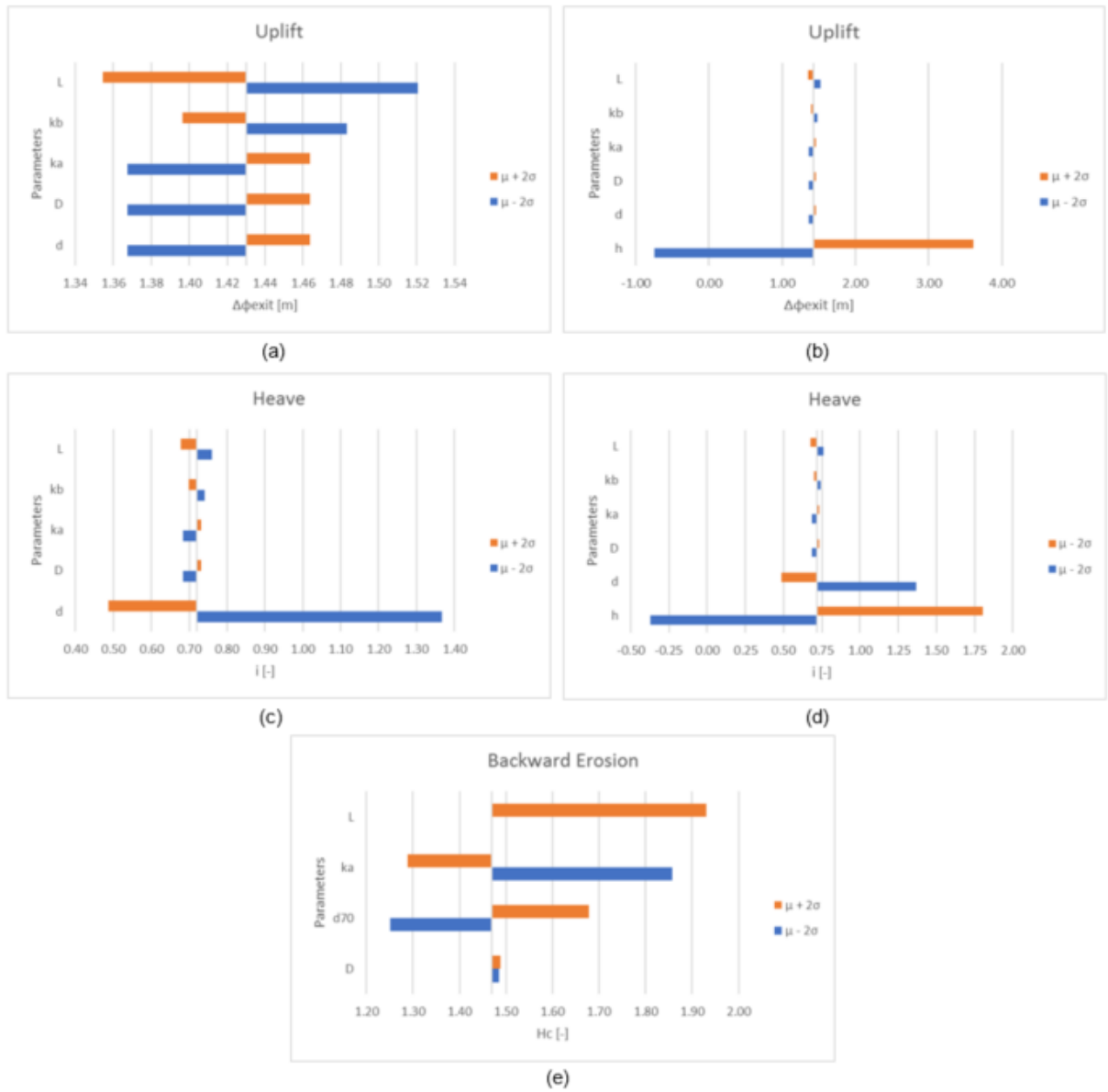
Figure D.7: Parameter sensitivity for the research location near Thorn
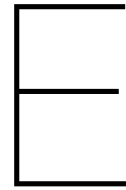
Appendix Numerical Analysis

This appendix corresponds to Chapter 5, the Numerical Analysis. The first section described and evaluates the modelling attempts for the research locations near Well, Beesel and Thorn. The second section includes the geometries of the model variations. The third section includes an extensive review of the variation study.

E.1. Modelling attempts for Well, Beesel en Thorn

For the benefit of the POV project an attempt was made to develop, in addition to the numerical model of Buggenum, numerical groundwater flow models for the other three research locations: Well, Beesel and Thorn. These numerical models do not directly contribute to the objectives of the numerical analysis as described in this report, but can be used within the POV Piping project to evaluate the likelihood to piping for the locations. However, it was found that there is a lot of information missing for these locations. This section describes the modelling obstacles and their causes for the models of Well, Beesel and Thorn. In addition, the relation between the modelling issues and the current assessment practice is discussed.

During the calibration phase of the model for Thorn it was found that the differences between the measured and modelled values of the potentials were too large to overcome by means of calibration. The numerical model resulted in far greater values for the potential than measured in the field. An explanation for this can be found in the fact that the dike near Thorn is not directly located along the Maas but next to a lake. The strong water level fluctuation on the Maas is most likely suppressed by the presence of that lake. Information about this resistance is lacking. Only the historic water levels of the Maas are known and not that of the lake. The lack of hydraulic data of the lake hindered the correct modelling of this location.

Subsequently, the possibility of a realistic model of the research location near Well was investigated. However, also at this location, the differences between the measured and modelled values of the potentials were too large to overcome in the calibration. The reason for this can be found in the presence of a very large foreland. Measurement point A is situated at about 300 meters from the river. To obtain a correct model, the complete foreland had to be included in the model. However, information about the hydraulic head, geometry and groundwater flow in this foreland was lacking.

In addition, the possibility of a realistic groundwater model of the location near Beesel was investigated. The dike near Beesel is located directly next to the river with only a small foreland. In contrast to the models of Well and Thorn, it was possible to calibrate to numerical model of Beesel. However, it should be noted that, under normal hydraulic circumstances the dike system of Beesel is a draining system. This means that the hydraulic head in the hinterland is higher than the water level of the Maas. Therefore, the water flows from the hinterland to the Maas instead of from the river to the hinterland. During the complete calibration period (2015), the water level of the Maas did not exceed the height of the hinterland as illustrated in Figure E.1. It can be expected that during extreme high-water periods,

such as that of 1993, the river water level will exceed the hinterland hydraulic level. This resulted in difficulties with respect to the simulation of the high water peak. Because, there are no measurements corresponding to an infiltrating situation it was not possible to determine the influence of a high river water level to the hinterland hydraulic level. Therefore, it was not possible to create a model that is suitable for the evaluation of high river water levels.
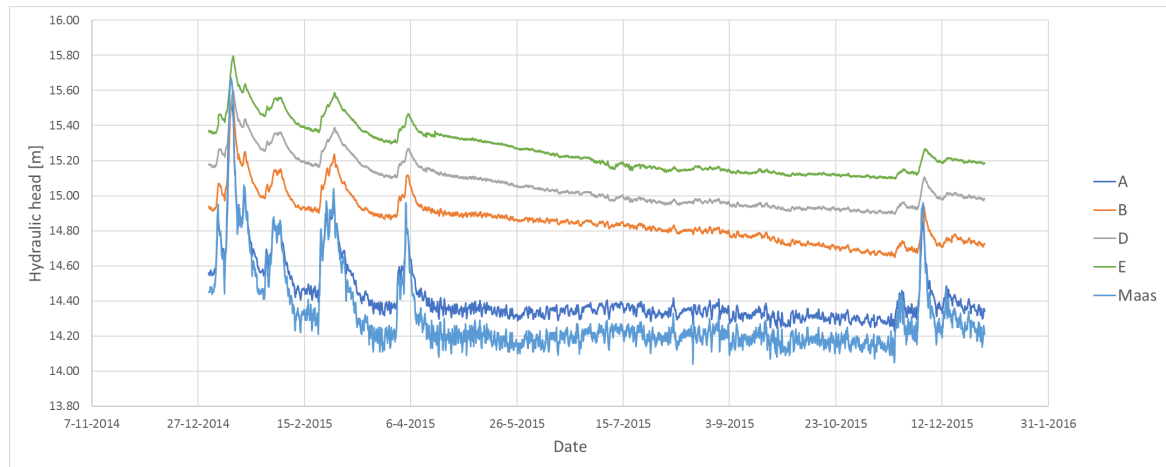
Figure E.1: Maas water level and water level measurements of the research location near Beesel for 2015

The modelling attempts for Well, Thorn and Beesel show that a lot of information is required to create a realistic calibrated groundwater flow model that matches field measurements in which a high-water peak can be simulated. Even when it is possible to develop and calibrate a model based on the normal situation, it is not always possible to investigate the piping likelihood. A high-water peak is required for this purpose and in order to implement such a peak correctly, information about the behaviour of the groundwater flow during those high water levels is required.

In all three cases a lot of information was available about the geometry, soil characteristics and hydraulic conditions. A large number of drillings and CPT's were performed and water level measurements of more than two years were available. The amount of information available in this study is larger than usually available for an assessment of the dikes. However, this information is still not complete and sufficient to obtain a correct groundwater flow model. One can then wonder if the results of an assessment based on such an amount of information or even less would be realistic. An example is the situation near Thorn. It has been found that, although the lake is situated in direct connection to the Maas, the water level at the lake is most likely lower than the water level of the Maas. When the dike is assessed based on the normative water level of the Maas, this will most likely result in a too conservative assessment of the Dike.

E.2. Geometries model variations

Figures E.2 to E.18 illustrate the geometries of the 23 model variations as presented in Table 5.1.
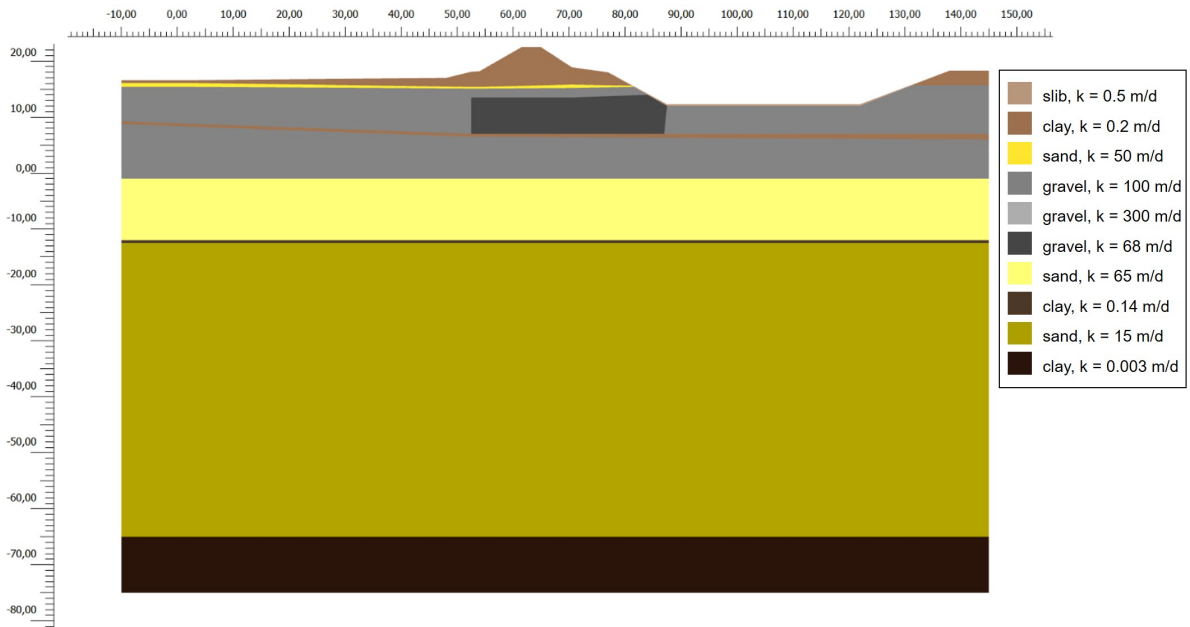
Figure E.2: Geometry model variation 3a
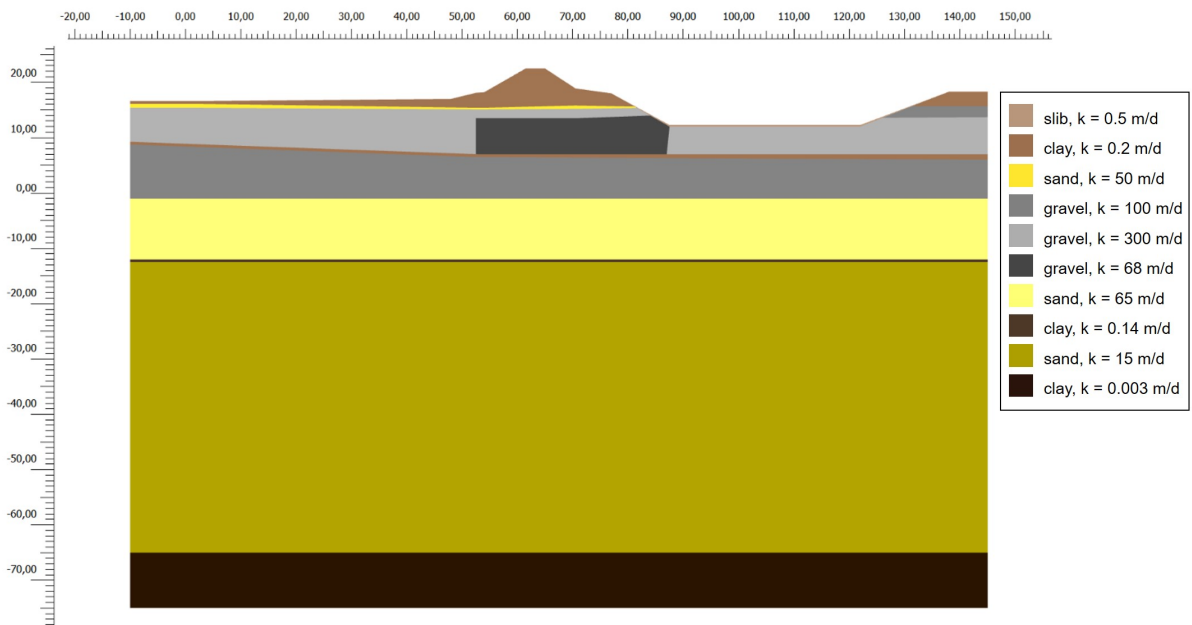
Figure E.3: Geometry model variation 3b
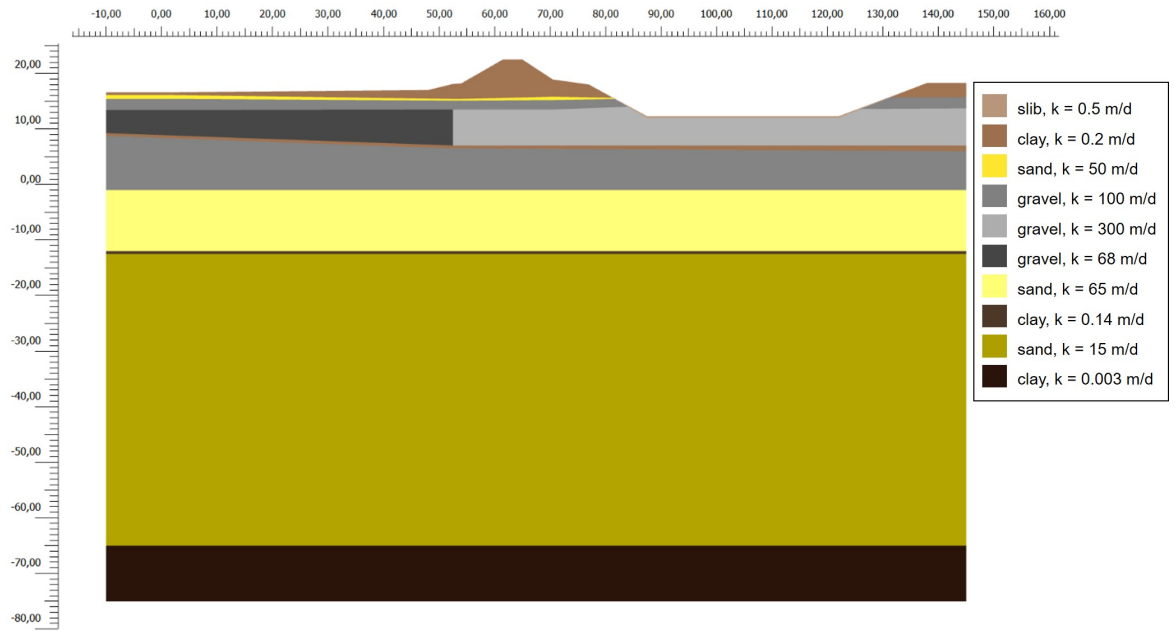
Figure E.4: Geometry model variation 3c
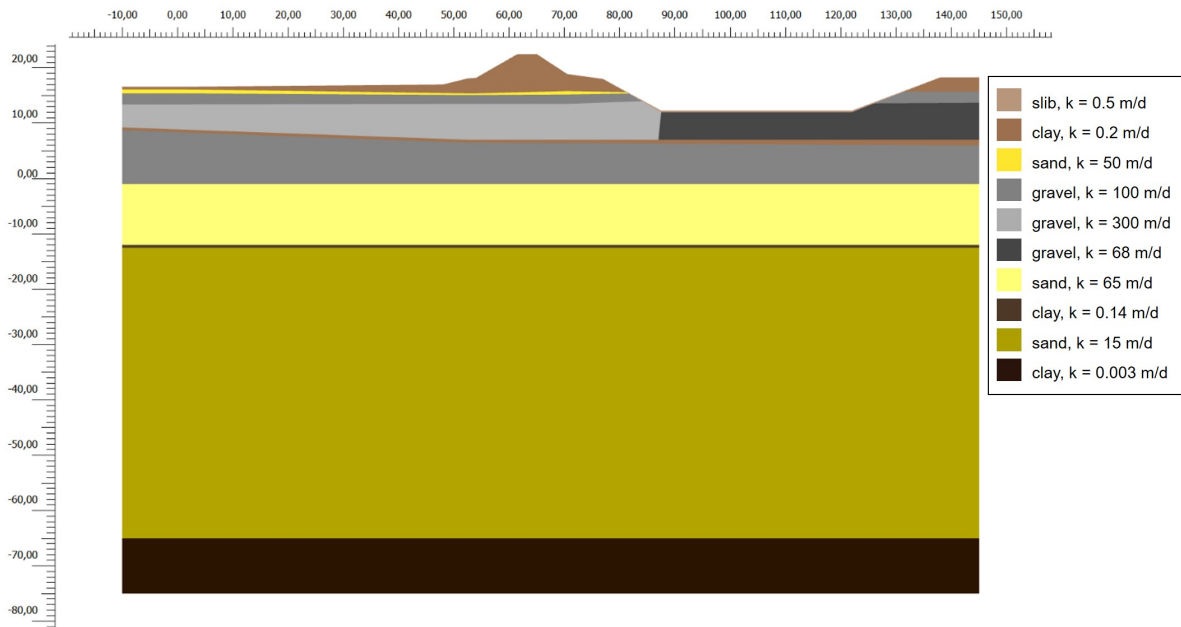
Figure E.5: Geometry model variation 3d
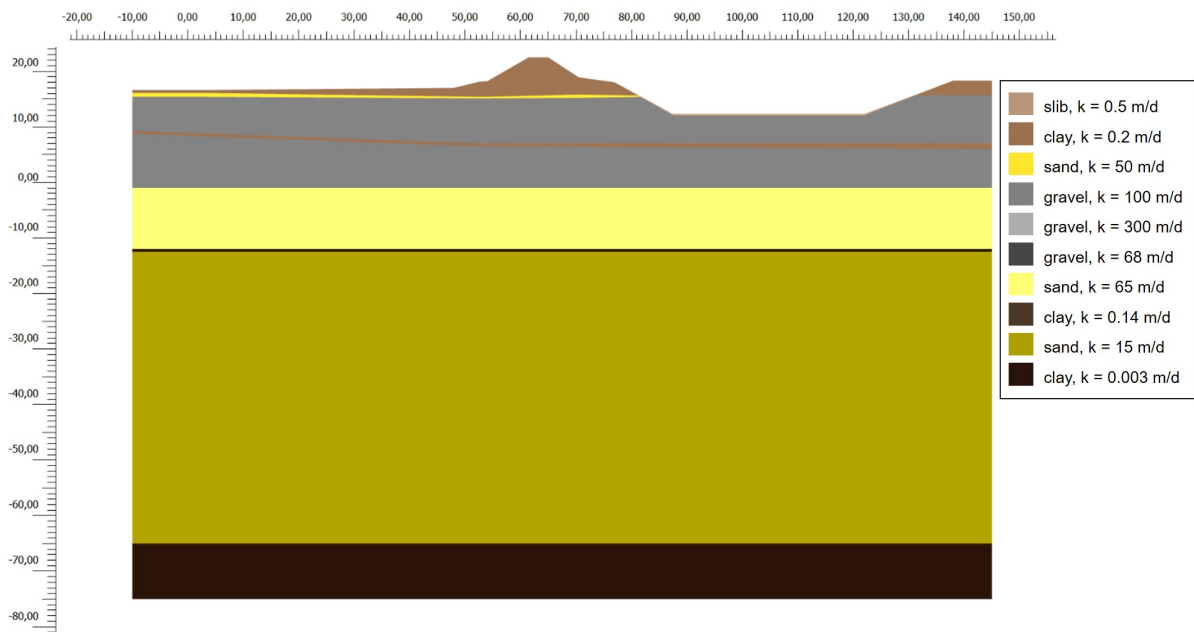
Figure E.6: Geometry model variation 3e
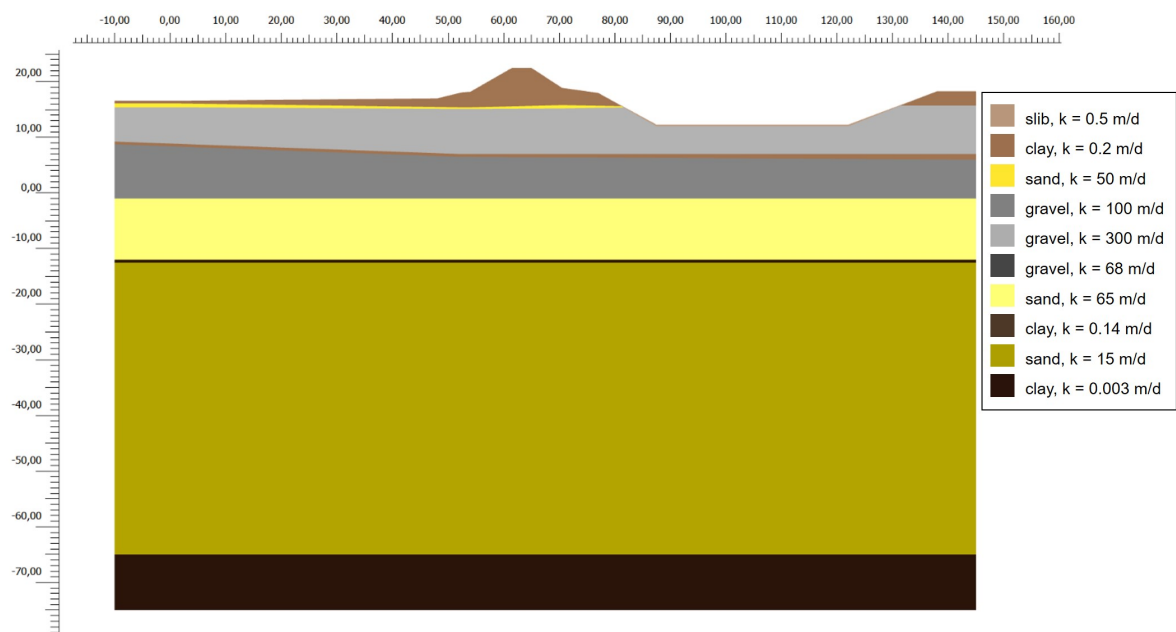
Figure E.7: Geometry model variation 3f
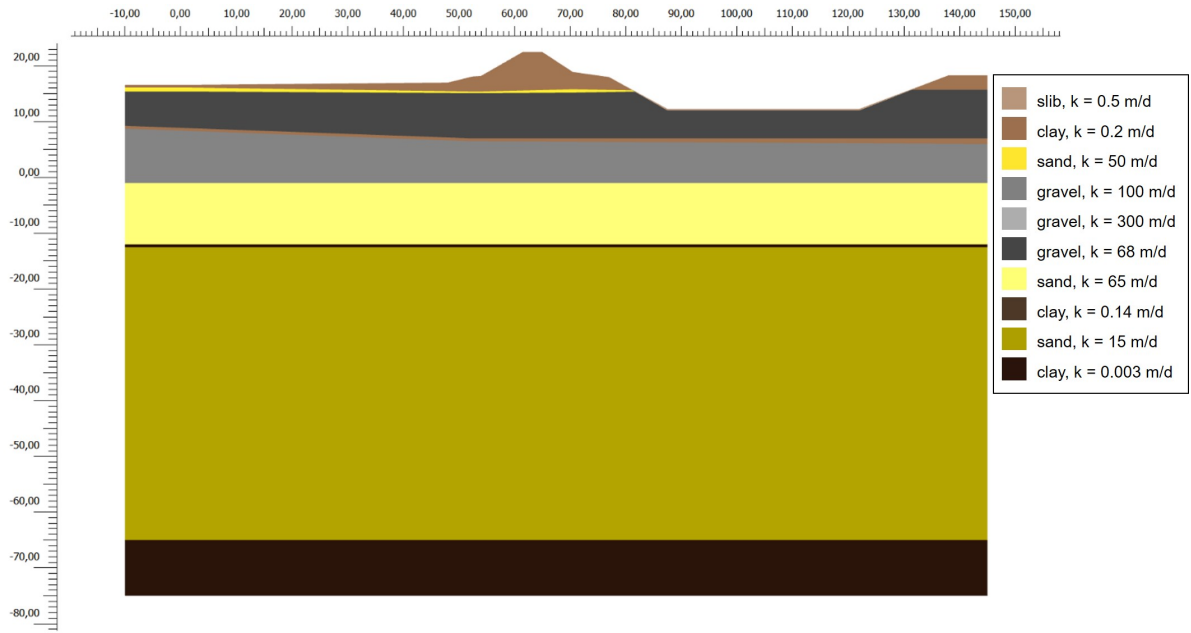
Figure E.8: Geometry model variation 3g
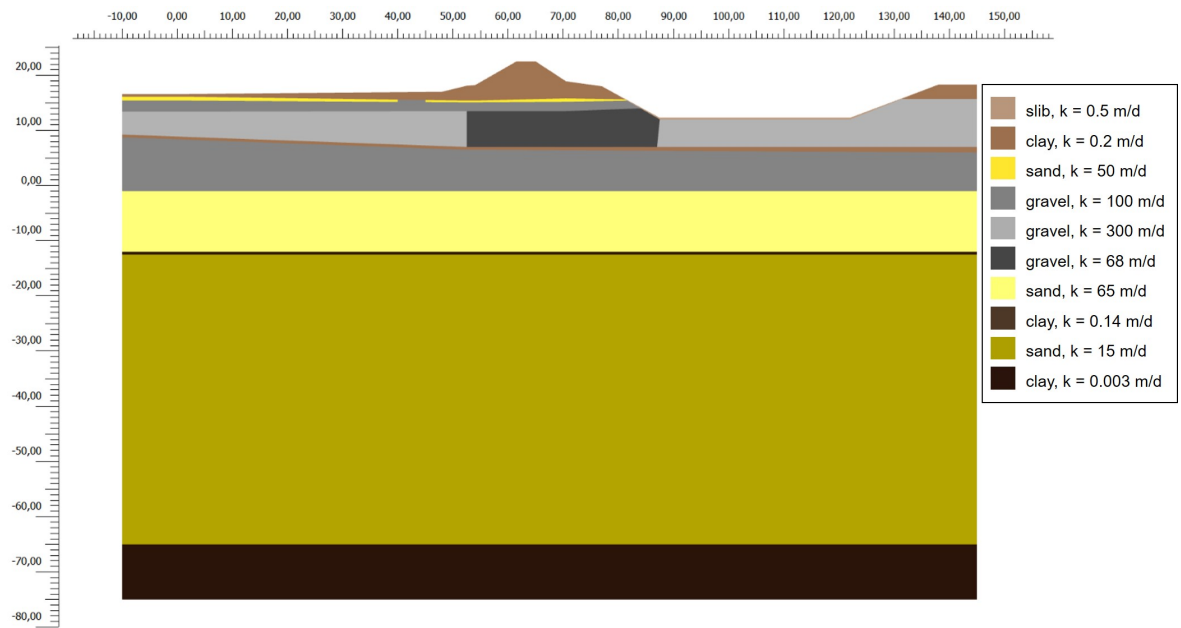
Figure E.9: Geometry model variation 3h
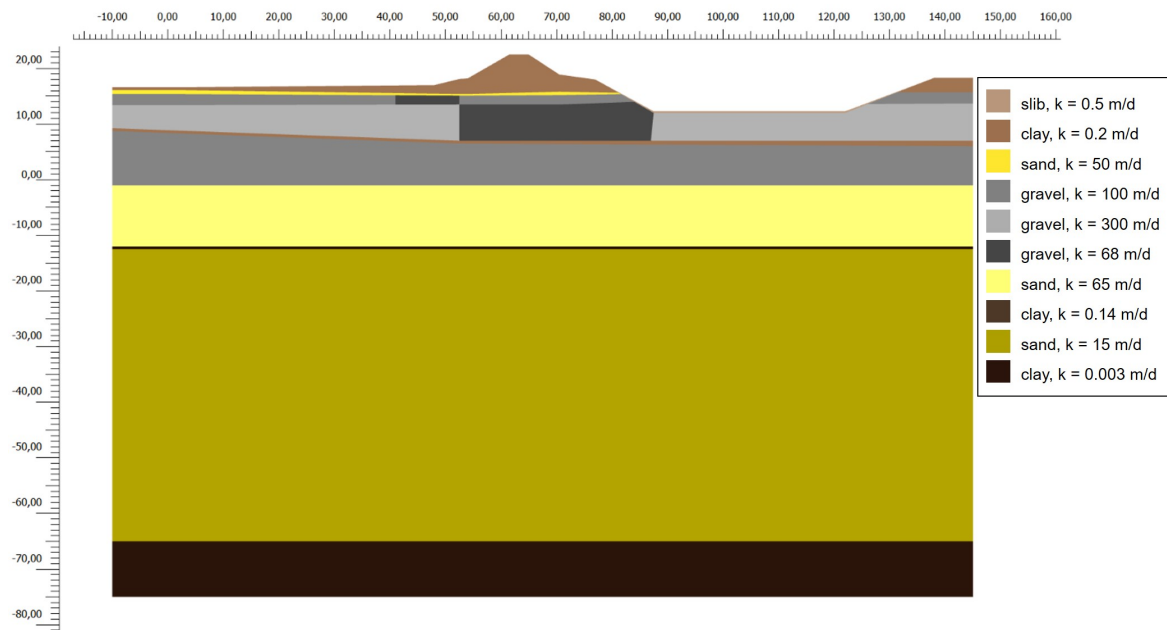
Figure E.10: Geometry model variation 3i
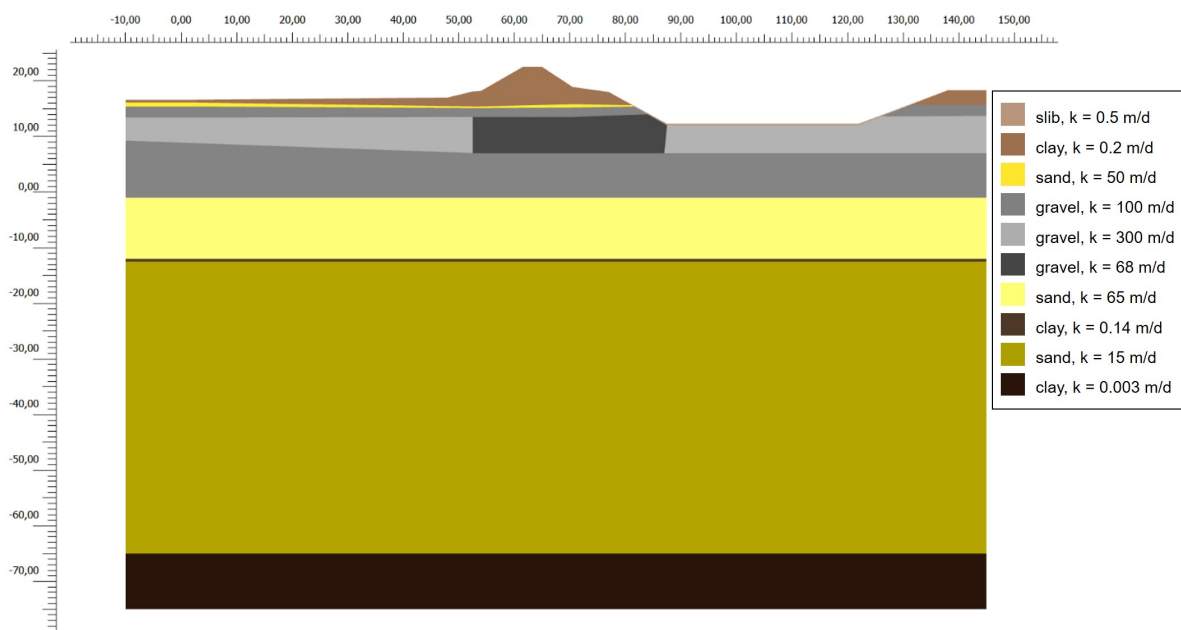
Figure E.11: Geometry model variation 4a
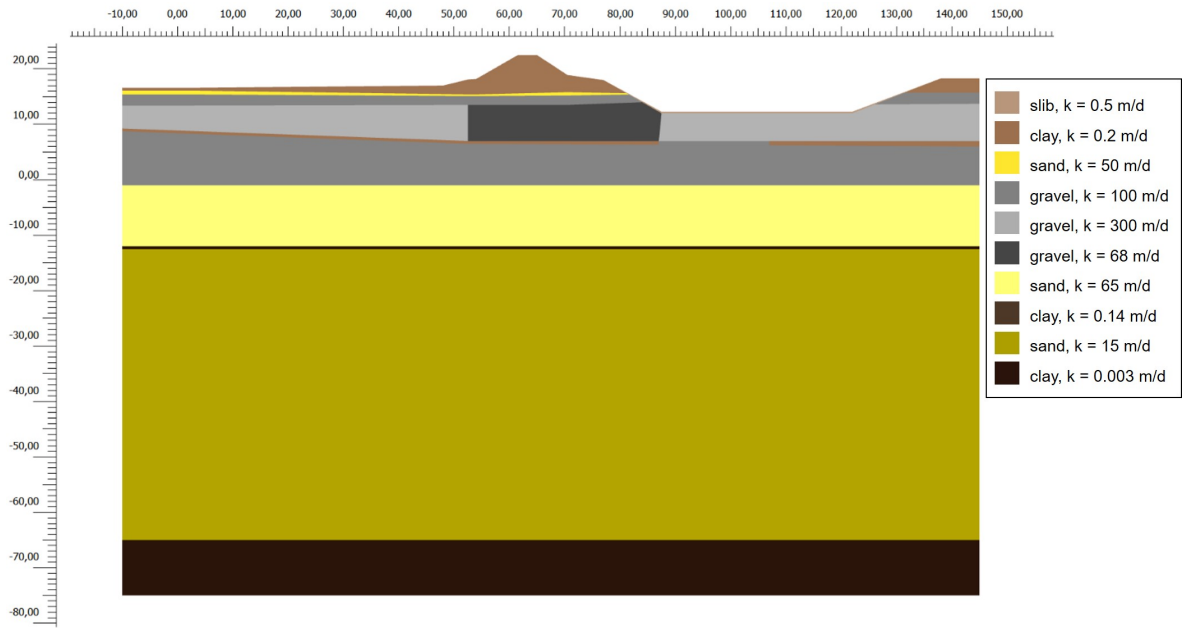
Figure E.12: Geometry model variation 4b
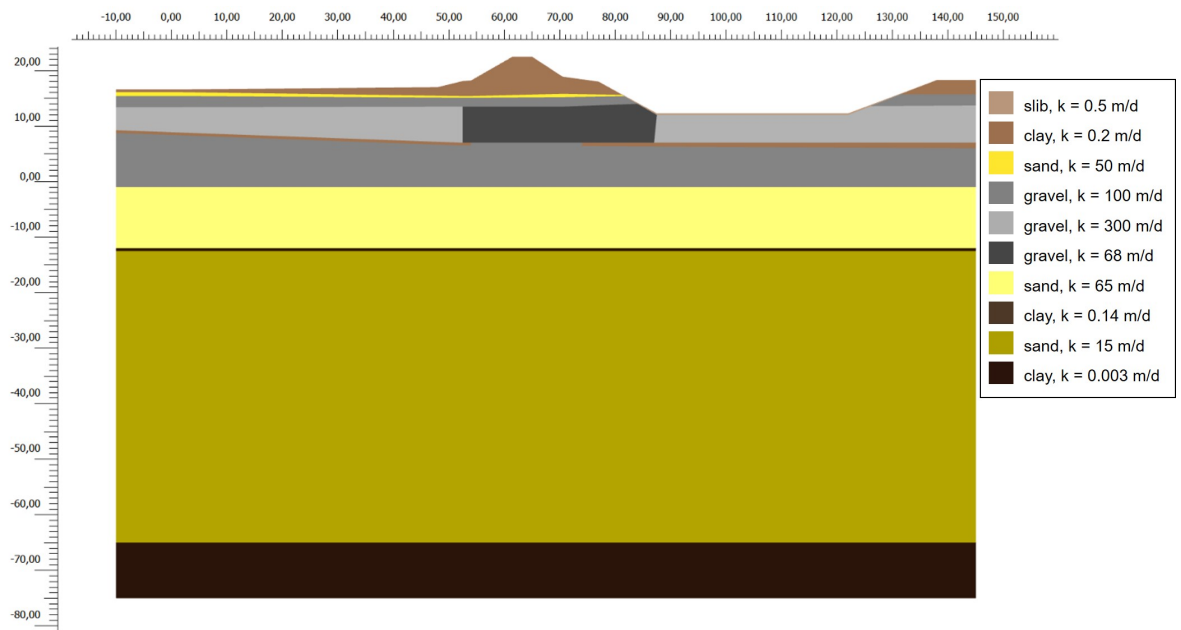
Figure E.13: Geometry model variation 4c
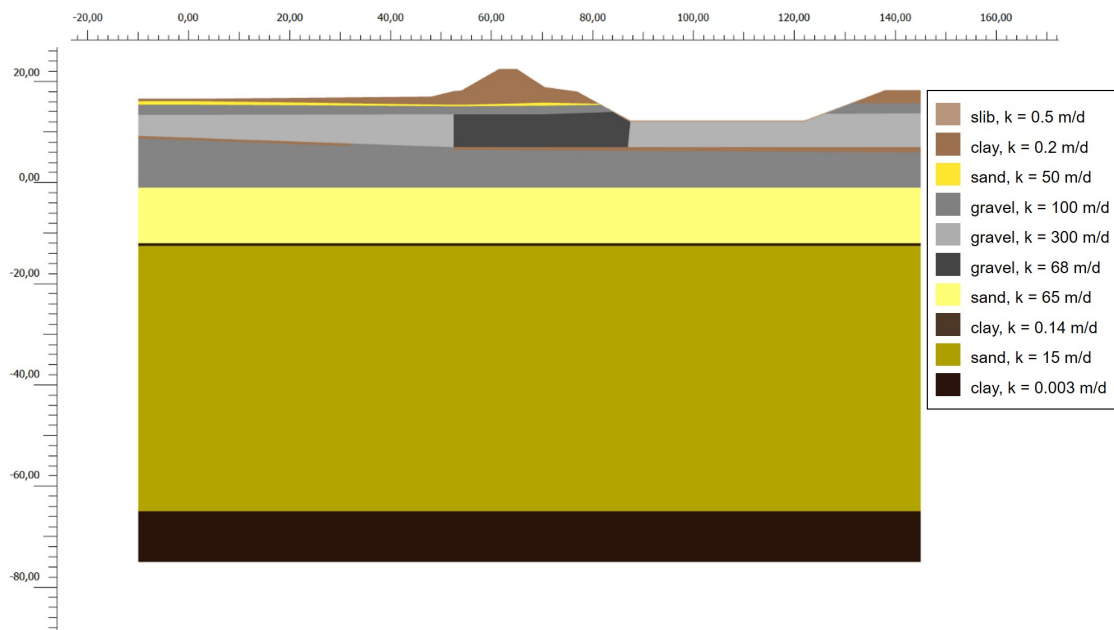
Figure E.14: Geometry model variation 4d
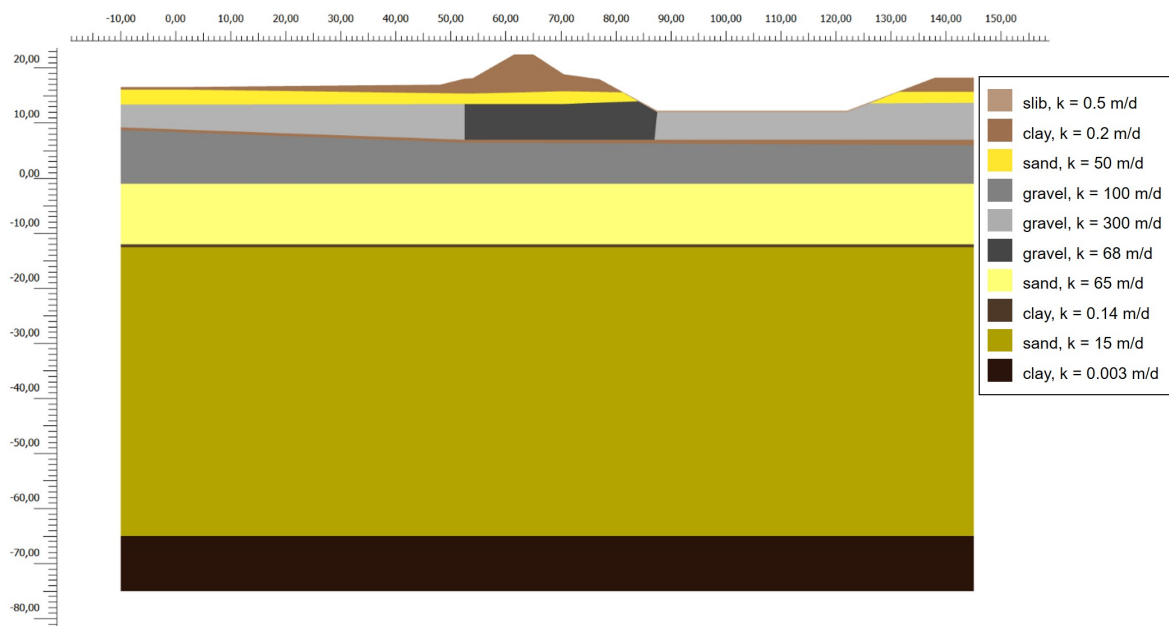
Figure E.15: Geometry model variation 5a
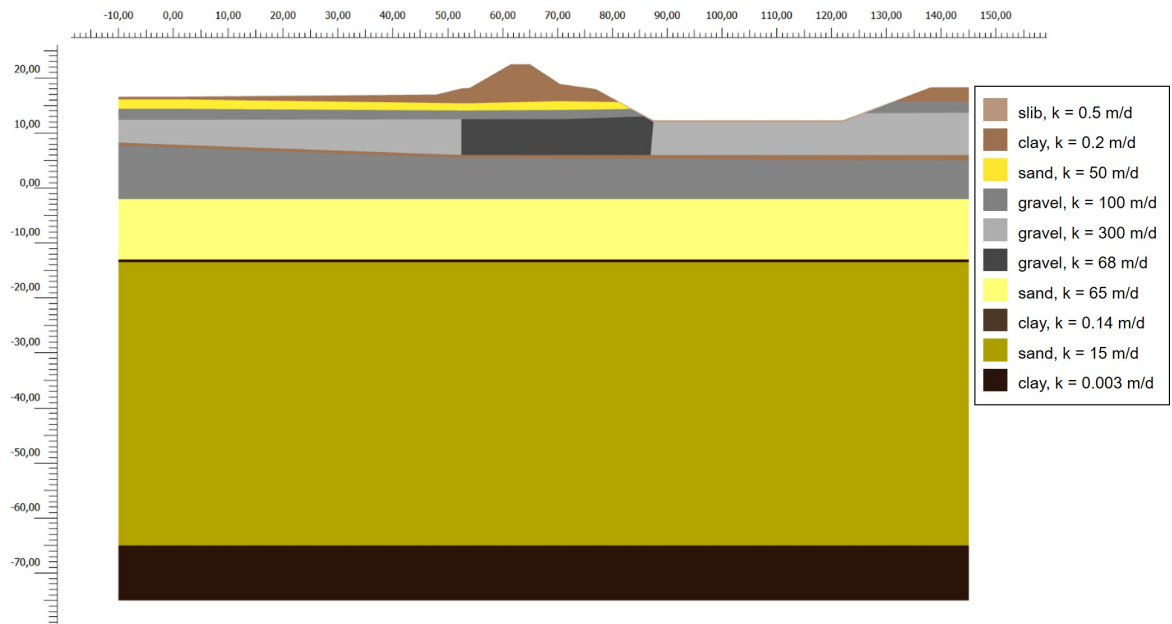
Figure E.16: Geometry model variation 5b
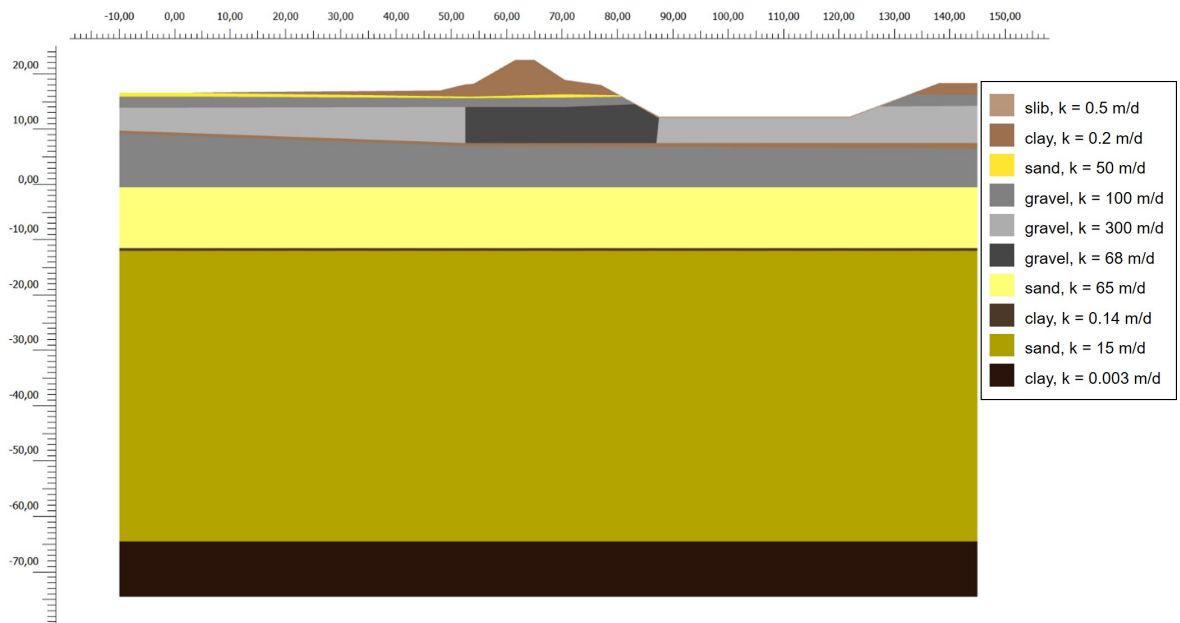
Figure E.17: Geometry model variation 6a
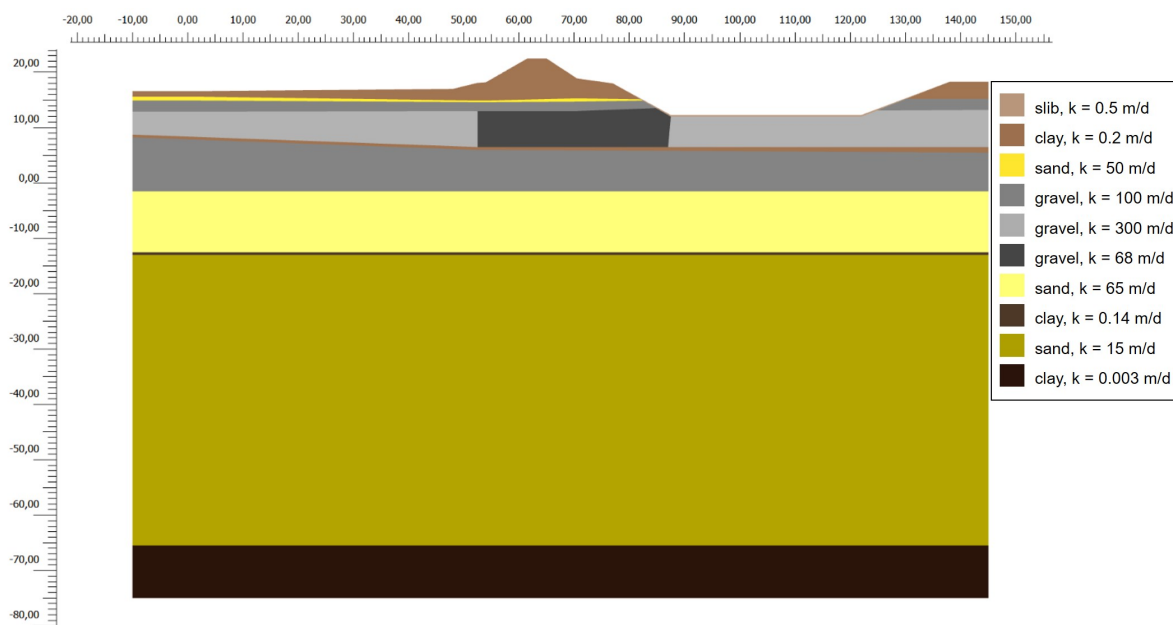
Figure E.18: Geometry model variation 6b

E.3. Explanation groundwater flow in model variations

Table 5.3 gave an overview of the model variations and their resulting potentials at the exit point at the time when the river water level reached its maximum value of 20.53 m + NAP. Model variations 1a to 1d showed that the permeability of the blanket layer has a significant effect on the likelihood for uplift. The greater the permeability of the blanket layer, the lower the maximum potential. With a hydraulic permeability of 0.5 m/d (model variation 1c), the potential even almost reaches the critical potential. The influence of the permeability of the sand layer, on the other hand, is not perceptible within the range in which the permeability was varied. The resulting potential of model variations 2a and 2b was similar to that of the original model. An increase of the thickness of the sand layer has little effect on the potential as shown by model variations 5a and 5b. The same applies to an increase of the thickness of the blanket layer (model variation 6b). However, reducing the thickness of the blanket layer does have a large effect (model variation 6a). This is not surprising, since the analytical analysis already showed that reducing the parameters has a greater effect than increasing the parameter values. It can be said that the characteristics of the sand layer (both the permeability and the thickness) do not significantly affect the potential. The characteristics of the blanket layer, on the other hand, are of great importance.

Model variations 3a to 3i are all related to the configuration and characteristics of the upper gravel layers (layers 4, 5, 6 and 7). Model variation 3a resulted in a higher potential than the original model. Figure E.19 shows that this is because the groundwater does not flow downwards into the second gravel layer at the inner toe. This is due to the fact that layers 4 and 7 have the same permeability of 100 m/d. In absence of the contrast between the permeability of layers 6 and 7 the groundwater continues to flow horizontally. Model variation 3b resulted in a potential that is higher than the potential of the original model, but lower than that of model variation 3a. Figure E.20 shows that the groundwater flows very fast in layer 4 in the part below the dike. This is due to the large difference in permeability between layer 4 and 6 (300 m/d versus 68 m/d respectively). The groundwater can easily access the aquifer via layer 4 due to the relatively low flow resistance as a result of the high permeability. Despite the equal hydraulic conductivities of layers 4 and 7, the groundwater is drawn deeper into layer 7 near the inner toe of the dike as shown in Figure E.21. Presumably, because the difference in permeability between layers 6 and 7 is relatively high in model variation 3b compared to model variation 3a. This explains why the potential resulted from model variation 3b is lower than that of model variation 3a.
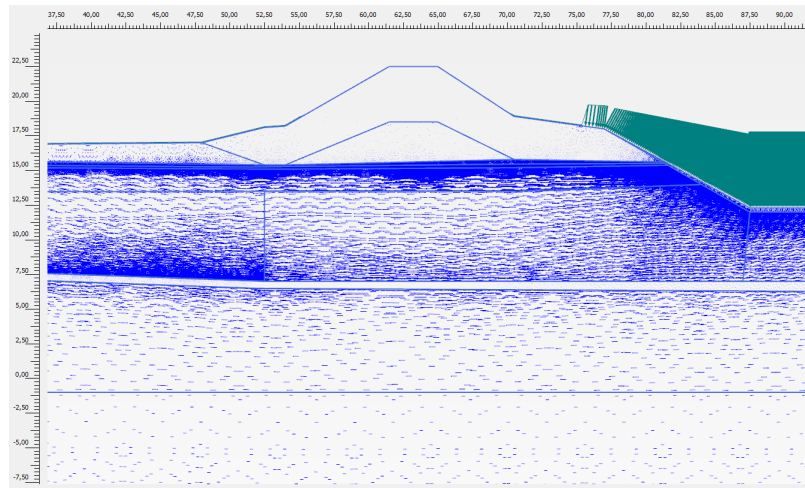
Figure E.19: Groundwater flow |q| [m/d] indicated by arrows for model variation 3a at the maximum river water level of 20.53 m +NAP
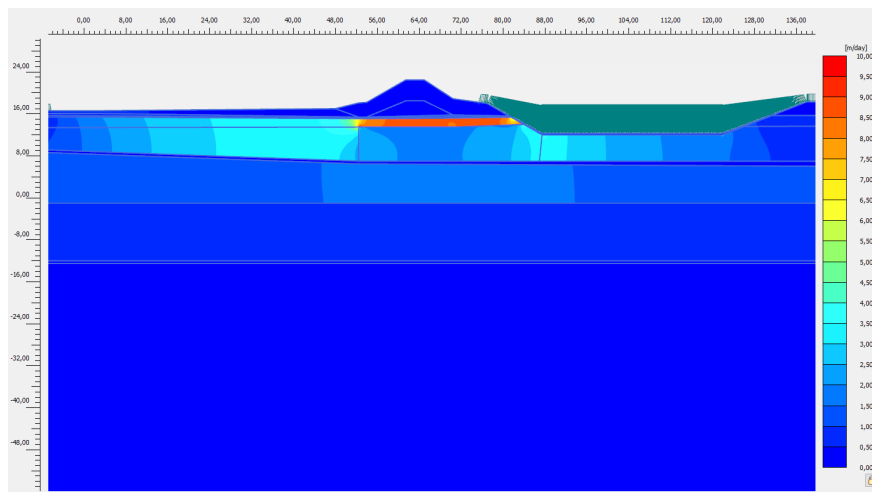
Figure E.20: Groundwater flow |q| [m/d] for model variation 3b at the maximum river water level of 20.53 m +NAP
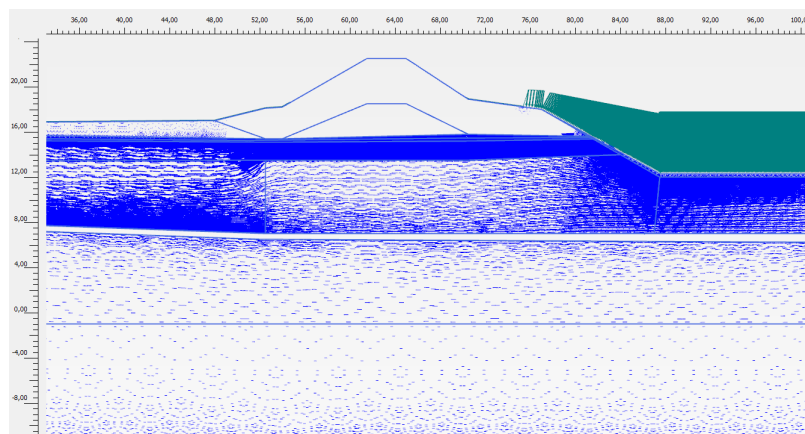
Figure E.21: Groundwater flow |q| [m/d] indicated by arrows for model variation 3b at the maximum river water level of 20.53 m +NAP

Model variation 3c results in an opposite groundwater flow pattern than the original model. At the inner toe the groundwater flow upwards due to the abrupt difference in permeability. The middle part of the second gravel layer (layer 6) has a high hydraulic conductivity of 300 m/d compared to the left part (layer 7) with a hydraulic conductivity of 68 m/d. Consequently, the groundwater moves to the layer with a hydraulic conductivity of 100 m/d, the first gravel layer (layer 4) resulting in the upward flow. This is clearly illustrated by Figure E.22. Due to the high flow velocity in the upper gravel layer (layer 4) left of the inner toe, the potential that resulted from this model variation was much higher than that of the original model. The potential was 19.47 m + NAP, 0.55 m above the potential of the original model.
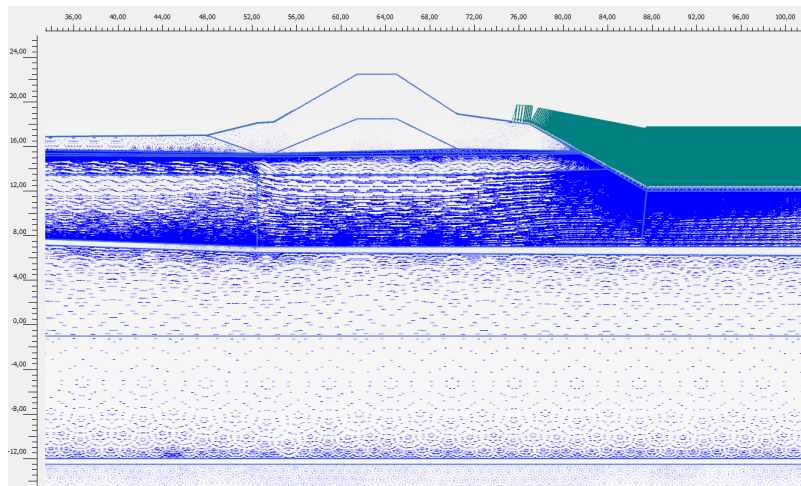
Figure E.22: Groundwater flow |q| [m/d] indicated by arrows for model variation 3c at the maximum river water level of 20.53 m +NAP

The maximum potential underneath the blanket layer at the exit point that resulted from model variation 3d was also significantly higher than the original model, 19.16 m + NAP a difference of 0.24 m. Comparing, Figure 5.5 and E.23 it can be seen that the flow velocity below the blanket layer at the exit point (layer 4) for model variation 3d is higher then the velocity in the original model. Comparing the original model and model variations 3c and 3d it can be concluded that the location of gravel zones with highly different permeabilities is of enormously important to the occurring potential. When a gravel zone with relatively low permeability is situated in the hinterland, it does not have a major effect on the groundwater flow. If this zone is located underneath the dike, as in the original model, then this results in a lower potential and thus a lower likelihood to piping. If the zone is situated in the hinterland, this causes the potential to increase very strongly and hence the piping likelihood. It should be noted that this relates to a system with two different layers of gravel underneath a sand layer, where the low permeability gravel zone is located in the second layer. This ensures that the groundwater flow can deviate from the upper to the lower gravel layer or vice versa as seen in the original model and model variation 3c respectively.
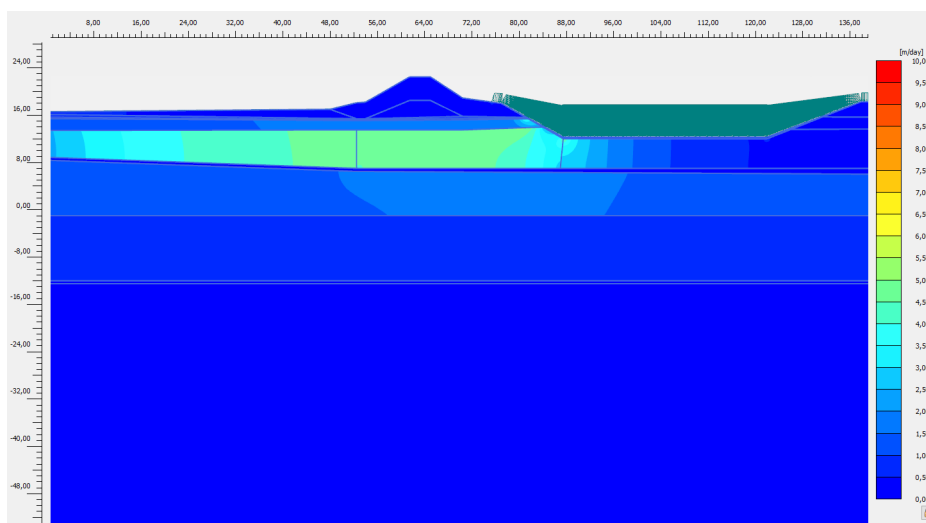
Figure E.23: Groundwater flow |q| [m/d] for model variation 3d at the maximum river water level of 20.53 m +NAP

Model variations 3e, f and g illustrate the role of the flow rate on the potential. The higher the permeability of the aquifer the higher the flow rate below the blanket layer and thus the higher the potential. Due to merging of the gravel layers, the heterogeneity in the aquifer is limited.

Model variation 3h includes a small gravel pocket with a permeability of 100 m/d in the sand layer left of the exit point. The gravel pocket has no observable effect on the groundwater flow. In addition, the moderately permeable gravel pocket in model variation 3i does not have a major effect on the groundwater flow either. Both model variations do not significantly influence the groundwater flow near the inner toe. The water is still drawn into the deeper gravel layer. This phenomenon completely determines the resulting potential. In addition, the contrast between the permeability of the gravel pocket and layer 4 is not very large (model variation 3i) as well as the contrast in the permeability between the sand layer and the gravel pocket (model variation 3h). As a result, it does not cause a major change in the groundwater flow.

The influence of the first clay layer, layer 8, has been studied in model variations 4a to 4d. In model variation 4a, this layer is completely removed resulting in a potential of 19.09 m, 0.17 m higher than the original potential. Replacing the clay layer by gravel results in an increase of the aquifer thickness. The larger the aquifer the higher the potential. This also follows from the analytical model. Model variation 4b illustrates the effect of local absence of the clay layer in the foreland (below the river). The resulting potential is equal to that of the original model. Logically, given that the water infiltrates only in the aquifer near the outer toe of the dike past this local absence. A local absence of the clay layer under the dike, model variation 4c, however, does have influence. The potential increases by 0.06 m to 18.98 m + NAP. This difference slightly increases when the clay layer is absent in the hinterland (model variation 4d). A potential of 19.04 m + NAP is then reached. Altogether, a (local) absence of the clay layer causes no major changes in potential.

List of Symbols

h	[m]	River water level w.r.t. NAP
h_p	[m]	Water level in hinterland w.r.t. NAP
d	[m]	Thickness of blanket layer
D	[m]	Thickness of aquifer
B	[m]	Width of the dike
L_f	[m]	Length of foreland
L_h	[m]	Length of hinterland
L	[m]	Seepage length
x_{exit}	[m]	Exit point w.r.t. center of the dike
k_a	[m/d]	Hydraulic conductivity of aquifer
k_b	[m/d]	Hydraulic conductivity of blanket layer
γ_{sat}	[kN/m^3]	Saturated volumetric weight of the blanket layer
γ_w	[kN/m^3]	Volumetric weight of water
γ_s	[kN/m^3]	Volumetric weight of sand grains
γ'	[kN/m^3]	Buoyant weight of sand grains
H	[m]	Head difference
H_c	[m]	Critical head difference
H_v	[m]	Vertical head difference
ϕ_{exit}	[m]	Potential at exit point
$\phi_{c,u}$	[m]	Critical potential
$\Delta\phi$	[m]	Difference between potential and hinterland water level
ζ	[-]	Damping factor of outside water level
λ	[m]	Leakage factor for leakage through blanket layer
i	[-]	Vertical exit gradient
$i_{c,h}$	[-]	Critical vertical gradient
n	[-]	Porosity
C_{creep}	[m]	Creep factor according to Bligh
$C_{w,creep}$	[m]	Weighted creep factor according to Lane
F_R	[-]	Resistance factor of Sellmeijer calculation rule
F_R	[-]	Scale factor of Sellmeijer calculation rule
F_R	[-]	Geometrical shape factor of Sellmeijer calculation rule
η	[-]	Whites constant (0.25)
θ	[degrees]	Bedding angle of sand (0.37)
RD	[-]	Relative density
RD_m	[-]	Mean value of relative density (0.725)
U	[-]	Uniformity coefficient
U_m	[-]	Mean value of uniformity coefficient (1.81)
KAS	[-]	Measure for the angularity of grains
KAS_m	[-]	Mean value angularity (0.498)
d_{70}	[m]	70%-fractile of the grain size distribution
d_{70m}	[m]	d_{70} reference value
κ	[m^2]	Intrinsic permeability ($k_a\, \nu/\gamma_w$)
ν	[Ns/m^2]	Kinematic viscosity of water at $10°C$ ($1.33 \cdot 10^{-6}$)
μ	[-]	Mean parameter value
σ	[-]	Standard deviation
V	[-]	Variation coefficient
q_c	[MPa]	Cone resistance
σ'_v	[kN/m^2]	Vertical effective stress

List of Figures

List of Tables